Rockefeller University
Digital Commons @ RU

Student Theses and Dissertations

1975

The Temperature Dependence of Reactions of Gaseous IONS: Kinetics and Thermodynamics of Transfer and Association Reactions

Michael Mautner

Follow this and additional works at: https://digitalcommons.rockefeller.edu/student_theses_and_dissertations

 Part of the Life Sciences Commons

RES
LD4711.6
M459
c.2

THE LIBRARY

LD 4711.6 M459 1975 c.1 RES
Mautner, MIchael.
The temperature dependence
of reactions of gaseous

Rockefeller University Library
1230 York Avenue
New York, NY 10021-6399

THE TEMPERATURE DEPENDENCE OF REACTIONS OF GASEOUS IONS: KINETICS AND THERMODYNAMICS OF TRANSFER AND ASSOCIATION REACTIONS

A thesis submitted to the Faculty of the
Rockefeller University in partial fulfillment
for the Degree of Doctor of Philosophy

by

Michael Mautner (Meot-Ner), M.Sc.

10 March 1975

The Rockefeller University
New York, New York 10021

DEDICATION

This work is dedicated to Mrs. Irene (Gigor) Horvath of Budapest, Hungary, who with a degree of human compassion uncommon at the time, risked her life to save mine as a Jewish child in Nazi Hungary. It is also dedicated to the memory of the six million victims, many of whom, undoubtedly more able than this author, were not fortunate enough to be permitted to make their contribution to human progress.

ACKNOWLEDGEMENTS

The help and encouragement of many people was instrumental for the completion of this work. I wish to thank Dr. J. H. Green and Dr. A. D. Adler for recommending me to be accepted as a student at Rockefeller University. I thank Professor F. H. Field for the generous amounts of time and effort he dedicated to my education in the ways of science. I also thank Professors H. Gershinowitz, D. Mauzerall, M. Schreiber, and R. Tilbury who taught and advised me in the course of my work. From my family, I wish to thank my wife Helene and my mother and stepfather, Mr. and Mrs. Martin Marx, for their continued encouragement and support during the course of this work.

ABSTRACT

The effect of temperature on the kinetics and thermodynamics of gaseous ion-molecule reactions were investigated by pulsed, high pressure (0.4 - 3.0 torr) mass spectrometry in the temperature range 100 - 650°K. In the context of kinetic temperature effects, the reactions investigated may be divided into three classes: (i) Fast bimolecular transfer reactions which proceed with collision rates, e.g. $N_2H^+ + X \longrightarrow XH^+ + N_2$ (X = CH_4, NH_3, CH_3CHO). These reactions exhibit no temperature dependences when X is nonpolar, and small temperature dependences resulting from the effects of the temperature on the average charge-dipole interaction, when X is polar. This behavior indicates, in the context of transition state theory (TST), that reaction complexes posses lose structures in which the reactants preserve the rotational degrees of freedom. (ii) Slow bimolecular ion-molecule transfer reactions. In this work the H^- transfer reactions $t\text{-}C_4H_9^+ + i\text{-}C_5H_{12} \xrightarrow{k} t\text{-}C_5H_{11}^+ + i\text{-}C_4H_{10}$ ($k = AT^{-3}$) and $NO^+ + CH_3CHO \xrightarrow{k} CH_3CO^+ + HNO$ ($k = AT^{-1.5}$) were investigated. The large negative temperature dependences are interpreted on the basis of TST as resulting from entropy loss associated with the formation of tightly bound transition complexes. (iii) Trimolecular association reactions. The mechanism $A^+ + B \underset{k_b}{\overset{k_c}{\rightleftharpoons}} AB^{+*} \xrightarrow[M]{k_s} AB^+$ was confirmed by pressure studies on $CH_3NH_3^+ + CH_3NH_2 \xrightarrow{M} (CH_3NH_2)_2H^+$; analogous reactions involving NH_4^+ and $(CH_3)_2NH_2^+$ were also investigated. The overall forward rate constants for such reactions exhibited large negative temperature dependences: $k_f \approx AT^{-3}$ to AT^{-7} for these reactions between 350 and 400°K; at lower temperature the magnitude of the temperature dependences decreases. These effects are interpreted on the basis of the effects of the temperature on k_b in the context of an RRKM-type model for the decomposition of coupled harmonic quantum oscillators.

The association reactions of $N_2^{+\cdot}$ and N_2H^+ with N_2 and of $CO^{+\cdot}$ and

HCO^+ with CO also exhibited negative temperature dependences ($k = AT^{-1.5}$ to AT^{-3}) which could be interpreted in a similar manner. Equilibrium studies in the latter reactions showed that the association reactions of $N_2^{+\cdot}$ and $CO^{+\cdot}$ with N_2 and CO are significantly more exothermic than those of the protonated ions N_2H^+ and HCO^+ with the same neutrals. Equilibrium studies were also performed to obtain the enthalpies ($\Delta H \approx -20 \pm 3$ kcal/mole) and entropies ($\Delta S \approx -20$ to -30 e.u.) for the association of $ValH^+$ and $ProH^+$ with Val, Pro, H_2O, NH_3 and CH_3NO_2.

CONTENTS

I. INTRODUCTION

MASS SPECTROMETRIC INVESTIGATIONS OF THE TEMPERATURE DEPENDENCES OF GAS PHASE IONIC REACTION RATES AND EQUILIBRIUM CONSTANTS

The investigation of gaseous ions under conditions where the effect of ion-molecule reactions is predominant received a major impetus from the discovery of the reaction

$$CH_4^+ + CH_4 \longrightarrow CH_5^+ + CH_3$$

in the early 1950's.[1,2,3] Instrumental developments[4] have made it possible to operate at pressures of 100 - 2000 microns, where the neutral and ionic components of the reactions plasmas are at thermal energies corresponding to the temperature of reaction vessel, i.e., the walls of the high-pressure mass spectrometric ion source.

In the conventional, low-pressure mass spectrometric ion sources ions are generated by electron impact, in energy states determined by the energy deposition function, usually with internal excitations of several e.V. The ions then decompose by mechanisms determined by their structures and the statistics of the distribution of the internal energy. In high-pressure mass spectrometry, however, the reactant ions of interest are usually either generated by electron impact and become thermalized by ion-molecule collisions prior to reaction, or the ions are generated by chemical ionization, i.e., in reactions between thermalized ions and thermalized neutrals, and become further thermalized prior to subsequent reactions. The reactions of interest in high-pressure mass spectra therefore usually take place in systems where the distribution of energy corresponds to the temperature determined by the temperature of the reaction vessel. Possible exceptions can exist if the ions of interest decompose at rates faster than that of their collisions with neutrals or if ions generated in exothermic reactions react in reactions of nearly unit efficiency with a major component of the neutral reaction mixture. Reactions of this second type would, however, be very fast since the rates of ion-molecule collisions are $\approx 10^{-9}$ cm.^{3}/molecule sec., and the usual

densities in the studies of interest here are $\geqslant 10^{16}$ mol. cm.^{3}. The rates of fast reactions between ions and the major neutral component of the reaction mixture are therefore on the order of $(10^{-9} \times 10^{16}) = 10^{7}$ sec.$^{-1}$. The overall rates of the reactions investigated in the present study are on the order of 10^{3} to 10^{6} sec.$^{-1}$. Reactions with rates $\geqslant 10^{7}$ sec.$^{-1}$ were used only to generate reactant ions which become thermalized before undergoing further slow reactions. In the reactions that were investigated the reactant ions either undergo many collisions with nonreactive components of the reaction mixture, or many nonreactive collisions with reactive components, before reaction takes place. In general, therefore, thermal distribution of the reactant species may be used.

Soon after the development of high-pressure, chemical ionization mass spectrometry, the significant temperature dependence of the mass spectra was observed.[5,6] The general expression of the rate constant may be written as

$$k(T) = A(T)\, e^{-E_a/RT}$$

where A(T) is a slightly temperature dependent pre-exponential factor and E_a is an activation energy practically independent of temperature. The value of temperature variation in the investigation of the kinetics of the reactions of gaseous ions may be briefly outlined as follows:

(i) Bimolecular exothermic ion-molecule transfer reactions are usually known to proceed with negligible activation energies. In the case that such reactions proceed via reaction complexes with lifetimes sufficient for the redistribution of internal energies, the temperature dependence of the reaction rates is determined by the pre-exponential factors. The temperature dependences of the reaction rates of such reactions can be related via transition state theory (TST) considerations to entropy changes upon the formation of the transition complex, and can, therefore yield information on the structure of the complex.

(ii) Bimolecular exothermic reactions may proceed via direct mechanisms or loose complexes. The temperature dependence of the rate

constants of such reactions is determined by collision kinematics and is best interpreted at this time by the Langevin-Giomousis Stevenson theory[7] that predicts no temperature dependence for fast ion-nonpolar molecule reactions and by the average dipole orientation (ADO) theory for reactions involving polar neutrals[8] which predicts slight negative temperature dependences for the rates of such reactions. The temperature dependence of the slow reactions involving tight complexes as predicted by TST considerations is of a functional form which is different and in general larger than the temperature dependence of the fast reactions. Consequently, the investigation of the temperature dependences of bimolecular reactions may be used to distinguish between direct and complex mechanisms, and to test kinematic theories concerning ion-molecule collision rates.

(iii) The rate constants of ion-molecule association reactions usually exhibit large negative temperature dependences. These temperature dependences may be used to test kinetic theories relating to ion-molecule association reactions such as the energy-transfer theory[9] or TST. Also by arguments similar to the previous paragraph, the temperature dependences may be used to distinguish between mechanisms in which the stabilization of association complexes occurs via direct mechanisms or through tightly-bound three-body complexes.

Temperature variation may also be applied to equilibrium studies. The van't Hoff plots of log k vs. $\frac{1}{T}$ yield the enthalpy of the reactions. Since

$$RT\ln K = \Delta G^{\circ} = \Delta H^{\circ} - T\Delta S^{\circ}, \qquad (I.1)$$

the measurement of K and ΔH° yields ΔS°. The study of temperature dependence of bimolecular reactions yields information on relative heats of formation of ions, proton affinities, ionization potentials, H^- affinities, etc. of neutral molecules. In association reactions, information on, for example, binding energies in ion-molecule association complexes and gaseous ion-solvent interactions may be obtained. (For a review, see Ref. 10.) The thermodynamic values, in turn, yield information of the structures of the stable ions produced in the association reactions. Comparison of the

thermodynamic and kinetic data on the intrinsic properties of gaseous ions with similar data in solution has great potential value to clarify the role of solvents in ionic processes.

The body of the data that has accumulated to date on mass spectrometry and ion-molecule reactions is very large, encompassing many thousands of journal articles and many books and review articles. References to literature related to the subject matters of the investigations reported in this work will be given in the individual chapter on each investigation. As opposed to the extensive amount of published information on mass spectrometry and ion-molecule reactions in general, the information available on the temperature dependence of ion-molecule reactions was scarce at the time that the work reported in this thesis was undertaken. The published data related mainly to the thermodynamic properties of ion-molecule association reactions involving small molecules and to some extent sporadic information on the temperature dependence of the kinetics of such reactions. At this state of the art, it appeared desirable to undertake more detailed investigation of the temperature dependences of ion-molecule reactions aimed at the goal of the systematic and comprehensive understanding of questions such as the relation between reaction mechanism, geometric and electronic structure of the reactants, the complexity of the reactants, kinetic and thermodynamic properties of both association and transfer reactions, and the temperature dependence of such reactions.

The studies reported in this thesis constitute research efforts aimed at these objectives. They also constitute an effort to explore the usefulness of temperature studies to clarify such fundamental problems, and to explore the potentials and limitations of pulsed high pressure mass spectrometry as a tool for such investigations.

The philosophy of the approach to the study of ion-molecule reactions followed in this work was to investigate selected problems which at this stage promise to yield insight into a particular aspect of ion-molecule chemistry. In bimolecular reactions one important problem of this kind

was the existence of slow ion-molecule transfer reactions, i.e., reactions which proceed with rates significantly slower than the collision rate. One class of such slow reactions are H^- transfer reactions, for example:

$$t\text{-}C_4H_9^+ + i\text{-}C_5H_{12} \longrightarrow t\text{-}C_5H_{11}^+ + i\text{-}C_4H_{10} \qquad (I.2)$$

which was known to proceed 40 times slower than the Langevin collision rate. The reaction may be slow because of the presence of an activation energy; or, alternatively because of entropic effects hindering the reaction rate. The study of the temperature dependence of the rate constant offers a possibility to distinguish between these factors and to gain insight into the reaction mechanism. Another important question is whether H^- transfer reactions involving more simple reactants will also proceed at slow rates and behave as reaction I.2 upon variation of the temperature. For this purpose we investigated the reaction:

$$NO^+ + CH_3CHO \longrightarrow CH_3CO^+ + NO \qquad (I.3)$$

With respect to fast ion-molecule reactions, the Langevin treatment[7] predicts no effect of the temperature on the reaction rate. This has not been proven systematically over a wide range of temperatures. As opposed to the Langevin treatment, the recently developed average dipole orientation theory[8] predicts a slightly negative temperature dependence. In the present work we undertook to investigate experimentally the predictions of these theories in reactions such as:

$$N_2H^+ + CH_4 \longrightarrow CH_5^+ + N_2 \qquad (I.4)$$

and

$$N_2H^+ + CH_3CHO \longrightarrow CH_3CHOH^+ + N_2 \qquad (I.5)$$

Ion-molecule association reactions are known to exhibit negative temperature dependences, these are often quoted as negative activation energies. The investigation of such reactions over wide ranges of temperature offers the possibility of establishing the true functional form of the temperature dependence of the rate constants for such reactions. Such investigations can be carried out down to low temperature ($\leq 100^\circ K$) in

the clustering reactions of $CO^{+\cdot}$, HCO^{+}, $N_2^{+\cdot}$ and N_2H^{+}, since CO and N_2 condense only at very low temperatures. Moreover, the fact that some of the above ions are radical and some are even-electron species offers the possibility to investigate the kinetic and thermodynamic effects of the presence of unpaired electrons on clustering reactions.

Another aspect of the effect of molecular structure on the rates of clustering reactions is the effect of molecular complexity on the rates. Both the temperature and structural effects on ion-molecule association reactions are expected to be due to the effects of these variables on the back-dissociation of the excited reaction complexes. This expectation is based on the energy-transfer mechanism which is also verified in this work. The effects of the temperature and of the molecular complexity are investigated experimentally in clusering reactions of NH_4^{+}, $CH_3NH_3^{+}$ and $(CH_3)_2NH^{+}$. These effects are also interpreted theoretically on the basis of the RRK coupled quantum harmonic oscillator model.

Studies of ion-molecular association reactions were also extended to the case of a reaction system of some biological and pre-biological interest, namely the clustering and solvation of protonated amino acids.

The present thesis reports the studies of these aspects of ion-molecule reactions, and discusses the implications of the results of these studies for the understanding of this class of natural phenomena.

REFERENCES

1. V.L. Tal'Roze and E. Lyubimova, Doklady, Akad. Nauk. SSR, 86, 909, (1952).
2. D.P. Stevenson and D.W. Schlisser, J. Chem. Phys., 23, 1353 (1955).
3. F.H. Field, J.L. Franklin and F.W. Lampe, J. Amer. Chem. Soc., 79, 2419 (1957).
4. F.H. Field, J. Amer. Chem. Soc., 83, 1523 (1961).
5. F.H. Field, J. Amer. Chem. Soc., 91, 2827 (1969).
6. P. Kebarle and A.M. Hogg, J. Chem. Phys., 42, 780 (1965).
7. G. Gioumousis and D.P. Stevenson, J. Chem. Phys., 29, 294 (1958).
8. T. Su and M.T. Bowers, Int. J. Mass Spectrom and Ion Phys., 12, 347 (1973).
9. A. Good, Trans. Faraday. Soc., 67, 3495 (1971).
10. P. Kebarle, in "Ion-Molecule Reactions," J.L. Franklin, ed., Plenum Press, New York, 1972, pp.315 ff.

II. EXPERIMENTAL:

THE TECHNIQUE OF PULSED, TIME-RESOLVED HIGH-PRESSURE MASS SPECTROMETRY

All the studies reported in this thesis were carried out on the Rockefeller University (formerly Esso) Chemical Physics Mass Spectrometer. The ion source in this instrument, which can be both cooled and heated, was described in detail by Beggs and Field.[1]

In the conventional, continuous mode operation of the mass spectrometric source an electron beam is continuously producing ions in the ion source. The ions produced in reactions in the source drift through in the source, leave through the ion exit slit and are continuously collected on an ion multiplier after mass analysis. In this mode of operation reaction times must be calculated from ion mobilities and the measured physical conditions in the ion source, such as the pressure, temperature and electric field strengths, and are subject to the uncertainties involved in such calculations.

The measurement of absolute rate constants usually requires an accurate knowledge of the reaction times. In systems where the inverse reactions may be significant and equilibria may be established, it is important to verify the establishment of equilibria by the establishment of a constant value for the observed equilibrium constant after sufficient reaction time has elapsed to achieve equilibrium. For these reasons, it is important that the composition of the reacting ion mixture will be subject to direct measurement as a function of reaction time. This objective can be obtained by the technique of pulsed, time-resolved mass spectrometry. Several methods of pulsed mass spectrometry were developed in recent years.[2-5]

A schematic illustration of the ion source used and voltages and pulse sequence typically applied in the studies reported in this thesis is shown in Fig. II.1. (All the potentials, pulse width and delay times

FIGURE II.1.

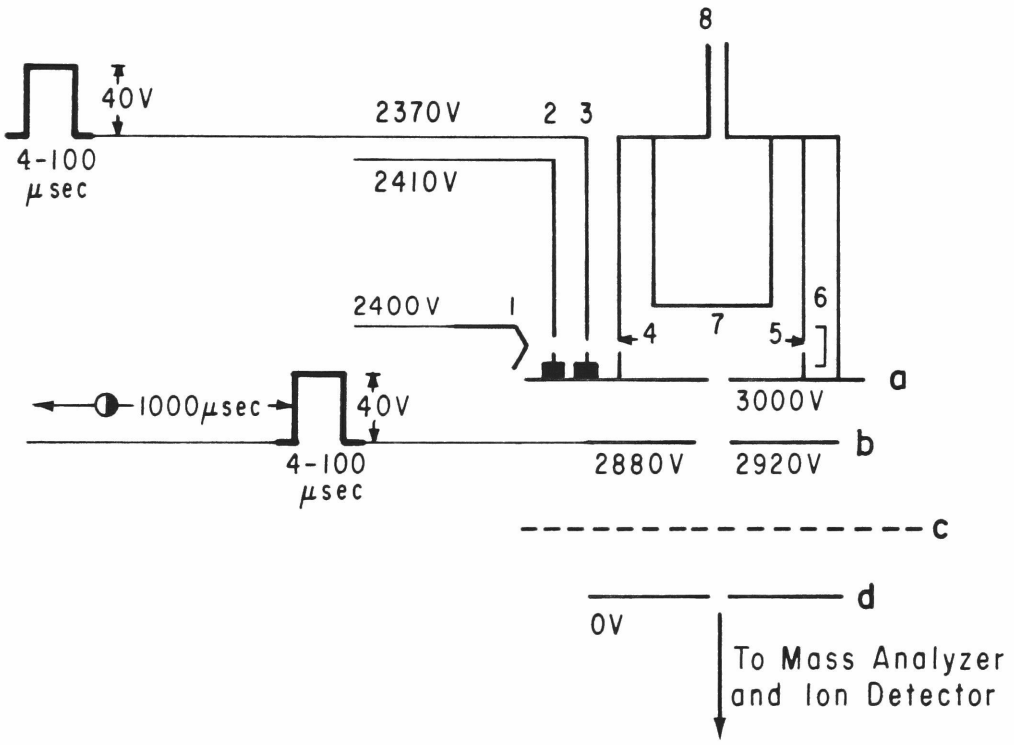

Schematic diagram of mass spectrometer ion source and potentials and pulse sequence applied in typical pulsed experiment. (1) filament; (2) electron drawout electrode; (3) gate electrode; (4) electron entrance slit; (5) electron exit slit; (6) electron collector; (7) ion repeller; (8) gas inlet, (a) ion exit electrode; (b) ion focus electrodes (c) 200 l./in. screen at focus elecgrode potential; (d) analyzer entrance slit. Slits (4) and (5) are at source block potential. In an alternative mode of operation, electrode (3) is at 3000 V, electrode (2) is at 2380 V and the 40 V pulse is applied to electrode (2) instead of (3).

shown are subject to some variation as required by experimental conditions.) A general schematic representation of the information flow in the system is shown in Fig. II.2.

The pulsed mode applied in the present studies is based on the production of the primary ions by a bombarding electron beam of known duration, and the focusing of the ions that leave the ion source into the ion detector by a voltage pulse applied to the focus electrode, a known and variable delay time after the initial electron beam.

As shown in Fig. II.1, the entire ion source block is maintained at +3000V with respect to ground potential. The electron gun filament is maintained at -600V with respect to the block, such that the bombarding electrons have an energy of 600 eV. In the pulsed mode, the electrons are retarded by a potential of -30 - -40 V with respect to the filament, applied to the gate electrode (electrode 3, Fig. II.1) or to the drawout electrode (electrode 2, Fig. II.1). The electrons are allowed to pass in into the reaction chamber only when a pulse of $\simeq$+40 V of variable duration (5 - 100 μsec.) is applied to the gate (or drawout, appropriately) electrode. Pulsing of the gate electrode was used in most of the studies. However, later it was found that pulsing the drawout electrode improves the signal yield and permits measurements at longer reaction times than with the pulsed gate electrode method.

The ions issuing from the source through the exit slit after the application of the electron beam pulse are defocussed by the application of the appropriate potentials to the focusing grids. After a known and variable delay time (usually between 10 to 1000 μsec. in these studies) after the application of the electron beam, a pulse of known duration is applied to one of the focusing grids. The height of the pulse is experimentally adjusted so that maximum focusing is obtained during the duration of this focusing pulse. In practice, a focusing pulse of constant height is used, and the potential difference between the focusing grids is adjusted to yield maximum focusing when the pulse is applied. In

FIGURE II.2

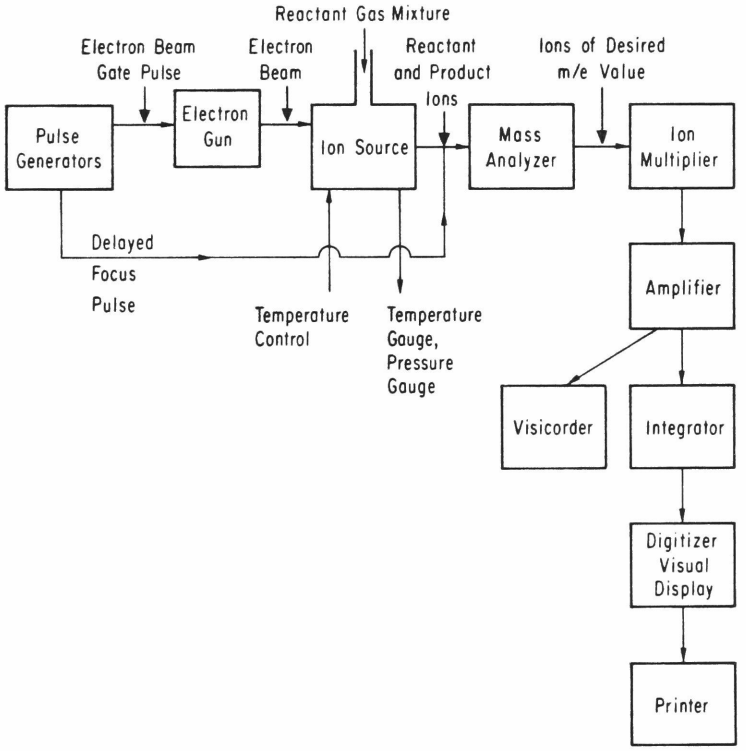

Schematic illustration of the overall information flow in the pulsed spectrometer system.

this manner, the intensity of the ion beam leaving the ion source and corresponding to the m/e value as determined by the setting of the mass analyzer, is mentioned as a function of the reaction time.

If operation of the mass spectrometer in the conventional continuous mode is desired, the gate electrode may be set at block potential and the potentials of the two focus plates set at values that maximize the continuous signal. Conversion between the two modes of operation requires about 1 - 2 minutes.

For the sake of the completeness of description, a schematic diagram of the pulse circuitry is also included in this thesis (Fig. II.3). The design and construction of this circuitry was largely due to the efforts of Dr. T.-Y. Yu; the drawing was done by Mr. A. Viscomi.

Initially, pulsed experiments were performed by adjusting the pulse widths and delay times at the desired values, and scanning through the desired range of m/e values to obtain the intensity of each peak after the desired length of reaction time. This method is applicable to intense peaks, but in the case of less intensity signals, individual pulses of signal, probably corresponding to individual ions, appear. In order to overcome problems caused by this phenomenon, and to increase sensitivity, integration of the output signal was required. In the integrating technique, after the desired values of pulse widths and delay time are set, the mass analyzer is adjusted to the center of the peak whose intensity is to be measured. The output from the ion multiplier (Bendix Model 4700 electron multiplier) and amplifier (Keithly Model 427 current amplifier) is introduced into a simple integrator unit (ZEOLITE ZA 801 M INTEGRATOR) and is integrated for a known length of time, usually 10 - 30 sec. The integrator curcuitry was also constructed by Dr. T.-Y. Yu.

The features, problems and techniques concerning the pulsed ion production detection technique call for several comments:

(i) The application of the pulse technique decreases the overall

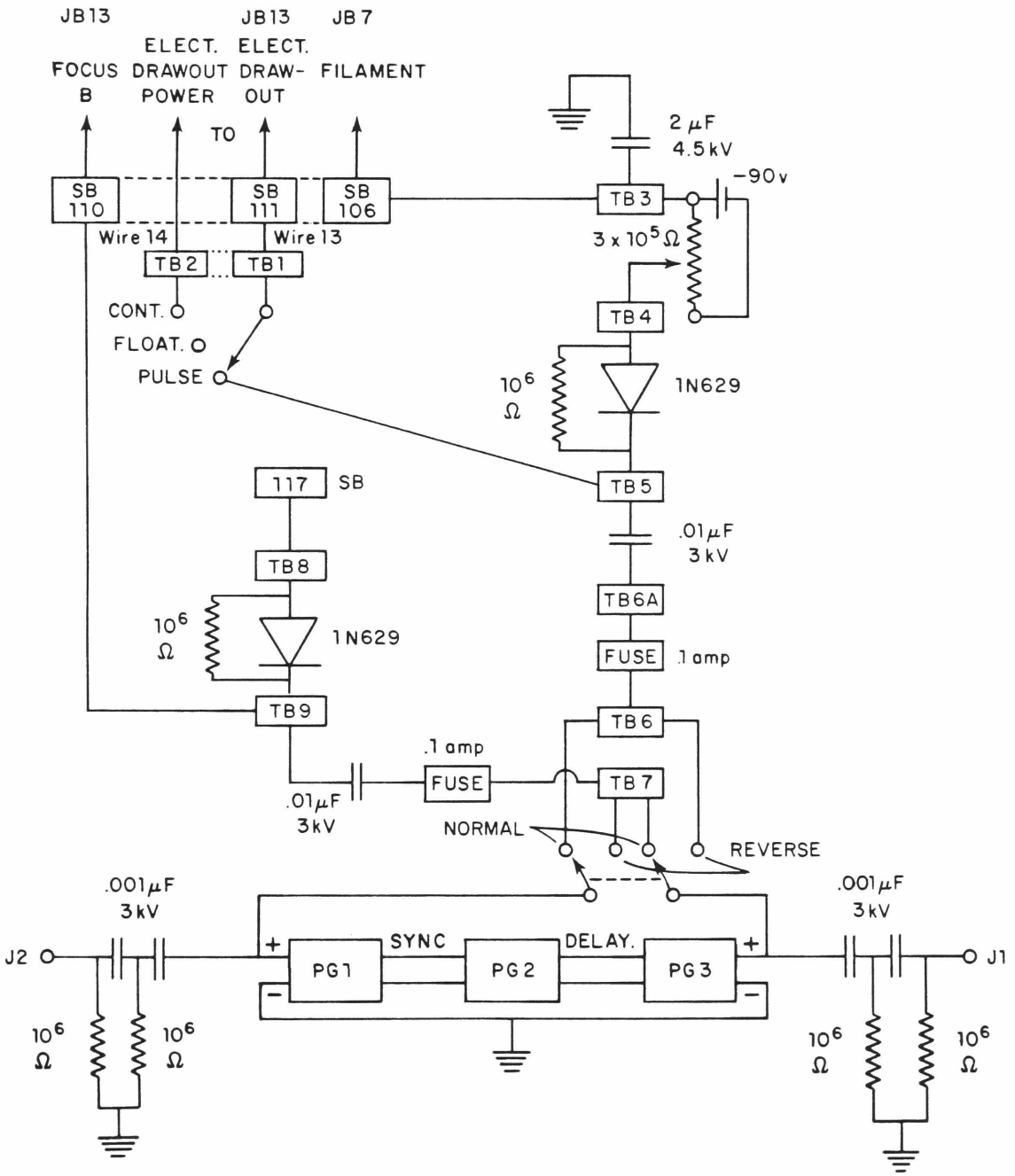
JB13
FOCUS B
JB13
ELECT. DRAWOUT POWER
ELECT. DRAW- OUT
JB7
FILAMENT
TO
SB 110
SB 111
SB 106
Wire 14
Wire 13
TB2
TB1
CONT.
FLOAT.
PULSE
2 μF 4.5kV
-90v
TB3
3 x 10^5 Ω
TB4
10^6 Ω
1N629
TB5
117 SB
TB8
10^6 Ω
1N629
TB9
.01μF 3kV
TB6A
FUSE .1amp
TB6
.1 amp
FUSE
TB7
.01μF 3kV
NORMAL
REVERSE
.001μF 3kV
.001μF 3kV
J2
J1
+
SYNC
DELAY.
+
PG1
PG2
PG3
−
−
10^6 Ω
10^6 Ω
10^6 Ω
10^6 Ω

Legend for Figure II.3 - Schematic diagram of the pulse generator pulse divider circuitry. The junction numbers shown correspond to junction labeling on the schematics of the mass spectrometer. The units PG 1, PG 2 and PG 3 are General Radio Model 1217-C pulse generators. In an alternative mode of operation (see footnote to Fig. II.1, and text) replace "gate" on this diagram by "drawout" and "JB 13" by "JB 12". JB in this diagram means Junction Box; SB Strip Terminal Board in junction cabinet; TB-Terminal Board in pulse equipment cabinet; J-Junction for oscilloscope.

sensitivity by a large factor as compared with the continuous mode. For example, if 10 μsec. wide electron beam and 10 μsec. wide focusing beam are used and the pulse sequence is repeated each 200 μsec. ions are produced only 5% of the total time and collected only 5% of the total time, i.e., total collected on yield is decreased by a factor of 20 x 20 = 400 as compared with the continuous method. To overcome this difficulty, a high voltage was applied to the ion multiplier to increase its gain, and signal integration was applied as described above.

(ii) The intensity of the ion current was found to decrease significantly with increasing delay time after the ionizing electron beam. The decrease becomes faster at high temperatures and at low pressures, i.e., when ion mobility is increased. In fact, the maximum ion yield was found usually at 0 - 10 μsec. delay times, indicating that initial ionization takes place over the entire source possibly due to the scattering of the bombarding electron beam. The ion loss processes cause decreased sensitivity at longer delay times and limits the use of the technique usually to delay times of less than 500 μsec., and sometimes as short as 50-100 μsec. Sensitivity may be somewhat increased at longer delay times by applying longer ionizing and focusing pulse widths. However, it is desirable to keep pulse widths as narrow as possible, since the finite pulse widths introduce indeterminacies into the time measurement.

Towards the completion of this work it was found that the alternative pulsing technique described earlier leads to higher ion yields, and gives better stopping of the electrons when the pulse is not applied. It appears that the larger ion yield results from the passage of more electrons into the source when this mode is applied. The effect of these improvements is that in this mode ions may be detected up to 1000 - 1500 μsec. delay times.

(iii) In our experiments we found that no repeller field was necessary to extract ions from the source. All pulsed experiments were conducted in field free conditions in the source, i.e., no magnetic or

electric fields were applied in the source during the course of the reactions. This condition is very important, since the application of fields in the source can introduce nonthermal contributions to the energies of the ions.

(iv) The application of the integrated signal technique requires that the peaks corresponding to ions of the given m/e being measured be at their maximum intensity during the integration period (10-30 sec.). Fortunately, the stability of the mass analyzer was found sufficient to fulfill this requirement, and usually several measurements on the same peak (at several delay times) could be carried out before refocusing of the mass analyzer was required.

In summary, the pulse technique described yields the advantage of explicit time resolution, which is essential for the reliable and accurate determination of rate and equilibrium constants for ionic reactions in a mass spectrometer. Mor sophisticated methods, especially the use of multichannel analyzers, can improve the sensitivity of the technique and the efficiency of data acquisition. However, the technique as described represents a relatively easy inexpensive ($\approx$ \$1,000) method to obtain quantitative physico-chemical data on reactions of gaseous ions.

To ensure the accuracy and reproducibility of the experimental results, as a general rule, each measurement was carried out at least twice. When pressure or temperature studies required an extensive amount of rate or equilibrium constant determinations, not every point was measured in duplicate, but at lease one in every five experimental points was duplicated. Also, in the cases where gaseous mixtures prepared in the laboratory were used, each mixture was prepared at lease in duplicate to assure reproducibility. The slopes of all van't Hoff and Arrhenius plots taken from the data were obtained by the least squares method.

Experimental details specific to each investigation will be given in the appropriate sections.

REFERENCES

1. D.P. Beggs and F.H. Field, J. Amer. Chem. Soc., 93, 1567 (1971).
2. V.L. Tal'Roze and A. K. Lyubimova, Dokl. Akad. Nauk. SSR, 86, 909 (1952).
3. T.W. Shannon, F. Meyer and A.G. Harrison, Can. J. Chem., 43, 159 (1964).
4. K. Birkinshaw, A.J. Masson, D. Hyatt, L. Matus, I. Opauszky and M.J. Henchman, Advances in Mass Spectrom., 4, 379 (1968).
5. D.A. Durden, P. Kebarle and A. Good, J. Chem. Phys., 50, 805 (1969).

III. TRANSFER REACTIONS

III.1. KINETICS, EQUILIBRIUM, AND NEGATIVE TEMPERATURE DEPENDENCE IN THE BIMOLECULAR REACTION $t\text{-}C_4H_9^+(i\text{-}C_5H_{12}, i\text{-}C_4H_{10})t\text{-}C_5H_{11}^+$ BETWEEN 190-570°K*

Introduction

The thermodynamics of the hydride-transfer equilibria occurring in the $t\text{-}C_4H_9^+(i\text{-}C_5H_{12}, i\text{-}C_4H_{10})t\text{-}C_5H_{11}^+$ system between 323-548°K was previously investigated in this laboratory[1] by high pressure mass spectrometry applied in the continuous mode of ion production and extraction. The kinetics of the hydride transfer reactions of t-butyl ion with 22 C_5-C_8 alkanes at 298°K was studied by Ausloos and Lias[2] using the technique of radiation chemistry. They found the rates of these reactions to be uncharacteristically slow for exothermic ion-molecule reactions, with rate constants generally between 10^{-10} - 10^{-11} cc/mol-sec., although hydride abstraction is the only reaction channel. An activation energy ($\lesssim$ 3.5 kcal/mole) inversely related to the exothermicity of the reaction was postulated.

In the present study, the temperature dependence of the equilibrium constant and the kinetics of the approach to equilibrium for the reversible reaction

$$t\text{-}C_4H_9^+ + i\text{-}C_5H_{12} \underset{k_r}{\overset{k_f}{\rightleftharpoons}} t\text{-}C_5H_{11}^+ + i\text{-}C_4H_{10} \qquad \text{(III.1.1)}$$

was investigated by means of pulsed high pressure mass spectrometry. This was undertaken in order to gain further insight into the kinetics of these slow ion-molecule reactions. In addition, we wanted to verify the previous continuous equilibrium measurements and to check if there were any discrepancies between the continuous and pulsed equilibrium techniques.

---

* The work reported in this section was performed in collaboration with Dr. J.J. Solomon: J.J. Solomon, M. Meot-Ner and F.H. Field, J. Amer. Chem. Soc., 96, 3727 (1974).

Experimental

Matheson Instrument grade (99.5%) isobutane and Matheson Coleman and Bell Spectroquality grade (99+mol %) isopentane were used. Gas mixtures of known composition of $i\text{-}C_4H_{10}/i\text{-}C_5H_{12}$ were prepared in 5 liter storage bulbs and were flowed directly into the ion source. Intensities of the t-butyl (m/e = 57) and t-pentyl (m/e = 71) ions were monitored at variable delay times at constant temperatures and pressures. The total source pressure was varied between 0.4 and 1.5 torr and for most experiments was adjusted to keep the total number density at about 1.7×10^{16} mol/cm.^{3}.

Results

A. Thermodynamics

The equilibrium constant for reaction (III.1.1) is given by:

$$K = \frac{(t\text{-}C_5H_{11}^+)(i\text{-}C_4H_{10})}{(t\text{-}C_4H_9^+)(i\text{-}C_5H_{12})} = \left(\frac{I_{71}}{I_{57}}\right)_{EQ} \times \frac{P_{i\text{-}C_4H_{10}}}{P_{i\text{-}C_5H_{12}}} \qquad \text{(III.1.2)}$$

The approach to equilibrium was examined by measuring the ion intensity ratio I_{71}/I_{57} as a function of reaction time. A sample plot of the apparent equilibrium constant, $K_a = (I_{71}/I_{57}) \times \frac{P_{i\text{-}C_4H_{10}}}{P_{i\text{-}C_5H_{12}}}$, vs. reaction time at constant temperature and pressure is shown in Fig. III.1.1. The achievement of equilibrium is observed above 100 μsec. where K_a becomes time independent. In Fig. III.1.1 we see that K_a does not go through the origin. If we make the reasonable assumption that the cross section for the initial formation of the $(M\text{-}1)^+$ ion in isobutane and isopentane are equal, then at t=0 we should expect an apparent equilibrium constant of unity ($I_{71}^o/I_{57}^o \propto \frac{P_{i\text{-}C_5H_{12}}}{P_{i\text{-}C_4H_{10}}}$ and therefore $K_a^o = \frac{I_{71}^o}{I_{57}^o} \times \frac{P_{i\text{-}C_4H_{10}}}{P_{i\text{-}C_5H_{12}}} = 1$). Plots analogous to Fig. III.1.1 were obtained for several temperatures between 328 - 570°K. The temperature dependence of the equilibrium constant is

FIGURE III.1.1

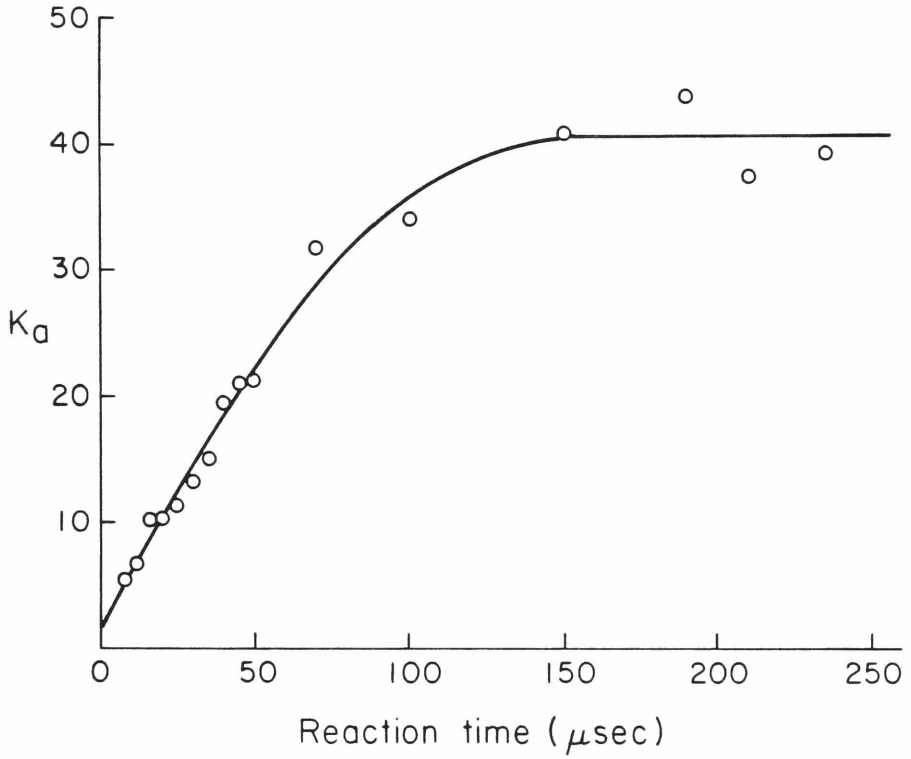

The apparent equilibrium constant vs. reaction time for reaction III.1.1
$T = 328^{\circ}K$, $P = 0.6$ torr, $P_{i\text{-}C_4H_{10}}/P_{i\text{-}C_5H_{12}} = 10.02$.

given in Fig. III.1.2. The solid line is obtained from a least squares analysis of the pulsed experimental points. The dotted line was obtained from the previous continuous high pressure equilibrium measurements on this system. The agreement between the van't Hoff plots obtained by the continuous and pulse techniques is excellent. The thermodynamic quantities obtained from the pulse experiments are ΔG^{o}_{300} = -2.5 kcal/mole, ΔH^{o} = -3.3 kcal/mole and ΔS^{o}_{300} = -2.7 eu.

B. Kinetics

A general bimolecular ion-molecule transfer reaction can be written as

$$A^+ + BX \underset{k_r}{\overset{k_f}{\rightleftharpoons}} B^+ + AX \qquad \text{(III.1.3)}$$

where k_f and k_r are the forward and reverse reaction rate constants. The equilibrium expression for reaction (III.1.3) is given by

$$K = k_f/k_r = (B^+/A^+)(AX/BX) \qquad \text{(III.1.4)}$$

Under typical pressure mass spectrometric conditions the neutral concentrations are much larger than the ionic concentrations; therefore reaction (III.1.3) can be treated as a system of opposing pseudo first-order reactions. Reaction (III.1.3) can now be rewritten as

$$A^+ \underset{k_{-1}}{\overset{k_1}{\rightleftharpoons}} B^+ \qquad \text{(III.1.5)}$$

where

$$k_1 = k_f\,(BX),\quad k_{-1} = k_r\,(AX) \qquad \text{(III.1.6)}$$

are the pseudo-first order forward and reverse rate constants, respectively. Following Benson's[4] treatment for opposing first order reactions we obtain the integrated rate expression:

$$\ln(A^+ \cdot K' - B^+) = \ln(A_o^+ \cdot K' - B_o^+) - (k_1 + k_{-1})t \qquad \text{(III.1.7)}$$

where A^+ and B^+ are the instantaneous concentrations of A^+ and B^+, A_o^+ and B_o^+ are the initial concentrations (at t = 0) of A^+ and B^+, and

FIGURE III.1.2

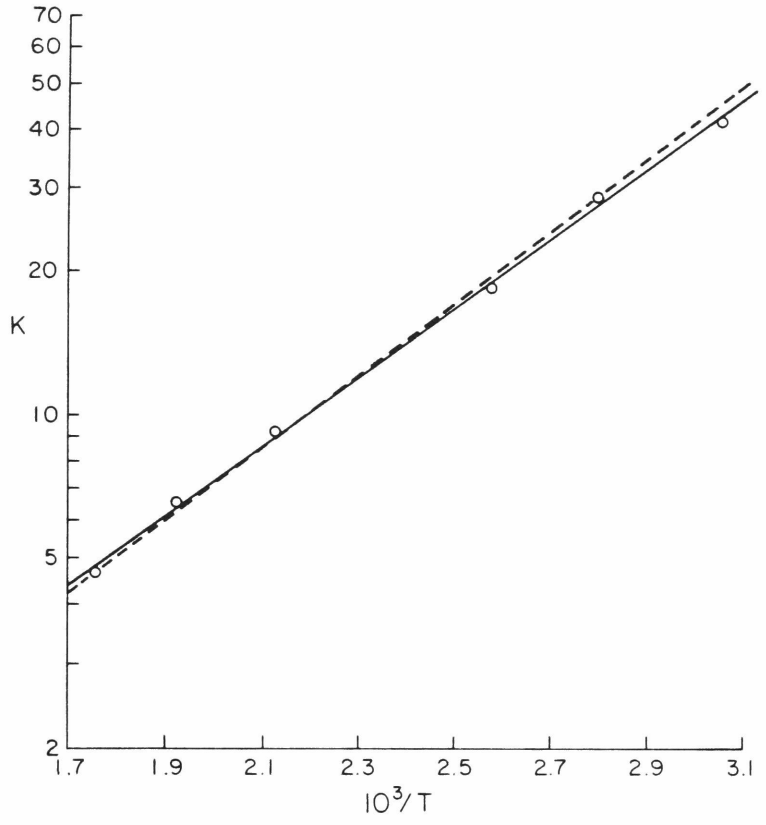

Comparison of van't Hoff plots: (——) pulse technique; (---) continuous technique.

$$K' = k_1/k_{-1} = (B^+/A^+)_{EQ} \qquad \text{(III.1.8)}$$

is the equilibrium ion ratio.

When $k_1 \gg k_{-1}$ or $k_{-1} \gg k_1$ we can neglect the slower reaction and equation (III.1.7) reduces to the rate expression for a simple first-order reaction. When this simplification cannot be made we must first measure K' and then applying equation (III.1.7). A plot of ln $(A^+ \cdot K' - B^+)$ vs. time yields a straight line whose slope is $-(k_1 + k_{-1})$. Combining this result with equation III.1.8 permits the calculation of k_1 and k_{-1}, and subsequently using equation (III.1.6) we can obtain k_f and k_r, the true bimolecular reaction rate constants.

A plot of ln $[I_{57}/(I_{57} + I_{71}) \times (I_{71}/I_{57})_{EQ} - I_{71}/(I_{57} + I_{71})]$ vs. reaction time is shown in Fig. III.1.3 where $I_{57}/(I_{57} + I_{71})$ and $I_{71}/(I_{57} + I_{71})$ are the normalized time dependent intensities of t-$C_4H_9^+$ and t-$C_5H_{11}^+$ ions, respectively, and $(I_{71}/I_{57})_{EQ}$ is the equilibrium ion intensity ratio (K') obtained from the time independent regime of K_a in plots such as Fig. III.1.1. We can calculate k_1 and k_{-1} from the slope $(= -(k_1 + k_{-1}))$ of the straight line in Fig. III.1.1 and from K' $(=k_1/k_{-1})$. In these experiments, the source temperature and pressure were kept constant, and therefore from the known neutral mixture ratio (i-C_4H_{10}/i-C_5H_{12}) we calculate the number densities of isopentane (N_P) and isobutane (N_B). Using equation (III.1.6) with $BX = N_P$ and $AX = N_B$, we calculate the forward and reverse bimolecular reaction constants for reaction (III.1.1).

The temperature dependence of k_f and k_r was determined by following the kinetics of the approach to equilibrium as described above for several temperatures. The results are presented in Table III.1.1. Included is the forward rate constant determined by Ausloos and Lias[5] at $T = 298^oK$ using t-butyl ions generated in the γ irradiation of neopentane. They measured this rate constant using the technique of end product analysis in deuterium labeled mixtures. Good agreement is found in the absolute reaction rate constant although very different experimental techniques were used.

FIGURE III.1.3

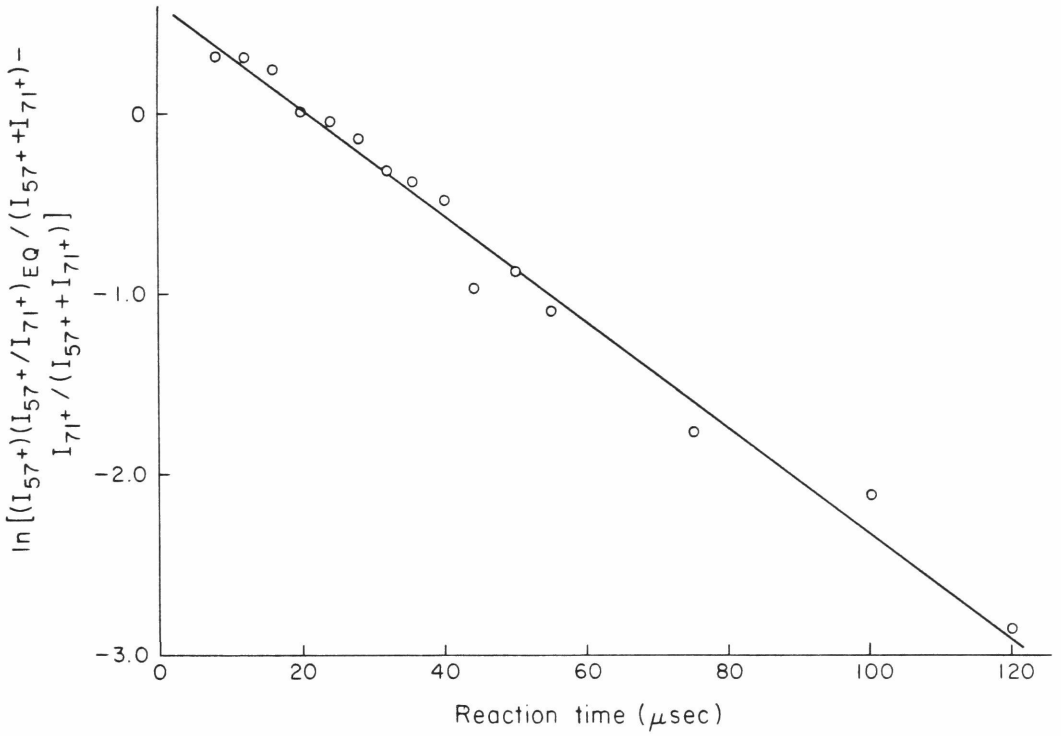

Determination of the (pseudo) first-order rate constants for reaction (1), slope = $-(k_1 + k_{-1})$: T = 358°K, P = 0.7 torr, $P_{i\text{-}C_4H_{10}}/P_{i\text{-}C_5H_{12}}$ = 10.02.

TABLE III.1.1

Experimental Temperature Dependence
of Biomolecular Reaction Rate Constants

T (^{o}K)	P_{TOTAL} (torr)	$N_B x10^{-16}$ (mol/cm.^{3})	$N_P x10^{-16}$ (mol/cm.^{3})	k	$k_f x10^{12}$ (cc/mol-sec.)	$k_r x10^{12}$ (cc/mol-sec.)
190	0.41	1.48	0.61	1763	52.1	0.03
262	0.47	1.23	0.51	155	27.5	0.18
298					25.0[a]	
328	0.59	1.58	0.16	41.5	15.6	0.38
358	0.70	1.72	0.17	28.7	12.7	0.44
385	0.54	0.88	0.48	18.6	8.5	0.46
388	1.49	2.63	1.09	19.1	7.8	0.41
389	1.18	1.91	1.03	18.6	7.3	0.39
470	0.82	1.19	0.49	9.2	3.6	0.39
520	0.91	1.20	0.50	6.5	4.0	0.61
570	1.04	1.25	0.52	4.7	2.3	0.50

a. Reference 5.

At the two lowest temperatures in the kinetic study the equilibrium constant K and hence K' were determined by extrapolating the least squares line of the van't Hoff plot to the desired temperature. This was done to overcome the experimental difficulty of measuring very large equilibrium constants. Uncertainty in the extrapolated value for K at low temperatures should not seriously effect the determination of k_1 and k_f, because as indicated in the general kinetic analysis, the values obtained for these quantities become largely independent of K' when it is large (i.e., $k_1 \gg k_{-1}$). However, the accuracy of k_{-1} and k_r are affected through the equilibrium constant relationship, equation (III.1.8).

As mentioned earlier, the finite pulse widths introduce an uncertainty in the assignment of the reaction time. This error is small.

When the pulse widths are negligible compared to the delay time. The error becomes potentially more significant when the kinetic study is restricted to a short reaction time. This was the case in our experiments at low temperature, when the rate of the forward reaction is fast, and the ion ratio, I_{71}/I_{57}, exceeds the dynamic range of the mass spectrometer after a short reaction time. The kinetic studies were also limited to a short reaction time when equilibrium is reached quickly because of the high total number density of the reactants. In our studies at the highest total number densities the equilibrium was achieved at $\approx$ 50 μsec.

We estimate the uncertainty in the tabulated rate constants given in Table III.1.1 to be 10 - 20% due to the inaccuracy in assigned reaction times. It is worth noting that since the ion intensity ratio is time invariant after the attainment of equilibrium, the accuracy of measured equilibrium constants is unaffected by any uncertainty in the estimated reaction time.

Another conceivable source of error in the rate constant determination is the possibility of alternate reaction channels. This was investigated, specifically the possibility of dimer formation. Stabilized addition complexes $(C_5H_{11}\cdot C_4H_{10})^+$, $(C_4H_9\cdot C_4H_{10})^+$, etc. were found to contribute

less than 1% of the total ionization even at the lowest temperatures employed in this study.

A large negative temperature coefficient for the forward reaction rate constant k_f is clearly evident in the data of Table III.1.1. Because of the prevalence of negative temperature coefficients in three body reactions,[6-12] the kinetic order of reaction (III.1.1) was investigated. This was done by changing the total pressure by a factor of three at constant temperature ($\sim 387^{\circ}K$). The bimolecular rate constants k_f and k_r obtained in these experiments were independent of pressure (see Table III.1.1).

Discussion

A novel aspect of the results is the finding (Table III.1.1) of a negative temperature coefficient for the rate of the forward component of reaction (III.1.1). The temperature dependence of bimolecular ion-molecule reactions involving the transfer of massive particles in reactions with very small or zero activation energies has not been investigated or observed previously, especially for reactions involving species of the degree of complexity of the reactants investigated in this study. However, a small number of bimolecular ion-molecule electron transfer reactions exhibiting a negative temperature dependence have been reported previously.[13-17] In all of the reported cases reactions between a monatomic and diatomic or between two diatomic species were involved, and the negative temperature dependence was relatively small (approximately $T^{-1/2}$).

The detailed mechanism of the forward processes in reaction (III.1.1) may be written as

$$t\text{-}C_4H_9^+ + i\text{-}C_5H_{12} \underset{k_d}{\overset{k_c}{\rightleftharpoons}} [(CH_3)_3C\text{---}H\text{-}C(CH_3)_2C_2H_5]^{+*} \xrightarrow{k_e} t\text{-}C_5H_{11}^+ + i\text{-}C_4H_{10} \cdot \qquad \text{(III.1.9a)}$$

In generalized notation the reaction is

$$A^+ + BH \underset{k_d}{\overset{k_c}{\rightleftharpoons}} (BHA^+)^* \xrightarrow{k_e} \text{Products} \qquad \text{(III.1.9b)}$$

Here $(BHA^+)^*$ is the energized collision complex formed in the ion-molecule collision of A^+ and BH, and k_e is the rate constant for the decomposition of $(BHA^+)^*$ to the products via an activated transition complex in which the proper amount of energy is concentrated in the reaction corrdinates.

It has been suggested[18-19] that such reactions may be treated in an approximate way using an expression for the rate of reaction of a complex consisting of s coupled oscillators. The applicability of this treatment to our reaction is discussed in Section V. We shall now apply the Eyring transition state theory to the forward process in reaction (III.1.1).

In most gas phase reactions the effect of pre-exponential terms on the temperature coefficient is masked by the much stronger influence of the activation energy. As was shown by Gershinowitz and Eyring[20] in their treatment of termolecular reactions, however, in the absence of an activation energy the temperature dependence of the partition functions can result in a substantial negative temperature dependence of the reaction rate.

Using transition state theory, the rate constant for the forward component of reaction (III.1.1) may be written as

$$k_f = C \frac{Q^*_{tr}\, Q^{\ddagger}_{rot}\, Q^{\ddagger}_{vib}\, Q^{\ddagger}_{el}}{(Q_{tr}\, Q_{rot}\, Q_{vib}\, Q_{el})_{i\text{-}C_4H_9} + (Q_{tr}\, Q_{rot}\, Q_{vib}\, Q_{el})_{i\text{-}C_5H_{12}}} \frac{kT}{h} e^{-E_a/RT} \qquad \text{(III.1.11)}$$

Here C is the transmission coefficient and Q's are the appropriate partition functions for the activated complex and reactants. The temperature dependence of the vibration and electronic partition functions may be assumed to be sufficiently small to be neglected. The partition function of the internal roatations that remain unchanged upon the formation of the transition complex cancel out in equation (III.1.11). Separating all the temperature independent terms in equation (III.1.11) and labeling the origins of the temperature dependent terms, equation III.1.11 may be

written as

$$k_f = \alpha C \frac{kT}{h} e^{-E_a/RT} \frac{(T^{\frac{3}{2}})_{tr} \; (T^{\frac{3}{2}})_{rot}}{(T^{\frac{3}{2}})_{tr}^{t\text{-}C_4H_9^+} \; (T^{\frac{3}{2}})_{tr}^{i\text{-}C_5H_{12}} \; (T^{\frac{3}{2}})_{rot}^{t\text{-}C_4H_9^+} \; (T^{\frac{3}{2}})_{rot}^{i\text{-}C_5H_{12}} \; (T^{\frac{r}{2}})_{int.rot.}}$$

$$= \frac{\alpha Ck}{h} \left(T^{-(2 + \frac{r}{2})} \right) e^{-E_a/RT} \qquad \text{(III.1.12)}$$

where r is the number of internal rotations that are converted to torsional oscillations in the transition complex. For simplicity it is assumed here that these torsional oscillations are of high enough frequency that they will not contribute a significant temperature dependence to the transition complex, and thus no terms corresponding to these oscillators appear explicitly in equation (III.1.12). If this assumption about the torsional oscillators frequencies is not valid, temperature terms approaching a linear T dependence will appear in equation (III.1.12) for each low frequency oscillator.

The linearity exhibited by the plot of ln k_f vs. ln T in Fig. III.1.4 constitutes evidence that the sxponential term in equation III.1.12 is not operative, presumably because E = 0.* Then the negative temperature dependence of the forward rate constant results from the transformation of rotational and translational degrees of freedom in the reactants to vi-

---

* We wish to note that E_a in equation III.1.11 and III.1.12 includes the additional zero point energy of the vibrations created upon the formation of the transition complex. In principle this term could introduce a positive activation energy for the formation of the complex and, consequently, for the rate constant of the transfer process. However, it is likely that any such term is more than counterbalanced by the energy released upon the formation of the ion-molecule association complex so that experimentally one finds $E_a = 0$.

FIGURE III.1.4

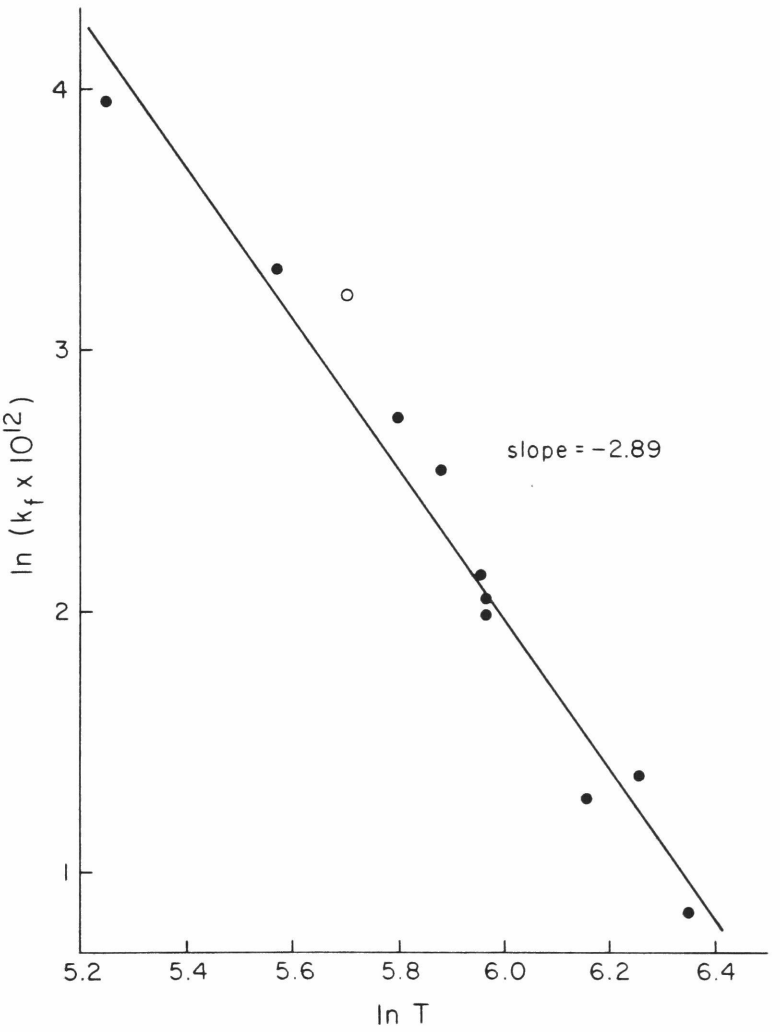

Temperature dependence of k_f. Solid circiles present data from pulse experiments; open circle taken from reference 5.

brational degrees of freedom in the transition complex. Examination of space filling models of the transition complex $(CH_3)_3C\cdots H\cdots C(CH_3)_2C_2H_5^+$ shows that up to six internal rotational modes may become hindered upon the formation of a tightly bound complex. Our result of $\frac{d \ln k_f}{d \ln T} \approx -3$ taken in conjunction with equation (III.1.12) suggests that only two internal rotations are lost upon the formation of the actual activated complex in the present reaction.

Although the linearity of the plot of $\ln k_f$ vs. $\ln T$ (Fig. III.1.4) does not suggest the presence of an activation energy, it is worthwhile to determine the extent to which an activation energy may be ruled out on the basis of the experimental data. For this purpose we used the hypothetical equations:

$$k = A' T^{-n} e^{-E_a/RT} \qquad \text{(III.1.13a)}$$

$$\ln k = \ln A' - n \ln T - E_a/RT \qquad \text{(III.1.13b)}$$

to calculate ln k as a function of T. We arbitrarily assumed the values of activation energy to be 1, 2, 3.....kcal/mole, and for each activation energy we found the value of n which gave the plot of equation (III.1.13b) most closely approximating the experimental plot of ln k vs. ln T. The results are illustrated in Fig. III.1.5 which shows that for activation energies larger than 2 kcal/mole no combination of activation energies and pre-exponential factors can yeild an acceptable curve that approximates both the slope and the linearity of the experimental plot in Fig. III.1.4. Consequently, the observed temperature dependence cannot result from a compensatory combination of a strongly temperature dependent term in the pre-exponential factor and a significant activation energy. Thus, as a conservative estimate, the presence of an activation energy larger than 2 kcal/mole may be ruled out by the experimental findings, although we think that the most reasonable interpretation of Fig. III.1.4 leads to a much smaller activation energy, namely, zero or very small. If an activation energy of 2 kcal/mole applied, the data would indicate the presence

FIGURE III.1.5

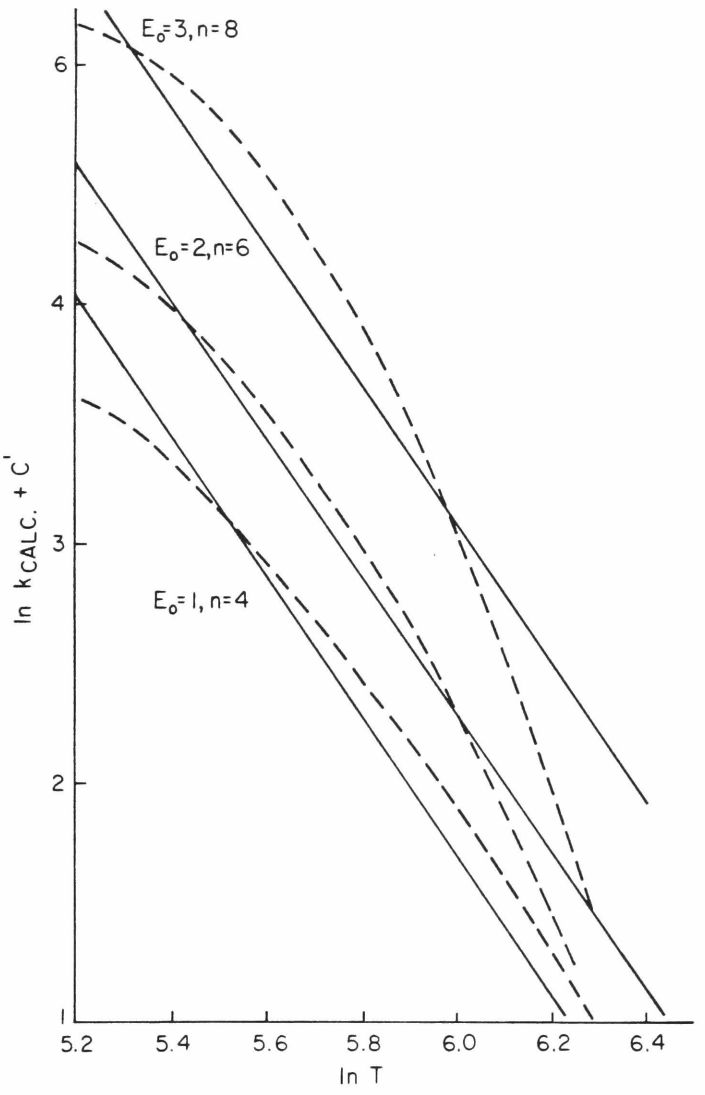

Several plots of $\ln k_{calc.} = \ln (A'T^{-n} e^{-E_a/RT}) = C' - n \ln T - E_a/RT$ vs. ln T, for the temperature range $200 \leq T \leq 600^{o}K$, for E_a = 1, 2 and 3 kcal/mole. For a given value of E_a, n is selected such that the hypothetical plot (---) will best approximate the experimental plot (——). The several pairs of lines (--- and ——) are arbitrarily separated on the drawing for the sake of clarity. The results illustrate that for hypothetical activation energies >2kcal/mole no combination of E_a and n can yield a curve that acceptably approximates both the slope and the linearity of the experimental plot.

of a T^{-6} term in the pre-exponential factor and the loss of 8 internal rotations on the formation of the association complex (from equation (III.1.12)). Thus the range of values of E_a which is compatible with our experimental data corresponds to the loss of 2 to 8 internal rotations. The maximum loss estimated from models is 6, and thus the guessed and calculated losses agree. This is encouraging, but the state of knowledge about the structures of the transition complex does not justify a more detailed speculation about it at the present time.

REFERENCES

1. J.J. Solomon and F.H. Field, J. Amer. Chem. Soc., 95, 4483 (1973).
2. P. Ausloos and S.G. Lias, ibid, 92, 5037 (1970).
3. Reference (1) Figure III.1.3.
4. S.W. Benson, "The Foundation of Chemical Kinetics," McGraw-Hill, New York, 1960.
5. P. Ausloos and S.G. Lias, "Ion-Molecule Reactions," J.L. Franklin, ed. Plenum Press, New York, 1972, Vol. 2, Chapter 16, p.729.
6. D.A. Durden, P. Kebarle and A. Good, J. Chem. Phys., 50, 805 (1969).
7. A. Good, D.A. Durden, and P. Kebarle, J. Chem. Phys., 52, 212 (1970).
8. A.J. Cunningham, J.D. Payzant, and P. Kebarle, J. Amer. Chem. Soc., 94, 7627 (1972).
9. M.A. French, L.P. Hills, and P. Kebarle, Can. J. Chem., 51, 4561 (1973).
10. A. Good, Trans. Faraday Soc., 67, 3495 (1971).
11. D.K. Bohme, D.B. Dunkin, F.C. Fehsenfeld, and E.E. Ferguson, J. Chem. Phys., 51, 863 (1969).
12. G. Porter, Disc. Faraday Soc., 33, 198 (1962).
13. N.G. Adams, D.K. Bohme, D.B. Dunkin and F.C. Fehsenfeld, J. Chem. Phys. 52, 1951 (1970).
14. D. Smith and R.A. Fouracre, Planetary Space Sci., 16, 243 (1968).
15. R. Johnsen, H.L. Brown and M.A. Biondi, J. Chem. Phys. 52, 5080 (1970).
16. E.E. Ferguson, D.K. Bohme, F.C. Fehsenfeld, and D.B. Dunkin, ibid., 50, 5039 (1969).
17. D.B. Dunkin, F.C. Fehsenfeld, A.L. Schmeltekopf and E.E. Ferguson, ibid., 49, 1365 (1968).
18. E.E. Ferguson, "Ion-Molecule Reactions," J.L. Franklin, ed., Plenum Press, New York, 1972, Vol.2, Chapter 8.
19. R. Wolfgang, Acc. Chem. Res., 3, 48 (1970).
20. H. Gershinowitz and Eyring, J. Amer. Chem. Soc., 57, 985 (1935).

III.2 THE TEMPERATURE DEPENDENCE OF SOME FAST ION-POLAR MOLECULE H^+ TRANSFER, AND OF SLOW H^- TRANSFER REACTIONS

Introduction

In the preceding study[1] of the slow bimolecular hydride-ion transfer reaction system

$$t\text{-}C_4H_9^+ + i\text{-}C_5H_{12}^+ \rightleftharpoons t\text{-}C_5H_{11}^+ + i\text{-}C_4H_{10}$$

we found that the forward, exothermic reaction proceeds significantly slower than the collision rate, and the rate constant exhibits an unprecedentedly large negative temperature dependence. The temperature dependence could be expressed as $k=AT^{-3}$ and interpreted as an entropy effect on the basis of transition state theory considerations. The question arises whether the slow rate of the reaction and its negative temperature dependence are related primarily to the nature of the particle transferred (H^-) or to special structural properties of the reactants.

As opposed to the above reaction, the majority of ion-molecule reactions involving the transfer of massive particles proceed at rates near the collision rate. The Gioumousis-Stevenson theory[2] predicts that the rates of such reactions are independent of temperature. If the reaction involves a neutral molecule with a permanent dipole moment, a small negative temperature dependence of the rate constant may be expected on the basis of the equation:

$$k = \frac{2\pi q}{\mu^{1/2}} \left[\alpha^{1/2} + c\mu_D \left(\frac{2}{\pi kT}\right)^{1/2}\right] \qquad \text{(III.2.1)}$$

Here μ is the reduced mass, μ_D the dipole moment, and α the polarizability of the neutral molecule. The locking constant c is 1 in the locked-dipole theory,[3] and a quantity related to the average orientation of the dipole in the ionic electric field according to the recently developed average dipole orientation (ADO) theory.[4] There appears to be little experimental information available on the temperature dependence of fast ion-molecule reactions.

In the present study we examined the temperature dependence of the hydride-ion transfer reaction

$$NO^+ + CH_3CHO \longrightarrow HNO + CH_3CO^+$$

This reaction involves the most simple reactants which we found suitable for an experimental study of an exothermic hydride-ion transfer reaction by our methods. We also investigated the temperature dependence of the rate constants of some fast proton-transfer reactions involving non-polar and polar neutral reactant molecules. These studies provide information on the interesting question of the nature of the reaction intermediates involved in ion-molecule transfer reactions.

In addition to the implications concerning basic reaction kinematics, the temperature dependences of ion-molecule reaction rates are also of potential significance in the chemistry of the thermally extreme planetary atmosphereic and interstellar environments.

Experimental

In the present investigations The Rockefeller University Chemical Physics Mass Spectrometer was used in the mode of pulsed, time-resolved high pressure mass spectrometry as described above. The reactions studied and the reaction mixtures used are summarized in Table III.2.1. The reactant ions of interest (N_2H^+, NO^+, t-$C_4H_9^+$, and H_3S^+) are produced by the major components of the reaction mixtures by fast reactions that go to conclusion in a few microseconds. The reactant ions then react more slowly with the minor components of the reaction mixture. The concentration of the neutral reactant of the reaction of interest in the reaction mixture and the total number densities were adjusted such that the reaction half-life was in the range of 25 - 50 μsec. The feasibility of these kinetic studies is largely dependent on the selection of appropriate reaction systems where competing transfer and association reactions of the reactant and product ions of interest with the components of the reaction mixtures and with impurities are negligible. In the present studies the ions of interest constituted at least 90% of the total ion current and the

TABLE III.2.1

Composition of Reaction Mixtures and Total Number Densities Applied in the Reaction Systems Investigated

Reaction	Composition of the Reaction Mixture	Total Number Density[a] $N \times 10^{16}$ molecules/cm.^{3}	Physical Properties of Neutral Reactant: Dipole Moment[b] μ_D (debye)	Physical Properties of Neutral Reactant: Electron Polarizability $\alpha \times 10^{24}$ cm.^{3}
$N_2H^+ + CH_4 \longrightarrow CH_5^+ + N_2$	95% N_2, 5% H_2, 0.056% CH_4	1.9	0.0	2.60[c]
$t\text{-}C_4H_9^+ + (C_2H_5)_3N \longrightarrow (C_2H_5)_3NH^+ + C_4H_8$	99.85% $i\text{-}C_4H_{10}$, 0.15% $(C_2H_5)_3N$	1.0	0.66	13.42[d]
$N_2H^+ + NH_3 \longrightarrow NH_4^+ + N_2$	95.1% N_2, 4.84% H_2, 0.064% NH_3	1.3	1.47	2.26[c]
$N_2H^+ + CH_3CHO \longrightarrow CH_3CHOH^+ + N_2$ $N_2D^+ + CH_3CHO \longrightarrow CH_3CHOD^+ + N_2$	95% N_2, 5% H_2 (or D_2) 0.048% CH_3CHD	1.3	2.69	4.56[d]
$H_3S^+ + CH_3CHO \longrightarrow CH_3CHOH^+ + H_2S$	95.8 N_2, 4.2% H_2S 0.042% CH_3CHO			
$NO^+ + CH_3CHO \longrightarrow CH_3CO^+ + HNO$	89.3% N_2, 10.5% NO, 0.2% CH_3CHO	1.0	2.69	4.56[d]

a. The total number density in each reaction system was kept constant by appropriate adjustment of the presure at the temperature of each kinetic study.

b. From "Selected Values of Electric Dipole Moment for Molecules in the Gas Phase," R.D. Nelson, D.R. Lide and A.A. Maryott, NSRDS-NBS, (1966) 10.

c. J.O. Hirschfelder, C.F. Curtiss and R.B. Bird, "Molecular Theory of Gases and Liquids," John Wiley and Sons, New York, 1964, p.950.

d. Calculated from the refraction index.

absence of possible competing reactions was carefully checked.

The materials used were Matheson Prepurified H_2, N_2, Chemical Purity NO, H_2S and D_2, Ultra High Purity CH_4, Anhydrous NH_3, MC&B CH_3CHO and $(C_2H_5)_3N$. In order to check the reproducibility of our mixture preparations, some rate measurements were performed on at least two separate reaction mixtures. Furthermore, duplicate determinations were made of each temperature study here reported.

The temperature range of the kinetic studies were determined by instrumental limitations or by the vapor pressures of the least volatile reaction components.

The mean free path under our experimental conditions is always at least 50 times smaller than the narrowest constriction between the source and the pressure measuring device. Thermal transpiration effects are therefore always absent in our experiments.

Errors in the rate measurements result from errors in mixture composition, the finite widths of the electron and gate pulses, and random scattering in the kinetic plots. We estimate that rate constants are measured with error limits of $\pm$ 20%. Reproducibility and relative rate constants are good to within 10%.

Since the concentrations of the ions in the reaction plasmas are many orders of magnitude smaller than the concentrations of the neutrals, all reactions exhibit pseudo-first-order kinetics. Equilibrium constants can be estimated from tabulated heats of formation of ions and neutrals, since entropy changes in the reactions of interest are small. From the calculated equilibrium constants we can conclude that our reactions were sufficiently removed from equilibrium at all points of the kinetic studies that the inverse reactions may be neglected. Representative pseudo-first-order kinetic plots are shown in Fig. III.2.1. The second-order rate constants can be obtained from the slopes of the pseudo-first-order plots and the known pressures and densities of the neutrals. The second-order kinetics of the reactions was confirmed by the observation that the

FIGURE III.2.1

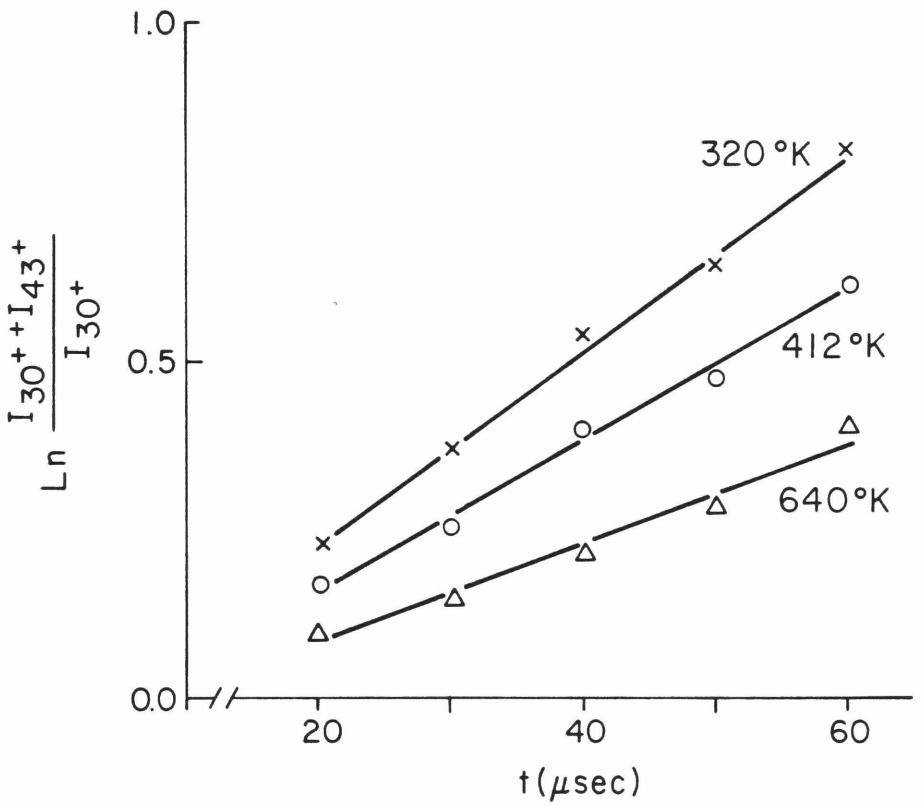

Representative kinetic plots for the reaction NO^+ (m/e = 30) + $CH_3CHO \longrightarrow CH_3CO^+$ (m/e = 43) + HNO.

Second-order rate constants measured at the densities quoted in Table III.2.1 were found to be equal within experimental error limits to rate constants measured at twice these densities.

Results

(i) Fast reactions: H^+ transfer

The experimental rate constants and the rate constants predicted by the locked dipole and ADO theories for the proton transfer reactions studied at 320 and 640°K are shown in Table III.2.2. The detailed forms of the temperature dependences of reactions 1-5* are shown in Fig. III.2.2 to III.2.4. For reaction 1 where the neutral reactant, CH_4, is nonpolar, equation (III.2.1) is equal to the Gioumousis-Stevenson equation. The rate constant is in good agreement with the theoretical value. The rate constant for this reaction is seen to be independent of temperature within experimental accuracy between 130 and 650°K, as expected (Fig. III.2.2). Similarly the contribution of the dipole moment of the slightly polar but highly polarizable molecule $(C_2H_5)_3N$ to the rate of reaction 2 is small. The experimental rate constant of this reaction is also in good agreement with the prediction of the parameterized ADO theory and exhibits negligible temperature dependence between 320 and 650°K, as predicted (Fig. III.2.2).

The neutral reactant in reaction 3, NH_3, is a polar molecule with a small polarizability (Table III.2.1). Comparing the measured rate of this reaction with the Langevin rate (=1.07 x 10^{-9}) cc/molecule sec.), one may easily calculate that the ion-dipole interaction contributes 30% to the reaction rate at 640°K, and 45% at 320°K. The experimental rate constants show that the contribution of the ion-dipole interaction to the rate constants causes a small negative temperature dependence of the rate constants, as predicted by equation (III.2.1) (Fig. III.2.3). The rate constants in this reaction are in good agreement with the predictions of the ADO theory.

---

* Reactions in Section III.2 will be referred to by their number in Table III.2.2

TABLE III.2.2

Experimental and Theoretical Rate Constants of some H^+ and H^- Transfer Reactions at 320 and 650°K

Reaction Number	Reactions	$10^9 k_{320}$ Experimental	$10^9 k_{320}$ Theoretical (Eq.1) Dipole Locking Constants= c^{300}_{ADO}	$10^9 k_{320}$ Theoretical (Eq.1) Dipole Locking Constants= 1.0	$10^9 k_{640}$ Experimental	$10^9 k_{640}$ Theoretical (Eq. 1) Dipole Locking Constants= c^{300}_{ADO}	$10^9 k_{640}$ Theoretical (Eq. 1) Dipole Locking Constants= 1.0	Dipole Locking Constants 300 c_{ADO}	Dipole Locking Constants 320 c_{EXP}
	H^+ and D^+ Transfer Reactions								
1.	$N_2H^+ + CH_4 \longrightarrow CH_5^+ + N_2$	1.3	1.2	1.2	1.3	1.2	1.2	-	-
2.	$t\text{-}C_4H_9^+ + (C_2H_5)_3N \longrightarrow (C_2H_5)_3NH^+ + C_4H_8$	1.6	1.5	2.1	1.6	1.5	1.9	0.05	0.09
3.	$N_2H^+ + NH_3 \longrightarrow NH_4^+ + N_2$	2.0	1.9	5.1	1.7	1.6	3.9	0.21	0.23
4.	$N_2H^+ + CH_3CHO \longrightarrow CH_3CHOH^+ + N_2$	5.8	2.6	6.9	4.2	2.2	5.2	0.25	0.78
5.	$N_2D^+ + CH_3CHO \longrightarrow CH_3CHOD^+ + N_2$	6.2	2.6	6.9	4.2	2.2	5.2	0.25	0.82
6.	$H_3S^+ + CH_3CHO \longrightarrow CH_3CHOH^+ + N_2$	5.1	2.5	6.5	4.2	2.1	4.9	0.25	0.87
	H^- Transfer Reactions								
7.	$NO^+ + CH_3CHO \longrightarrow CH_3CO^+ + HNO$	0.76	2.6	6.9	0.34	2.2	5.2	-	-
8.	$t\text{-}C_4H_9^+ + i\text{-}C_5H_{12} \longrightarrow t\text{-}C_5H_{11}^+ + i\text{-}C_4H_{10}$	0.014	1.3	1.5	0.0017	1.3	1.5	-	-

[a] Calculated from equation (III.2.1) with the dipole locking constant c as given for the particular collision system by the parameterized ADO theory[4b]. Note that this is not exactly the ADO value, in particular at 640°K, since c has been given only for 300°K in Reference 4b.

Calculated from the experimental rate constants and equation (III.2.1), i.e., $k_{EXP} = \frac{2\pi q}{\mu^{1/2}} \left[q^{1/2} + c_{EXP} \mu_D \left(\frac{2}{\pi kT} \right)^{1/2} \right]$.

The values of c_{EXP} can be seen as the experimentally determined average locking of the dipole in the electric field of the ion.

FIGURE III.2.2

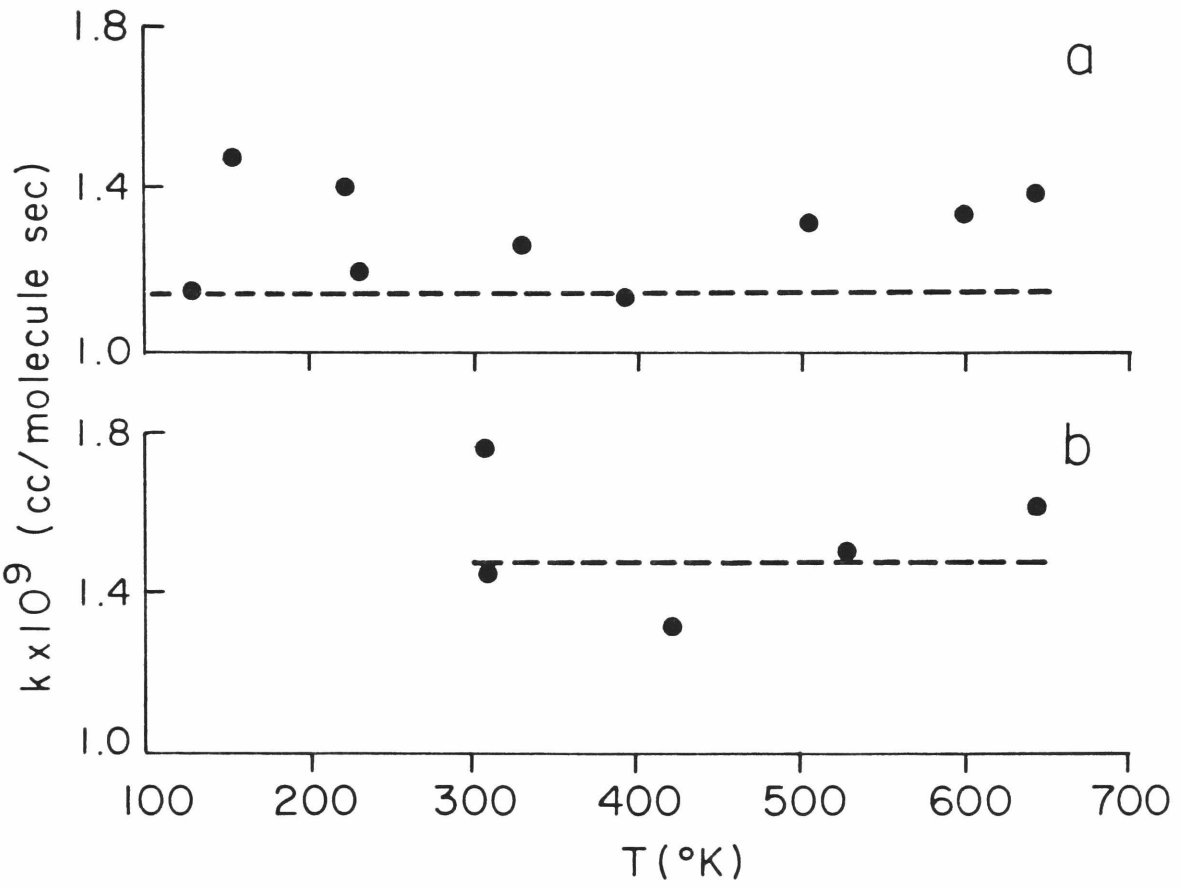

a. The temperature dependence of the rate constant of the reaction $N_2H^+ + CH_4 \longrightarrow CH_5^+ + N_2$ between 130 and 640°K.

b. The temperature dependence of the rate constant of the reaction $t\text{-}C_4H_9^+ + (C_2H_5)_3N \longrightarrow (C_2H_5)_3NH^+ + C_4H_8$ between 310 and 640°K. Points represent experimental measurements; broken lines theoretical (ADO) capture rate constants.

FIGURE III.2.3

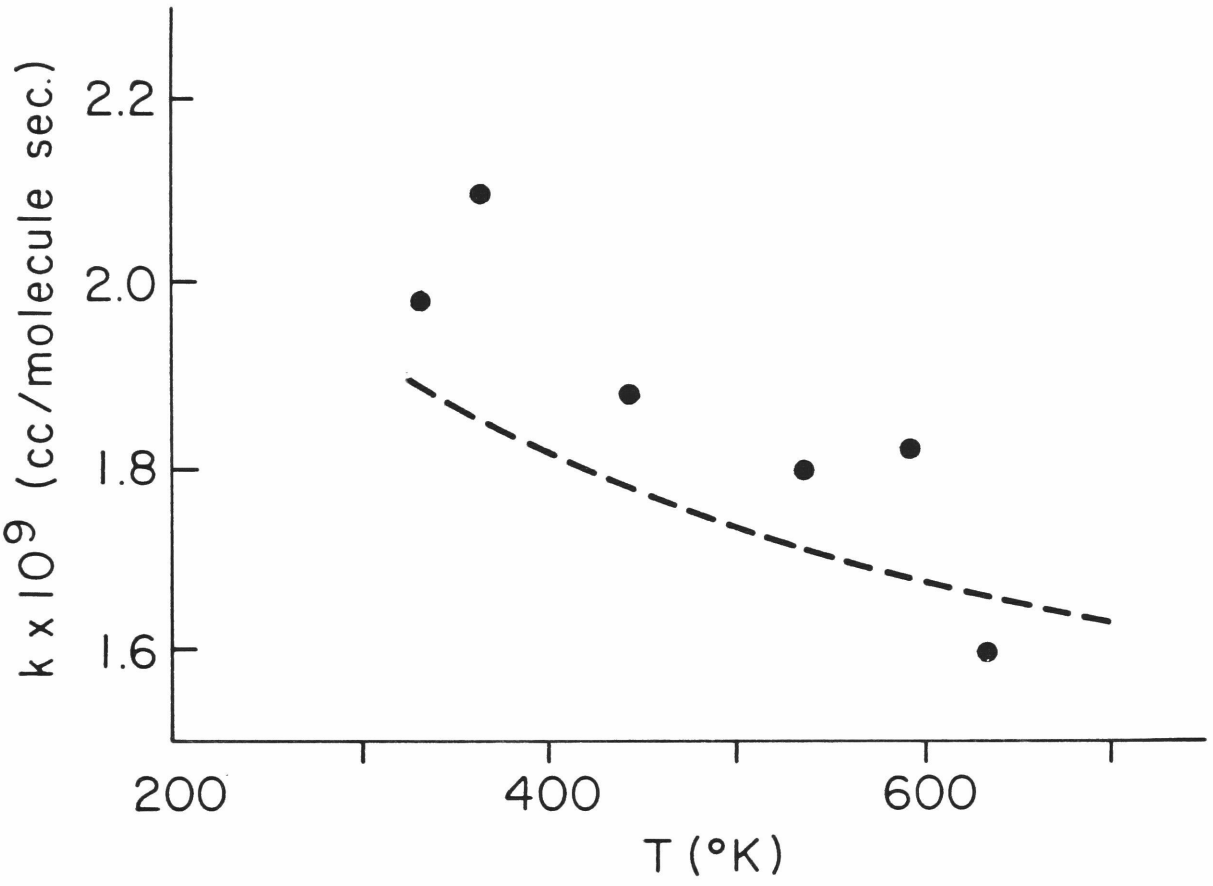

The temperature dependence of the rate constant of the reaction $N_2H^+ + NH_3 \longrightarrow NH_4^+ + N_2$ between 320 and 640°K. The broken line represents the theoretical rate constants calculated from equation (II.2.1) with the dipole locking constant $c = 0.21 = c_{ADO}^{300}$.

FIGURE III.2.4

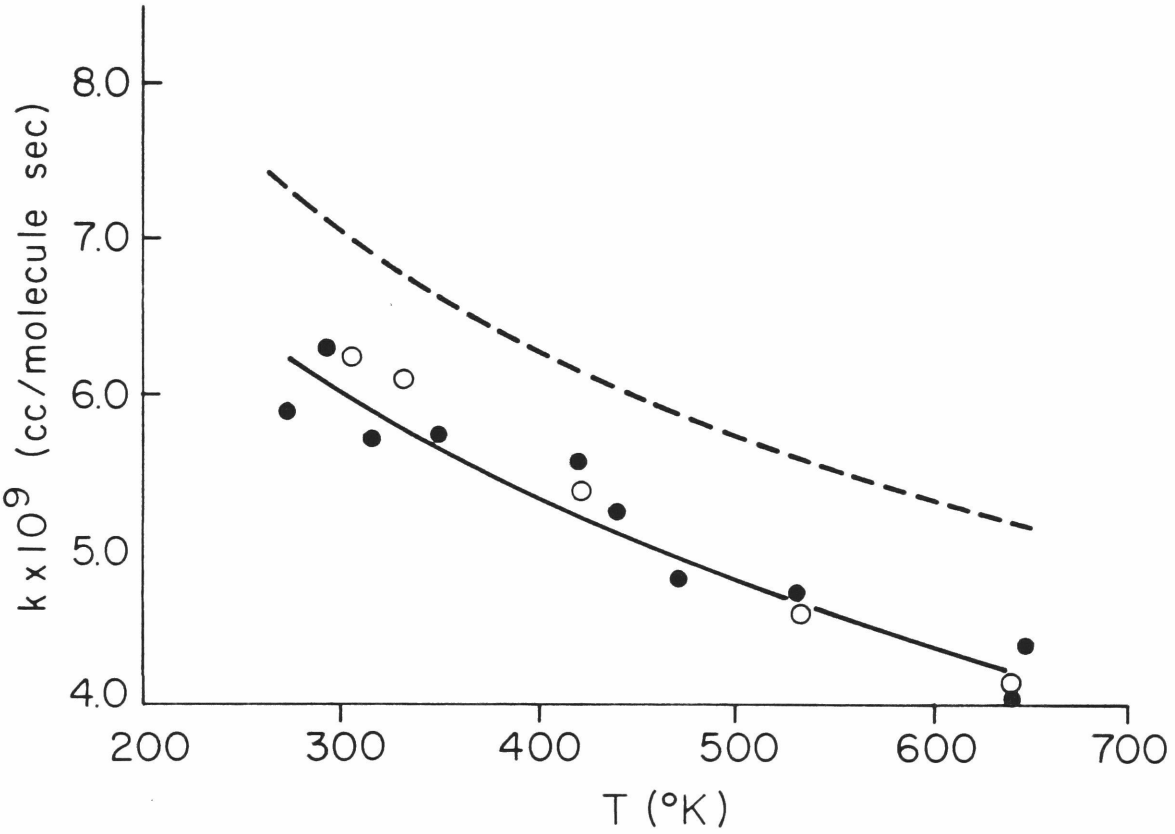

The temperature dependence of the rate constant of the reaction $N_2H^+ + CH_3CHO \longrightarrow CH_3CHOH^+ + N_2$ between 270 and 640°K. Solid circles represent experimental values and the solid line shows the experimental temperature dependence. The broken line represents the theoretical (locked dipole) rate constants. Open circles are experimental rate constants for the reaction $N_2D^+ + CH_3CHO \longrightarrow CH_3CHOD^+ + N_2$.

k_{320} is in good agreement with the experimental rate constant for this reaction published recently by Hemsworth et al.[5]

The neutral reactant in reactions 4-6, CH_3CHO, is a highly polar molecule (μ_D = 2.67 debye). Comparing the Langevin rate (=1.20 x 10^{-9} cc/molecule sec.) with the experimental rate constants shows that the ion-dipole interaction contributes 78% of the rate of reaction 4 at 320°K and 70% at 640°K. These results are consistent with a dipole locking constant of 0.78, rather than the ADO value of 0.25. Similar results are found in reactions 5 and 6. In light of the general success of the ADO theory,[5] the large locking of the dipole found in the reactions of this highly polar molecule is somewhat of an anomaly. We do not know the reason for this behavior.

The similarity between the rate constants of reactions 4 and 5 shows the absence of kinetic isotope effects in this reaction.

The temperature dependences of the rates of reactions 4 and 5 are shown in Fig. III.2.4. The experimental rate constants again show the negative temperature dependence caused by the contribution of the ion-dipole interaction to the rate constant. To the best of our knowledge, these results are the first experimental demonstrations of the effect of ion-dipole interactions on the temperature dependence of the rate constants of fast ion-molecule reactions.

(ii) Slow reactions: H^- transfer

The experimental rate constants and the calculated collision rates of two hydride-ion transfer reactions at 320 and 640°K are shown in Table III.2.2. The experimental values may be compared with the corresponding theoretical values for each reaction. In addition the experimental values for reaction 7 and 8 may be compared with those of reactions 4 and 2, respectively, since the collision properties of the respective reaction systems involved, i.e., the reduced masses, polarizabilities and dipole moments are comparable. It is seen that in contrast to the proton-transfer

reactions, the rates of the hydride-ion transfer reactions are significantly slower than the capture rates. In the investigation of reaction 8 we found that the plot of ln k vs. ln T for that reaction was linear with a slope of -3 between 190 and 570°K.[1] This temperature dependence is significantly larger than the temperature dependence of the collisional rate of the comparable proton-transfer reaction 2 which is of the form $k = AT^{o}$.

We show the temperature dependence of the rate constant of reaction 7 in a plot of ln k vs. ln T in Fig. III.2.5. The rate constant of this hydride-ion transfer reaction is seen to show a temperature dependence that may be expressed at $k = AT^{-1}$. This temperature dependence is significantly larger than the temperature dependence of the capture rate of the comparable proton transfer reaction 4 (Fig. III.2.5).

Discussion and Conclusion

In the study of the reaction system $t\text{-}C_4H_9^+(i\text{-}C_5H_{12}, i\text{-}C_4H_{10})t\text{-}C_5H_{11}^+$ we found that the negative temperature dependence of the forward reaction could be interpreted on the basis of transition-state theory (TST) considerations. The temperature dependence of the rate constant may be expressed by TST equations for the general case of:

$$k_r(T) = c\,\frac{kT}{h}\,\frac{Q^{\ddagger}_{tr}\,Q^{\ddagger}_{rot}\,Q^{\ddagger}_{vib}\,Q^{\ddagger}_{elec}}{\prod_{i=1}^{n}(Q_i)_{tr}\,(Q_i)_{rot}\,(Q_i)_{vib}\,(Q_i)_{elec}}\,e^{-E_o/RT} =$$

$$A\,\frac{\left(T_{tr}^{3/2}\right)^{\ddagger}\left(T_{rot}^{j/2}\right)^{\ddagger}}{\prod_{i=1}^{n}\left(T_{tr}^{3/2}\right)_i\left(T_{rot}^{j/2}\right)_i}\,T^{r/2}_{\text{int. rot}}\,e^{-E_o/RT} \qquad \text{(III.2.2)}$$

Here Q and Q_i are the partition functions of the transition complex and the n reactants that form it. The temperature dependence of the vibrational and electronic partition functions may be neglected for the present purposes. The activation energy for exothermic ion-molecule reactions is usually assumed to be zero or negligibly small. This was shown to be true for reaction 8. Our findings of zero or negative temperature coefficients

FIGURE III.2.5

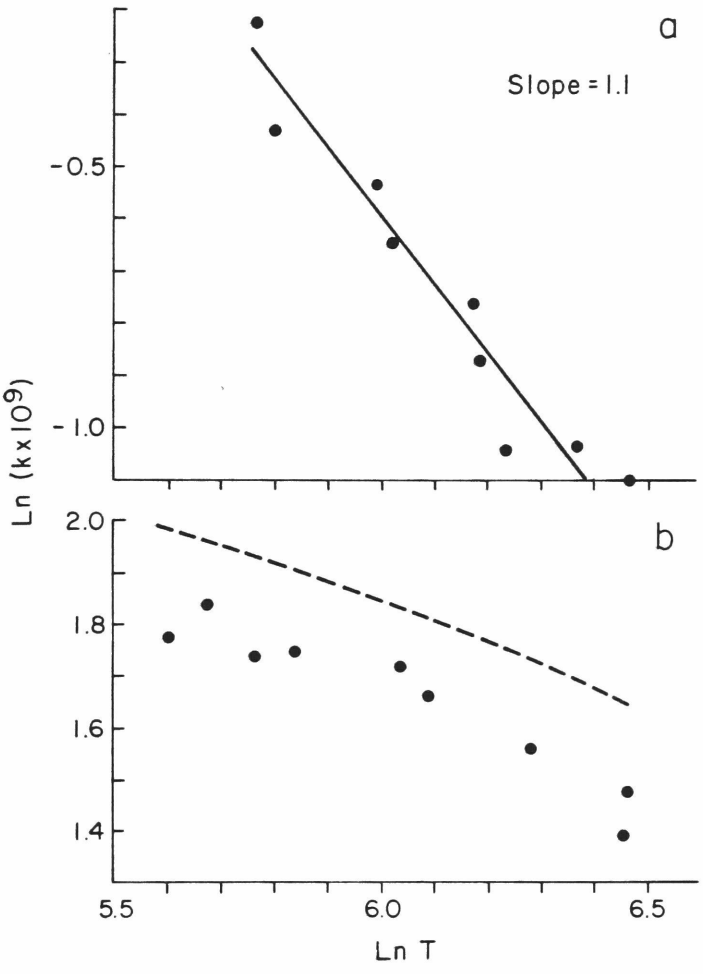

a. The temperature dependence of the rate constant of the reaction $CH_3CHO + NO^+ \longrightarrow CH_3CO^+ + HNO$ between 320 and 640°K. A plot of ln k x 10^9 vs. ln T is shown. Solid line is the least squares plot through experimental points.

b. For comparison the plot of ln k x 10^9 vs. ln T for the comparable proton-transfer reaction $N_2H^+ + CH_3CHO \longrightarrow CH_3CHOH^+ + N_2$ (solid circles) and the plot of the logarithm of the theoretical capture rate ln(k locked dipole x 10^9) vs. ln T (broken line) are also shown.

found in the present study indicate that the activation energies are also negligible for exothermic ion-molecule reactions here investigated. Thus the exponential term in equation (III.2.2) is effective unity.

Labeling the origin of the temperature dependent term, the second expression in equation (III.2.2) is obtained. In this expression A is a constant; j is 3 for nonlinear and 2 for linear molecules; and r is the change in the number of internal rotations upon the formation of the transition complex. Applying this equation to reaction 8, for which it was found experimentally that $k = AT^{-3}$, we obtained r = -2, i.e., two internal rotations become hindered upon the formation of the transition complex. This is a reasonable number for the molecular structures of the reactants in that reaction. For reaction 7 we obtain

$$k = AT \frac{\left(T_{tr}^{3/2}\right)^{\ddagger}\left(T_{rot}^{3/2}\right)^{\ddagger}}{\left(T_{tr}^{3/2}\right)_{CH_3CHO}\left(T_{tr}^{3/2}\right)_{NO^+}\left(T_{rot}^{3/2}\right)_{CH_3CHO}\left(T_{rot}^{2/2}\right)_{NO^+}} T^{\frac{r}{2}} = AT^{\frac{r-3}{2}} \qquad \text{(III.2.3)}$$

from the slope of Fig. III.2.5 we get $\frac{r-3}{2} = -1$, r=1. One internal rotation is created upon the formation of the transition complex. The axis of this rotation is easily seen as the $H\text{----}NO^+$ bond in the complex

$$CH_3\text{-}\overset{O}{\overset{\|}{C}}\text{-}H\text{---}NO^+$$

Thus, transition state theory account for hydride ion transfer reactions in a simple and satisfactory way. However, it must be recognized that these reactions may also in principle be described by RRK or quasi-equilibrium theory treatments. This point will be discussed in Section V.

Turning to the H^+ transfer reactions, TST considerations applied to such reactions proceeding via tightly bound complexes would also predict generally a temperature dependence of T^{-1} or $T^{-1.5}$. This behavior is clearly not observed in our data on the fast proton-transfer reactions. However, Eyring et al[6] applied transition state theory methods to fast ion-molecule reactions which proceed through loose complexes. In this

model the distance between the reactants in the activated state is determined by the position of the maximum in the potential energy surface of the reaction, and this distance is in turn determined by the difference between the rotational and ion-induced dipole interactions. In these loose complexes* the reactants retain their individual rotational and vibrational degrees of freedom, and the treatment leads to an expression for the rate constant which is similar to the Langevin expression and is likewise independent of the temperature. It does not appear that the transition state theory treatment has been extended to ion-polar molecule reactions.

In conclusion, H^- transfer reactions exhibit large negative temperature dependences which can be successfully interpreted using theoretical considerations based on the formation of tight transition complexes and cannot be accounted for satisfactorily by collisional considerations based on loose or orbiting complexes. In contrast, the absolute rates of H^+ transfer reactions, and the small negative temperature dependences thereof which we measured, and be successfully accounted for by such collisional considerations and are inconsistent with the formation of tightly bound transition complexes.

There is no obvious explanation for the fundamental differences between the nature of H^+ and H^- transfer reactions, although it is obviously a matter of much interest.

---

* For example, according to this treatment the mean distance between N_2H^+ and CH_4 in the activated state of the corresponding H^+ transfer reaction at 300^oK turns out to be $3.9A^o$.

REFERENCES

1. J.J. Solomon, M. Meot-Ner and F.H. Field, J. Amer. Chem. Soc., 96 3727 (1974).
2. G. Gioumousis and D.P. Stevenson, J. Chem. Phys., 29, 294 (1958).
3. S.K. Gupta, E.G. Jones, A.G. Harrison and J.J. Myher, Can. J. Chem. 45, 3107 (1967).

4a. T. Su and M.T. Bowers, J. Chem. Phys., 58, 3027 (1973).

b. T. Su and M.T. Bowers, Int. J. of Mass Spectrom. and Ion Physics, 12, 347 (1973).

5. R.S. Hemsworth, J.D. Payzant, H.J. Schiff and D.K. Bohme, Chem. Phys. Letters, 26, 417 (1974).
6. S. Glasstone, K.J. Laidler, and H. Eyring, "The Theory of Rate Processes," McGraw Hill Co., New York, 1941, pp.220ff.

IV. ASSOCIATION REACTIONS

IV.1 KINETICS AND THERMODYNAMICS OF ASSOCIATION REACTIONS OF $CO^{+\cdot}$ AND HCO^{+} WITH CO AND OF $N_2^{+\cdot}$ AND N_2H^{+} WITH N_2 BETWEEN 120 AND 650°K*

Introduction

Gaseous ion-molecule association reactions have been investigated in recent years in this laboratory and by other workers. A thorough understanding of reactions of this type requires the clarification of such questions as the relation between the electronic and steric structure of the reactants and the thermodynamic parameters of the reactions and the significance of purely physical or of chemical forces in the formation of the association complexes. The understanding of the kinetics of formation of ion-molecule complexes involves such problems as, for example, the relation between structure and reaction rates, the relation between the thermodynamics of the reaction and the reaction rates, and the functional dependence of the rate constants on the temperature and the pressure. Deeper understanding of all of these questions should be facilitated by comprehensive comparative studies of reactions of molecules of related structures.

With these considerations in mind we undertook in the present study the investigation of the thermodynamic and kinetic parameters of the association reactions of the protonated even-electron ion HCO^{+} and the radical ion $CO^{+\cdot}$ with carbon monoxide within the temperature range experimentally presently accessible to us, i.e., 120 - 700°K. We also investigated some aspects of the association reactions of N_2H^{+} and $N_2^{+\cdot}$ with nitrogen.

Experimental

Mass spectra were recorded in the conventional mode of continuous ion production and detection.[1] Kinetic and equilibrium studies were conducted

* M. Meot-Ner and F.H. Field, J. Chem. Phys., 61, 3742 (1974).

by the pulsed high pressure mass spectrometric technique, applied to our apparatus, which has been described above.[2]

Materials used in the present study were Matheson CO, N_2, H_2 and He, all of purity > 99%. The gases were passed through a glass coil immersed in liquid nitrogen to remove any condensable impurities. No significant impurities were observed in the mass spectra of the reaction mixtures.

Results and Discussion

1. Mass Spectra

The mass spectra of the reaction mixtures used in this study were obtained at 120°K at the number densities used in the kinetic studies and at high densities, where a greater number of higher association products are observed. Many of the ions observed in these spectra are reported here for the first time. The ion observed in the mass spectra of pure CO and of the He - CO mixture (Table IV.1.1) corresponds to sets of ion clusters produced by the association of CO molecules with the molecular and fragment ions $CO^{+\cdot}$, C^+, and $O^{+\cdot}$. The most prominent are the ions of the general formula $(CO^{+\cdot}\cdot nCO)$, n = 1-6. Next in significance are the ion of the formula $C^{+\cdot}\cdot nCO$, n = 1-5. The very small intensity of the $C_2O^{+\cdot}$ $(C^{+\cdot}\cdot CO)$ ion compared with the $C_3O_2^{+\cdot}(C^{+\cdot}\cdot 2CO)$ ions is to be noted. The formation of $C_2O^{+\cdot}$ and $C_3O_2^{+\cdot}$ ion in carbon monoxide plasmas was reported previously.[3,4,5] $C_2O^{+\cdot}$ was presumed to be very reactive and the carbon suboxide ion $C_3O_2^{+\cdot}$ was presumed to be formed by association reactions of $C^{+\cdot}$. Comparison of the mass spectra given in Table IV.1.1 shows a greate increase of both the $C^{+\cdot}$ ion and the $C_3O_2^{+\cdot}\cdot nCO$ ions in the He + CO plasma vs. the CO plasma, presumably due to the abundant formation of the $C^{+\cdot}$ ion in the He + CO plasma by the reaction.

$$He^{+\cdot} + CO \longrightarrow He + C^{+\cdot} + O$$

A significant increase of the $C_3O_2^{+\cdot}\cdot nCO$ intensity compared with that of the $C^{+\cdot}$ ions with increasing pressure is also noted in both plasmas. These observations given support to previous suggestions[3] that $C_3O_2^{+\cdot}$ is a product of the overall reaction

TABLE IV.1.1

The Mass Spectra of Pure CO

and a Mixture of He and 2% CO at 120°K

		CO		2% CO + 98% He	
Total Pressure (torr)		0.12	0.60	0.60	2.0
m/e	Identification	I (%)		I (%)[a]	
4	$He^{+\cdot}$	-	-	0.3	-
12	$C^{+\cdot}$	7.4	3.2	40.9	19.4
16	$O^{+\cdot}$	2.7	1.0	1.4	1.8
28	$CO^{+\cdot}$	41.6	25.8	36.0	10.7
32	$O_2^{+\cdot}$	1.1	0.2	0.5	-
40	$C_2O^{+\cdot} = C^{+\cdot}\cdot CO$	-	0.2	0.7	-
44	$CO_2^{+\cdot} = O^{+\cdot}\cdot CO$	-	0.2	-	-
56	$(CO)_2^{+\cdot}$	43.9	24.5	17.6	17.2
68	$C_3O_2^{+\cdot} = C^{+\cdot}\cdot 2CO$	0.9	1.5	2.8	12.4
84	$(CO)_3^{+\cdot}$	2.4	8.2	0.5	4.0
88	$C_2O_4^{+} = O_2^{+\cdot}\cdot 2CO?$	-	0.7	-	-
96	$C_3O_2^{+\cdot}\cdot CO$	-	2.2	-	16.7
100	$O^{+\cdot}\cdot 3CO$	-	0.2	-	-
112	$(CO)_4^{+\cdot}$	-	22.2	-	4.2
116	$O_2^{+\cdot}\cdot 3CO$	-	1.1	-	-
124	$C_3O_2^{+\cdot}\cdot 2CO = C^{+\cdot}\cdot 4CO$	-	1.9	-	7.5
128	$O^{+\cdot}\cdot 4CO$	-	0.9	-	-
140	$(CO)_5^{+\cdot}$	-	5.8	-	4.8
144	$O_2^{+\cdot}\cdot 4CO$	-	1.9	-	-
152	$C_3O_2^{+\cdot}\cdot 3CO = C^{+\cdot}\cdot 5CO$	-	-	-	1.3
156	$O^{+\cdot}\cdot 5CO$	-	0.2	-	-
168	$(CO)_6^{+\cdot}$	-	0.1	-	-
172	$O_2^{+\cdot}\cdot 5CO$	-	0.1	-	-
184	$O^{+\cdot}\cdot 6CO$	-	0.1	-	-
196	$(CO)_7^{+\cdot}$	-	0.1	-	-

a. Intensities expressed as percent of the total ion current , i.e, $\frac{100I}{\Sigma I}$.

$$C^{+\cdot} + nCO \longrightarrow C_2O_3^{+\cdot} + (n-2)CO$$

In the CO plasma at higher pressures, ions of the general formulas $O^{+\cdot}\cdot nCO$, n = 1-6, and $O_2^{+\cdot}\cdot nCO$, n = 2-5, are also observed.

The mass spectra of the mixtures of 10% H_2 in CO and 10% CO in H_2 were simple, with the ions $HCO^+\cdot CO$, n = 1-5 constituting the only significant species. These spectra are not presented here for the sake of space economy, HCO^+ is presumably formed in these plasmas by fast reactions between the reactant ions $CO^{+\cdot}$, $H_2^{+\cdot}$ and H_3^+ and the neutral components of the plasma. The absence of any significant amounts of the ions $He^{+\cdot}$ in the mass spectra of the He + CO mixtures and of $H_2^{+\cdot}$, H_3^+, and $CO^{+\cdot}$ in the mass spectra of H_2 + CO mixtures shows that the primary reactions leading to the formation of $CO^{+\cdot}$ and $HCO^{+\cdot}$ in the two reaction systems respectively go to completion in a few μsec. These observations present an example of the application of the chemical ionization method to generate ions for kinetic and equilibrium studies in pulsed high pressure mass spectrometry.

2. Equilibrium and Thermodynamic Studies

The approach to equilibrium in the reaction

$$HCO^+ + CO + H_2 \rightleftharpoons HCO^+\cdot CO + H_2 \qquad (1)^*$$

between 343 and 408°K is shown in Fig. IV.1.1. The figure shows a monotonic rise with time in the value of the observed equilibrium constant, i.e., of $\frac{I_{HCO^+\cdot CO}}{I_{HCO^+}\cdot P_{CO}}$ until a constant value is obtained. The constancy of k_{obs} indicates that equilibrium has been reached. Fig. IV.1.1 shows that equilibrium is reached faster as the temperature increases, and the value of the equilibrium constant decreases. Equilibrium constants obtained from the plateau regions of plots of K_{obs} vs. reaction time were used in the van't Hoff plots shown in Fig. IV.1.2 for reaction 1 and for the reaction

$$N_2H^+ + 2N_2 \rightleftharpoons N_4H^+ + N_2 \qquad (3)$$

* Throughout Section IV.1 reactions will be numbered and referred to according to their number in Table IV.1.2.

FIGURE IV.1.1

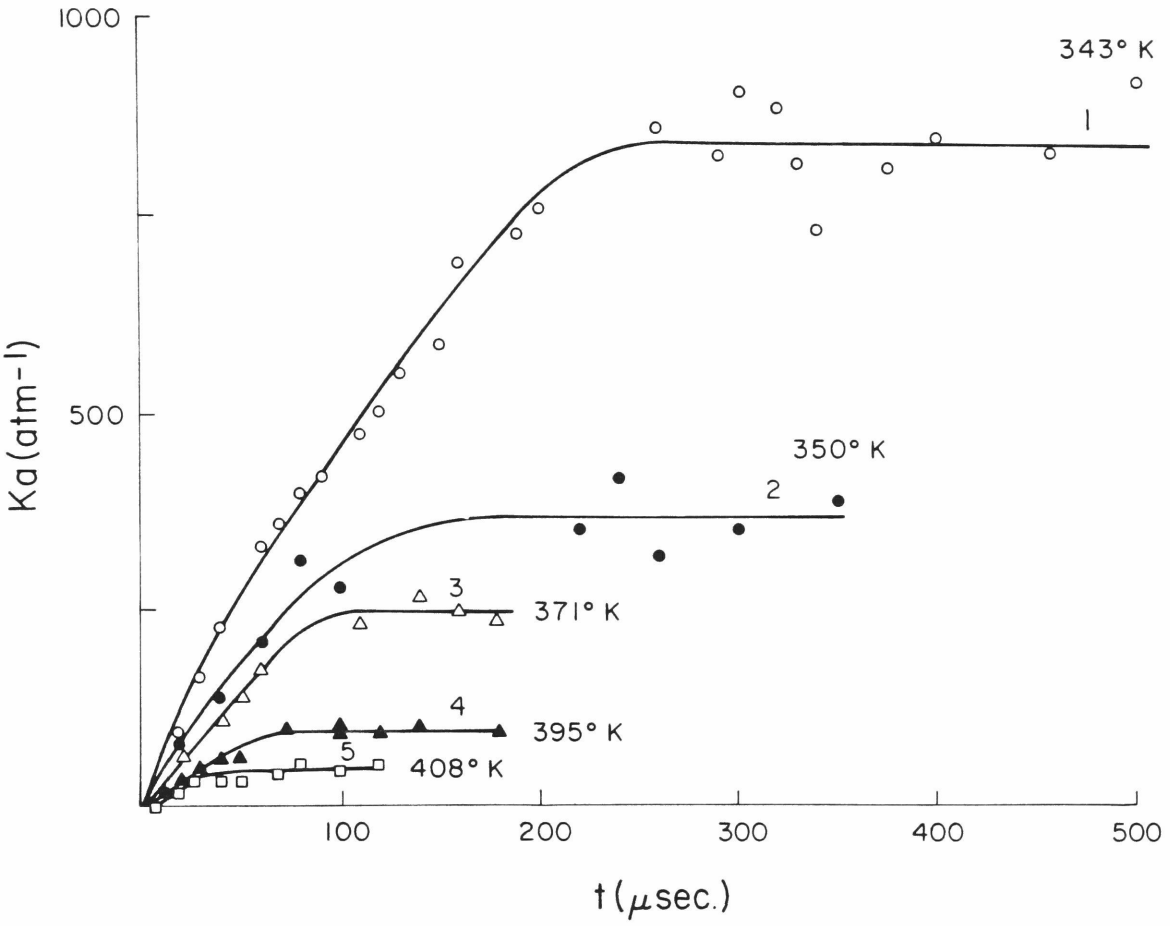

Sample plots illustrating the approach to and attainment of equilibrium in the reaction $HCO^+ + CO + H_2 \longrightarrow HCO^+ \cdot CO + H_2$ in a reaction mixture of 20% CO in H_2. Experimental conditions: (1) T = 343°K, $P_{CO + H_2}$ = 2.97; (2) T = 350, P = 2.9; (3) T = 371, P = 2.73; (4) T = 395, p = 2.48; (5) T = 408, P = 2.58.

FIGURE IV. 1.2

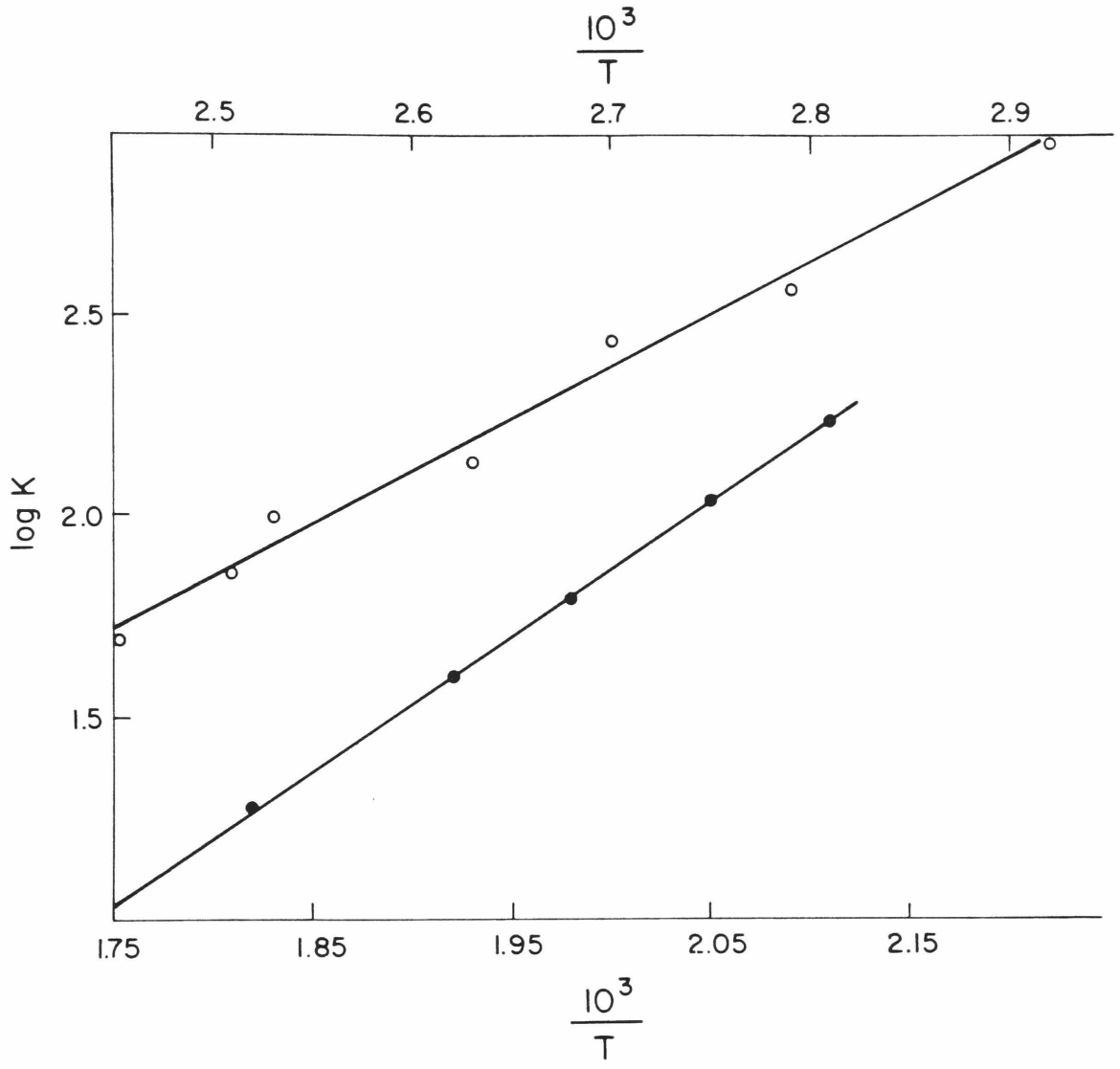

van't Hoff plots for the reactions: o $HCO^+ + CO \rightleftharpoons HCO^+ \cdot CO$ and $N_2H^+ + N_2 \rightleftharpoons N_4H^+$. Upper scale of abscissa corresponds to the former, lower scale to the latter reaction.

which was investigated by similar methods between 474 and 571°K.

For further verification of the attainment of equilibrium we measured the equilibrium constant for the formation of $HCO^+ \cdot CO$ at 395°K in a mixture of 20% CO in H_2 at 1.25 torr and 2.50 torr total pressures. We also measured the equilibrium constant for the formation of N_4H^+ at 472°K, in a mixture of 10% H_2 in N_2 at 5 different total pressures between 1.2 and 4.2 torr. In these experiments the measured equilibrium constants proved to be 90 ± 10 and 130 ± 15, respectively, independent of pressure.

We attempted to measure the equilibrium in constant for the reaction

$$CO^{+\cdot} + 2CO \rightleftharpoons C_2O_2^{+\cdot} + CO \qquad (5)$$

However, at the highest temperature available to us (700°K) and at the longest delay time attainable within the limitations of instrumental sensitivity, equilibrium could not be obtained in this reaction system. From the highese value of the apparent equilibrium constants, i.e., of $\frac{I_{C_2O_2^{+\cdot}}}{I_{CO^{+\cdot}} \cdot P_{CO}}$ at 695°K we estimate that $K_{695} \gtrsim 4130$ atm.$^{-1}$. The entropies of association of the related reactions investigated here, as well as those of the analogues reactions of $N_2^{+\cdot}$ and $O_2^{+\cdot}$, are all 20 ± 1 e.u.[6,7] We assume this value for our present purposes, and it leads to an estimated value of $-\Delta H^\circ \gtrsim 25.4$ kcal/mole for the reaction producing $C_2O_2^{+\cdot}$. This estimate agrees with previous estimates for the enthalpy of the association of $CO^{+\cdot}$ with CO, obtained by different techniques.[3,5]

The thermodynamic values obtained from the van't Hoff plots for the association reactions of HCO^+ with CO and N_2H^+ with N_2, and the available information on the thermodynamic parameters for the analogous association reactions of the corresponding radical ions $CO^{+\cdot}$ and $N_2^{+\cdot}$ are summarized in Table IV.1.2.

The most notable feature of the observed values is the remarkable difference between the enthalpies of the association reactions with the appropriate neutral molecules of the protonated even-electron ions and

the corresponding radical ions. From quantum chemical calculations Conway[8] concluded that delocalization of the unpaired electron in $N_2^{+\cdot}$ contributes significantly to the enthalpy of formation of $N_4^{+\cdot}$. Our results and general chemical knowledge suggest that the difference between enthalpies of association of the radical ions with neutrals and between the even-electron ions with neutrals results from the occurrence of chemical electron-delocalization effects in the radical ion case, while in the even-electron ions only physical, electrostatic forces between the ion and the neutral molecule may be significant.

3. Kinetic Studies

In the present study we have investigated some aspects of the kinetic behavior of the association reactions 1-6, Table IV.1.2. Ion-molecule reactions occurring under high pressure mass spectrometric conditions may be considered to follow quasi-first-order kinetics in general since the concentrations of the neutrals are essentially constant during the reactions. Thus the quasi-first-order rate constants for the association reaction can be obtained from the slopes of the plots of $\ln \sum_{i=0}^{n} I_{M^+\cdot iCO}/I_{M^+}$ vs. reaction time Here $\sum_{i=0}^{n} I_{M^+\cdot iCO}$ represents the sum of the intensities of the ions $CO^{+\cdot}$, $C_2O_2^{+\cdot}$, $C_2O_2^{+\cdot}\cdot CO$..., or the corresponding ions involving HCO^+. $M^+\cdot nCO$ is the highest association complex observed. We also assume that the higher association ions are formed from $M^+\cdot CO$ by further association reactions. We observed ions higher than $M^+\cdot CO$ only in a few instances at temperatures below 150°K. At all points of the kinetic studies the reactions were sufficiently far from equilibrium for the inverse reactions to be neglected. Sample kinetic plots are shown in Fig. IV.1.3.

The kinetic order of the association reactions of interest was tested by the effect of the variation of the pressure on the reaction rate. As an example the results for reaction 4 at 120°K are shown in Fig. IV.1.4. The results show a linear increase of the second order rate constant with in-

FIGURE IV.1.3

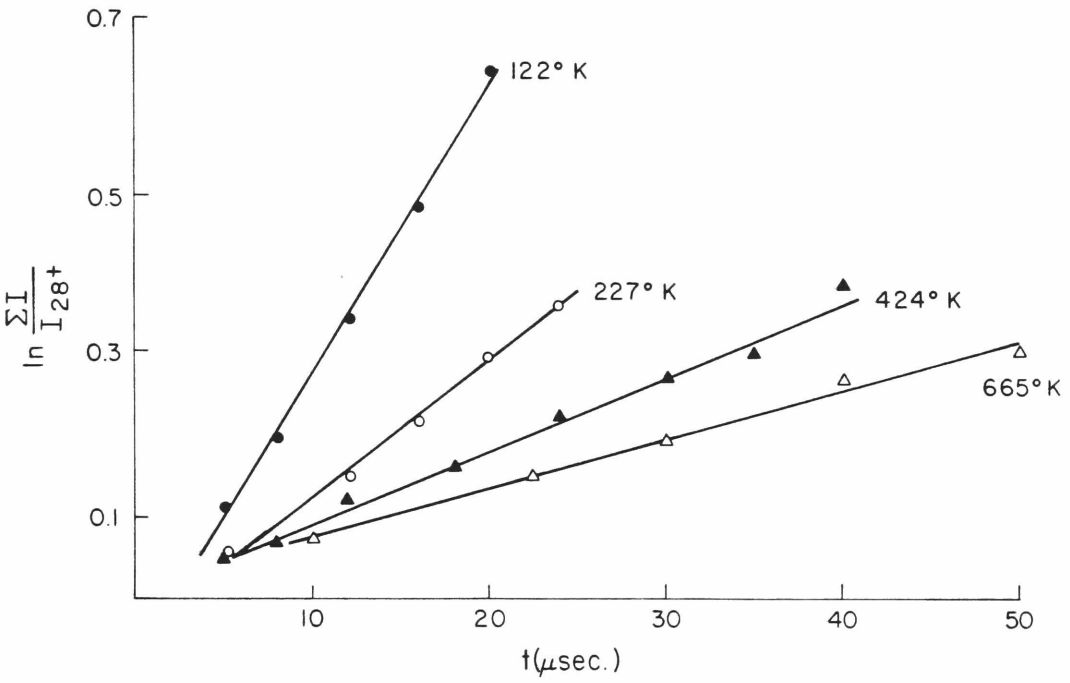

Quasi first-order kinetic plots for the reaction $CO^{+\cdot} + 2CO \longrightarrow C_2O_2^{+\cdot} + CO$. (1) T = 122°K, P_{CO} = 0.145 torr; (2) T = 227, P_{CO} = 0.24; (3) T = 424, P_{CO} = 0.52; (4) T = 665, P_{CO} = 1.01.

FIGURE IV.1.4

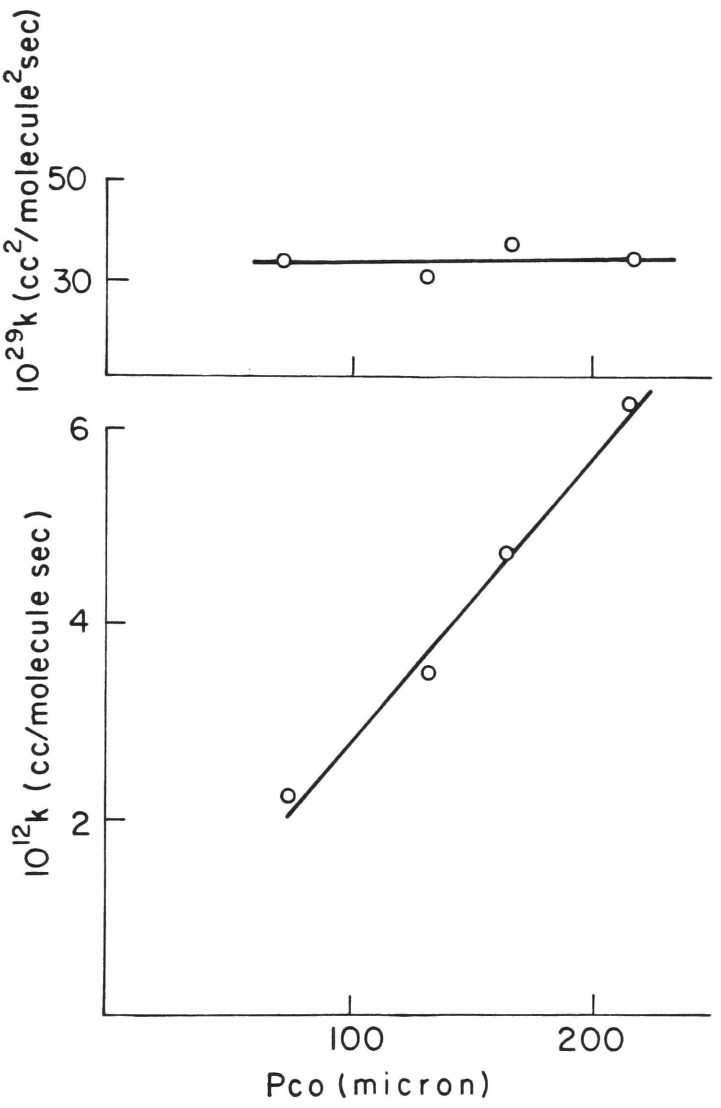

The dependence of the rate constants for the reaction $CO^{+\cdot}$ + nCO $\longrightarrow$ $C_2O_2^{+\cdot}$ + (n-1)CO on the pressure of CO, at 122°K. The second and third order rate constants were calculated from the experimental quasi-first order rate constants and the density of CO.

creasing pressure or, alternatively, constancy of the third order rate constant over the pressure range investigated. The results thus demonstrate that reaction 4 is of third order between 0.075 and 0.25 torr at 122°K. By similar experiments we found linear dependence of the second-order constants on third-body concentration, or overall third-order behavior for reaction 5 between 0.2 and 0.8 torr, for reaction 2 between 0.2 and 0.8 torr and for reaction 1 between 0.5 and 2.0 torr, all at 120°K, and for reaction 3 between 0.6 and 2.7 torr at 320°K. Reaction 6 was shown to be of third-order by Good et al.[9]

Since all of our kinetic studies were conducted at temperatures equal to or higher than those at which the pressure studies in each reaction system were conducted, and at total densities intermediate between the densities corresponding to the lower and upper limits of the pressure studies, all of the reactions that are reported may be considered to be of third order.*

Bohme et. al.[10] reported a change from third-order to second-order kinetics in the reaction $H_2^{+\cdot} + N_2 + He \longrightarrow N_4^{+\cdot} + He$ and $O_2^{+\cdot} + O_2 + He \longrightarrow O_4^{+\cdot} + He$, both at pressures lower than 0.8 torr, at 82°K. The higher temperature in our experiment (120°K) may be accountable for the fact that we did not observe a similar behavior in our reaction systems at densities similar to or higher than those applied in the study of Bohme and co-workers.

The rate constants for reactions 1-6 at 328°K are shown in Table IV.1.2. Our measured value for reaction 6 is in very good agreement with the values quoted for this reaction in Reference 11. Our rate constant for reaction 4 is somewhat higher than that obtained in Reference 3 by more indirect methods. (14.3×10^{-29} cm.^{6} molecule^{-2} sec.$^{-1}$)

It is to be noted that the rate of association reaction of $CO^{+\cdot}$ with

---

* It should be noted that the reaction $HeCO^{+\cdot} + CO \longrightarrow C_2O_2^{+\cdot} + He$ is unlikely here since no $HeCO^{+\cdot}$ was observed in this study. This is significant because the argon analogue of the reaction has been reported.[5]

CO (reaction 5) is faster by a factor of 68 than the analogous reaction of HCO^+ (reaction 2), which is less exothermic by at least 13.7 kcal/mole. The association of $N_2^{+\cdot}$ with N_2 is faster by a factor of 14.6 than the analogous reaction of N_2H^+, which is less exothermic by 8.3 kcal/mole. The reaction of $CO^{+\cdot}$ with CO is faster than the less exothermic reaction of $N_2^{+\cdot}$ with N_2. Thus throughout Table IV.1.2 a direct correlation is observed between the enthalpy of an association reaction and its forward rate constant.

Comparison between the rate constant values in rows (1) and (2) of Table IV.1.2 shows that H_2 is more efficient as a third body than CO by a factor of 2 for these reactions, while rows (4) and (5) show that CO is more efficient than He by about 50%. These observations are in agreement with the general knowledge on the efficiency of third bodies, at least in a qualitative sense.

4. The Temperature Dependence of the Rate Constants

The rate constants of three-body ion-molecule association reactions usually exhibit negative temperature dependence, i.e., the rate increases with decreasing temperature. The temperature dependence of the rate constants of clustering reactions in nitrogen, oxygen and water were investigated by Kebarle, et. al.,[9,7b,12] each over a temperature range spanning 100 - 150 degrees. In the present study we investigated the temperature dependence of the rates of reactions 4 and 5 between 120 and 650°K and of reaction 1 and 2 from 120°K to the temperatures where no association products could be seen, i.e., 500 - 550°K.

The studies of the dependence of the rate constants on the temperature were conducted at constant mixture compositions and constant total particle densities for each reaction. The experimental conditions were as follows: For reaction 1, a mixture of 10% CO, 90% H_2 at a total density of 5.04×10^{16} molecules/cc; reaction 2, 10% H_2, 90% CO, total density 4.79×10^{16}; reaction 3, 10% H_2, 90% N_2, total density 4.60×10^{16}; reaction 4, 2% CO, 98% He, total density 2.57×10^{16}, reaction 5, 100% CO,

density 1.40 x 10^{16}, and reaction 6, 100% N_2, density 1.83 x 10^{16} molecules/cc.

The dependence of the rate constant of reaction 4 on the temperature is shown in Fig. IV.1.5.

In most of the studies reported in the literature on the temperature dependence of ion-molecule reactions the results are exhibited in plots of log k vs. $10^3/T$, and negative activation energies are obtained from the slopes of such plots. It has, however, also been stated that negative activation energies are not necessarily meaningful.[12,13] For the purposes of the present discussion we wish to point out that, a priori, negative activation energies could have physical meaning if a reaction mechanism required that only molecules possessing energy below a certain critical energy will react.* In such a mechanism, a negative activation energy would appear in a mathematical form similar to the ordinary positive activation energy due to the form of the Maxwell-Baltzmann distribution. On the other hand theoretical treatments also predict, as will be discussed presently, a pre-exponential factor of the form T^{-n}, which is determinant in reactions which proceed with a negligible activation energy. Therefore a negative temperature dependence of a rate constant could arise, a priori, from a negative activation energy or a pre-exponential of the form T^{-n} or a combination of both. Because of this reason and because of the conflicting practices and opinions in current literature, it is important to investigate the actual form of the temperature dependence of the rate constants of ion-molecule reactions. It is worth noting that measurements over extended temperature ranges, in particular including low temperature, are necessary for definitive results, since over the limited temperature ranges that the rates of termolecular reactions have been reported to date, log T and $10^3/T$ are approximately linear with respect to each other, and therefore a variable that is linear with respect to $10^3/T$ will appear to be linear with respect to log T, or vice versa, within experimental accuracy

---

* I wish to thank Dr. H. Gershinowitz for raising this point.

limits. For example, both plots IV.1.5a and IV.1.5b appear to be linear between 650 and 450°K.

For the above reasons we plotted the measured values of log k for reaction 4 vs. both log T and $10^3/T$ (Fig. IV.1.5). While both plots are approximately linear between 650 and 450°K, the results over the whole extended range of this study show unequivocally that the plot of log k vs. log T, rather than log k vs. $10^3/T$ exhibits a linear relationship. Similar behavior is observed for the other reactions investigated in this study Fig. IV.1.6 and IV.1.7. This behavior rules out significant negative or positive activation energies in these reactions.

In the $CO^{+\cdot}$ and HCO^+ reactions where CO serves as a third body some negative deviation from linearity is observed at the lowest temperatures investigated even in the plots of log k vs. log T (Fig. IV.1.6 and IV.1.7). The deviation would be, of course, even worse in plots of log k vs. $10^3/T$. Even though the scattering of experimental points at these lowest temperatures is large (the experimental difficulties are quite serious), the deviation from linearity seems to be greater than that to be attributed to random errors. Since the density used in these reaction systems was necessarily small in order to keep the reaction rates measurable, the observed deviation from linearity could result from incomplete thermal relaxation of the ions at these temperatures. However, the measured rate constants are independent of the total pressure (see Section III). This indicates that deviations from thermal relaxation are not significant after 5 - 10 μsec. reaction time. We also checked the possibility of insufficient thermal equilibrium of the neutral gas with the walls by preheating the gas before the point of entrance to the source to 200°C with the source at 120°K. We observed no effect of this on the measured rate constant.

It can be shown that a very small positive activation energy could be sufficient to cause an effect of the necessary direction and magnitude

FIGURE IV.1.5a

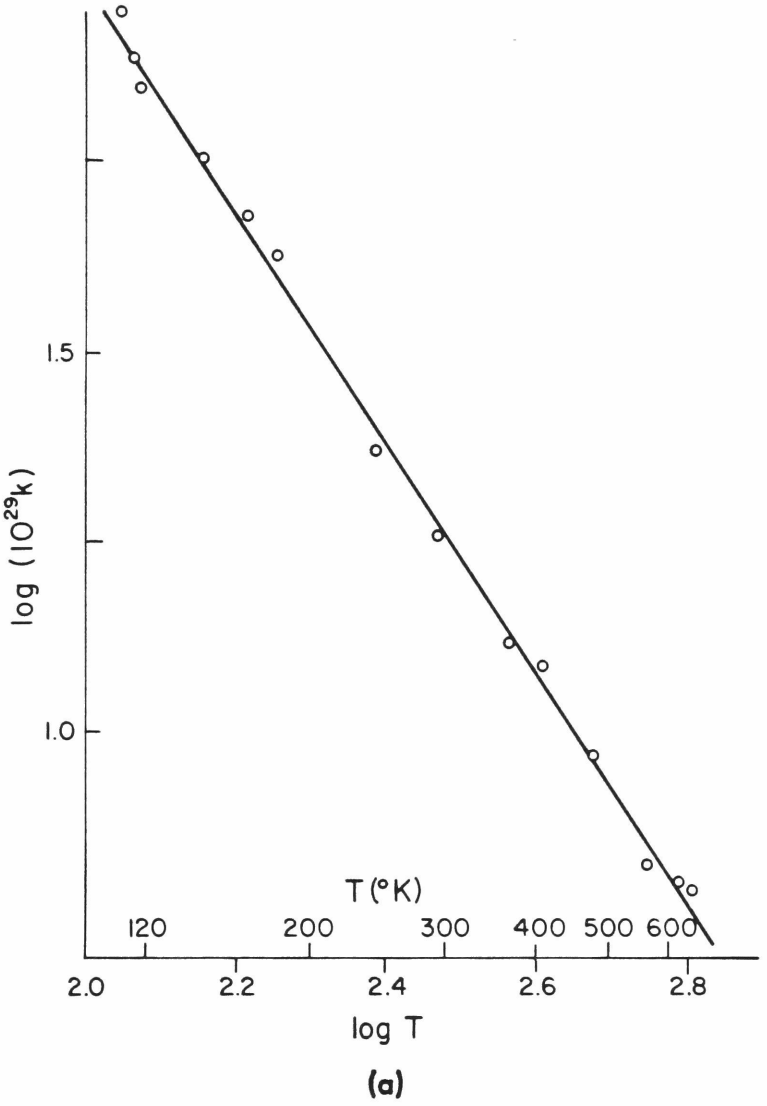

The dependence of the rate constant of the reaction $CO^{+\cdot}$ + CO + He $\xrightarrow{k}$ $C_2O_2^{+\cdot}$ + He on the temperature. (a) The plot of log k vs. log T. (b) The plot of log k vs. $10^3/T$. For ease of reference, scale of absolute temperature is also indicated in this and following figures.

(Fig. IV.1.5b see on next page).

FIGURE IV.1.5b

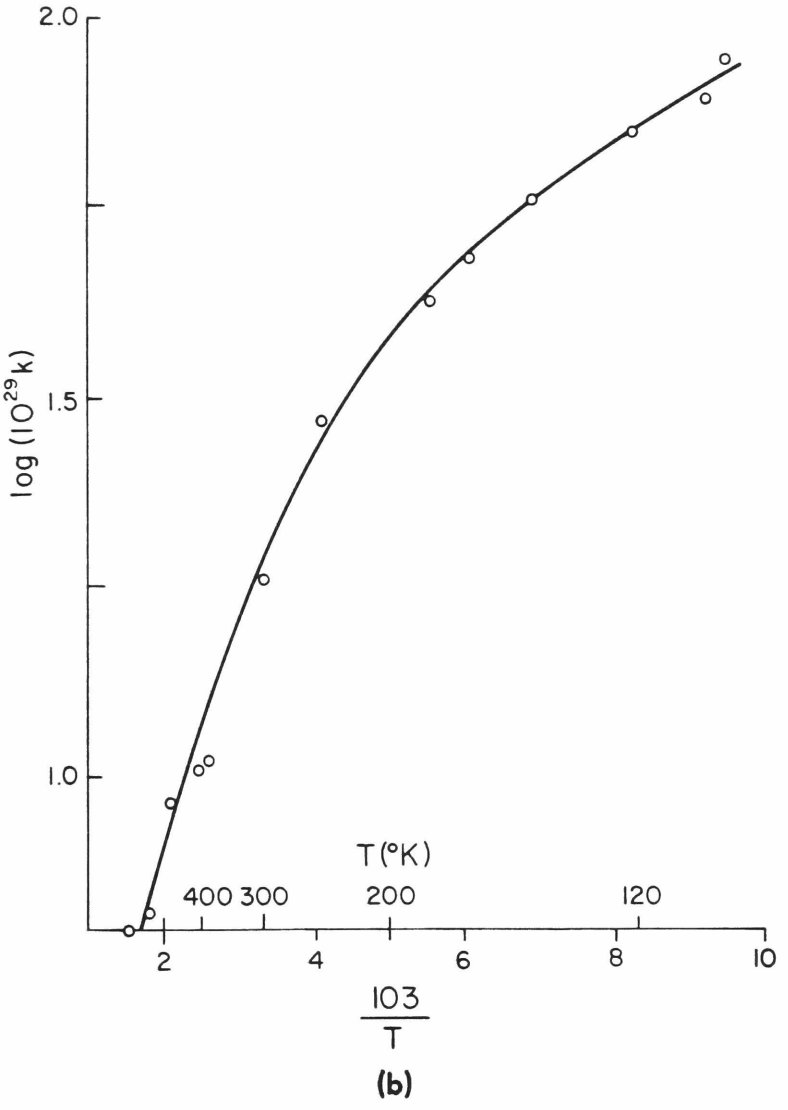

See legend on preceding page.

FIGURE IV.1.6

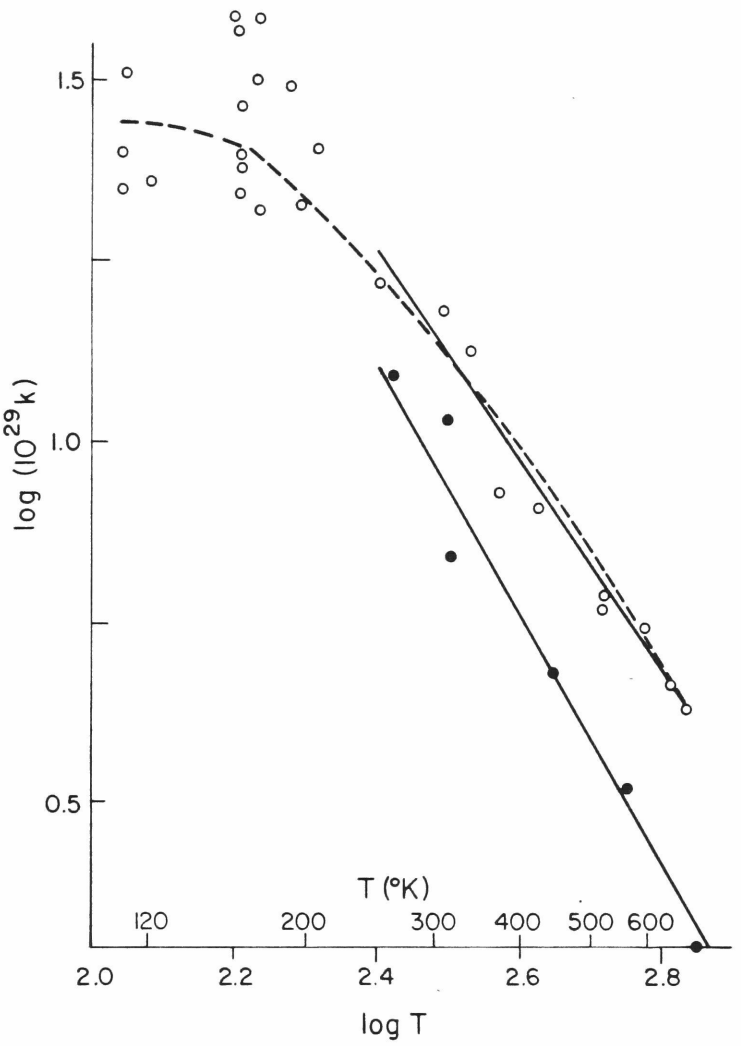

The temperature dependence of the rate constants of the reactions $CO^{+\cdot} + 2CO \longrightarrow C_2O_2^{+\cdot} + CO(o)$ and $N_2^{+} + 2N_2 \longrightarrow N_4^{+} + N_2(\bullet)$. The broken line is the plot of the logarithm (base 10) of the hypothetical rate constant $k_n = CT^{-2}e^{-E_a/RT}$ for an activation energy of 0.2 kcal/mole. C is arbitrarily chosen such that k_n equals the experimental rate constant for reaction 5 at 328°K.

FIGURE IV.1.7

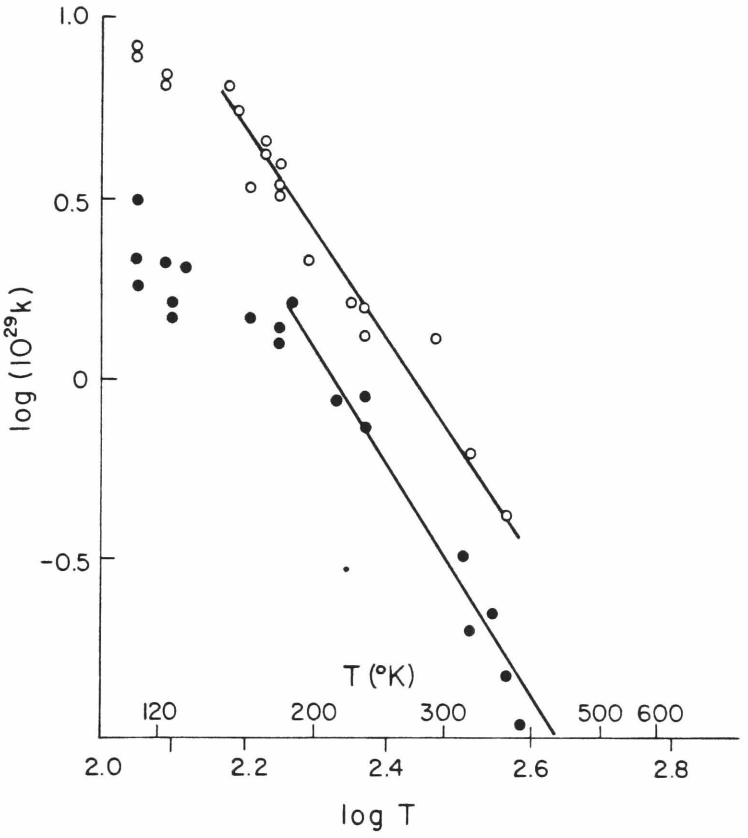

The temperature dependence of the rate constants of the reactions $HCO^+ + 2CO \longrightarrow HCO^+ \cdot CO + CO$ (•) and $HCO^+ + CO + H_2 \longrightarrow HCO^+ \cdot CO + H_2$ (o).

at these low temperatures.* This is demonstrated by the broken line in Fig. IV.1.6 for an activation energy of 0.2 kcal/mole. Since no published study to date for similar reactions includes more than two kinetic points between 80 and 280°C it is impossible to check this observation against other independent data at this time. At higher temperatures the effect of such a small activation energy would not, of course, be detectable.

Although the possibility of a positive activation energy for such highly exothermic ion-molecule reactions is unusual, a rotational barrier, as proposed by Eyring et. al. and by Wolfgang,[14] may contribute a small energy maximum on the potential surface of the reaction. Another possible source of such a small potential energy barrier could be the zero-point energies of the vibrations formed in the association process. We observe (see Fig. IV.1.5a, IV.1.6 and IV.1.7) that the deviation from linearity is more significant when CO is used as the third body than when He or H_2 are used. The energy of interaction of the CO molecules with the excited complex must be significantly larger than those of He and H_2 with the complexes, as is also seen by the formation of higher complexes including CO. Therefore, the zero-point energy is also larger in these cases, and this explanation for a small positive activation energy is compatible with our data. Naturally these considerations should be considered highly tentative until further information on the functional form of ion-molecule reaction rate constants at very low temperatures becomes available.

The temperature dependence of the reactions of interest in the present study can be obtained from the slopes of thelinear portions of the plots of log k vs. log T, Figs. IV.1.5 - IV.1.7. The experimental results are summarized in Table IV.1.2.

---

* Calculations based on a model of the decomposition of a system of coupled harmonic oscillators for the back-dissociation of the association complex can also explain this effect. This will be discussed in more detail in Section V.

5. Theoretical Considerations Concerning the Temperature Dependence of the Rate Constants.

The temperature dependence of ion-molecule association reaction rate constants has generally been interpreted on the basis of a model consisting of the following set of reactions:

$$A^+ + B \rightleftharpoons (AB^+)^* \qquad \text{(IV.1.7)}$$

$$(AB^+)^* + M \rightleftharpoons AB^+ + M \qquad \text{(IV.1.8)}$$

The back-dissociation of the excited complex $(AB^+)^*$ is treated by RRK considerations in Section V.

The temperature dependence of the rate constants may also be interpreted on the basis of the transition state theory (TST). This theory has been applied with success to the termolecular reaction $2NO + O_2 \longrightarrow 2NO_2$.[15] In Section III.1 we applied it to interpret the large negative temperature dependence ($k = CT^{-3}$) of the bimolecular ion-molecule reaction of the transfer of a hydride ion from i-C_5H_{12} to t-$C_4H_9^+$. We also found that simple TST considerations accounted successfully for the temperature dependence of termolecular ion-molecule reactions with experimental temperature dependences between T^{-1} to $T^{-4.6}$.[16]

The TST expression for the rate constant of a reaction of the type and under the conditions of interest in this study may be written (see equation (III.2.2)) as:

$$k_f \approx AT \frac{\left(T_{tr}^{3/2}\right)^{\ddagger} \left(T_{rot}^{j/2}\right)^{\ddagger}}{\prod_i \left(T_{tr}\right)_i^{3/2} \left(T_{rot}\right)_i^{j/2}} \qquad \text{IV.1.9}$$

Here we can disregard changes in the number of internal rotations upon the formation of the complex. This seems justified in the simple molecules of interest.

For the purposes of TST considerations a reaction of the general scheme of equation (IV.1.7) and (IV.1.8) may involve a termolecular complex $(ABM^+)^{\ddagger}$ and be classified as properly termolecular. Alternatively, a reaction may

proceed through a bimolecular activated complex $(AB^+)^{\ddagger}$ which can be deactivated by M in an elastic collision without forming an activated complex in the TST sense, and be classified as a bimolecular reaction proceeding with third-order kinetics.* In the termolecular case the denominator of the detailed expression in equation (IV.1.9) includes the contributions from the partition functions of A, B^+, and M; for a bimolecular mechanism only A and B^+. We used equation (IV.1.9) to calculate the temperature dependence predicted by TST of the reactions investigated in this study for both the bimolecular and termolecular mechanisms. The calculated temperature dependences and those obtained from the experimental data, i.e., from the slopes of the straight lines in Figs. IV.1.5a, IV.1.6 and IV.1.7 are shown in Table IV.1.3. For reaction 4 - 6 the experimental temperature coefficients agree well with the calculated temperature coefficients for bimolecular, linear complexes. For reactions 1 and 2 reasonably good agreement is observed between experimental temperature coefficients and those calculated for termolecular, non-linear complexes.

Moreover, from equation (IV.1.9) it is also observed that TST considerations predict a direct relation between the negative temperature dependence and the slow absolute rate of a reaction. A relation of this kind is certainly borne out by the general magnitude of the measured rate constant and the temperature dependences of reactions 1 and 2 vs. reactions 4 - 6 (Table IV.1.2).

Since all the experimental parameters, both thermodynamic and kinetic, of the reactions 1 - 3 of the even-electron ions and of the reactions 4 - 6 of the radical ions differ significantly, it is reasonable that the fundamental reaction mechanisms might also be different. However, at the present time we do not wish to speculate as to why some of these reactions should involve bimolecular and some termolecular transition complexes.

---

* Alternatively, a process of this type may be seen to proceed via a loose AB^+* - M complex, while the termolecular process via a tight AB^+*M complex, in analogy with the fast H^+ and slow H^- transfer processes of Section III.2.

TABLE IV.1.2

Thermodynamic Values, Forward Rate Constants and the Temperature Dependence of the Rate Constants for Association Reactions of HCO^+, $CO^{+\cdot}$ and $N_2^{+\cdot}$

Reaction	$-\Delta H^o$ (kcal/mole)	$-\Delta S^o$ (cal/mole degree)	$-\Delta G^o$ (kcal/mole)	$10^{29} \times k_{328}$ (cc^2/mol^2 sec)	Temperature Dependence of the Rate Constants[b]
1. $HCO^+ + CO + H_2 \longrightarrow HCO^+ \cdot CO + H_2$	11.7	20.9	5.4	0.61	$T^{-3.0}$
2. $HCO^+ + 2CO \longrightarrow HCO^+ \cdot CO + CO$	11.7	20.9	5.4	0.29	$T^{-2.9}$
3. $N_2H^+ + 2N_2 \longrightarrow N_4H^+ + N_2$	14.5	20.4	8.4	0.54	-
4. $CO^{+\cdot} + CO + He \longrightarrow C_2O_2^{+\cdot} + He$	25.4	-	-	14.2	$T^{-1.5}$
5. $CO^{+\cdot} + 2CO \longrightarrow C_2O_2^{+\cdot} + CO$	≥ 25.4	-	-	19.8	$T^{-1.5}$
6. $N_2^{+\cdot} + 2N_2 \longrightarrow N_4^{+\cdot} + N_2$	≥ 22.8[a]	19.5[a]	17.1[a]	7.9	$T^{-1.7}$

a. J.D. Payzant and P. Kebarle, J. Chem. Phys., 53, 4723 (1970).

b. For the rate constants expressed as $k = CT^n$, C are constants with respect to T, e.g. $k = k_{328}\left[\frac{T(^oK)}{328}\right]^n$.

TABLE IV.1.3

The Experimental and Predicted (TST) Temperature Dependences of Forward Rate Constants

Reaction	Experimental Temperature Dependence[a]	Temperature Dependence Predicted by TST[a]			
		Termolecular Complex		Bimolecular Complex	
		Linear Complex	Nonlinear Complex	Linear Complex	Nonlinear Complex
1. $HCO^+ + CO + H_2 \longrightarrow HCO^+ \cdot CO + H_2$	$T^{-3.0}$	T^{-4}	$T^{-3.5}$	$T^{-1.5}$	T^{-1}
2. $HCO^+ + 2CO \longrightarrow HCO^+ \cdot CO + CO$	$T^{-2.9}$				
4. $CO^{+\cdot} + CO + He \longrightarrow C_2O_2^{+\cdot} + He$	$T^{-1.5}$	T^{-3}	$T^{-2.5}$	$T^{-1.5}$	T^{-1}
5. $CO^{+\cdot} + 2CO \longrightarrow C_2O_2^{+\cdot} + CO$	$T^{-1.5}$	T^{-4}	$T^{-3.5}$	$T^{-1.5}$	T^{-1}
6. $N_2^{+\cdot} + 2N_2 \longrightarrow N_4^{+\cdot} + N_2$	$T^{-1.7}$				

a. For the rate constants expressed as $k = CT^n$.

Conclusions

Comparing the thermodynamic data for the HCO^+-CO and N_2H^+-N_2 association reactions with the thermodynamic data for the analogous reaction of $CO^{+\cdot}$ and $N_2^{+\cdot}$, it is apparent that the enthalpy of association with a neutral molecule is significantly smaller for the even electron than for the radical ions, and that forces of different nature must be effective in these reactions.

The magnitude of the rate constants of the reactions investigated in this study show a general correlation with the enthalpy of the reaction and also with the temperature dependence of the rate constants. Thus the reactions of the even-electron ions are both less exothermic, slower, and exhibit a larger negative temperature dependence than the analogous reactions of the radical ions. The temperature dependence of the rate constants exhibits a form of $k = CT^{-n}$, proving that the pre-exponential factor, rather than an activation energy is mainly responsible for the temperature dependence.

The temperature dependence of the rate constants and the other experimental correlations noted above may be interpreted qualitatively both on the basis of a model based on the RRK type unimolecular back dissociation of the excited complex and on the basis of transition state theory considerations, which have not been applied previously for termolecular ion-molecule reactions. The TST considerations offer such kinetic insights as whether the reaction proceeds through a termolecular or bimolecular excited complex. More experimental data is necessary to decide which theory is more useful and preferable.

The application of an extended range of temperatures in our study was found to be helpful in the determination of the functional dependence of the rate constant on temperature. The results at the lowest temperatures applied indicate that a very small activation energy may be present in these reactions. The investigation of the exact dependence of the rate constants on temperature is important both for the understanding of the

reaction dynamics and for the understanding of ion-molecule reaction systems at very low temperatures, such as under upper atmospheric or interstellar conditions.[17] For example, the extension of a function similar to the one that yielded the broken line on Fig. IV.1.6 shows that the reaction would be slower by a factor of about 1000 at 20°K due to an activation energy of only 0.5 kcal/mole.

The decrease of the temperature dependence of the association rate constant below ≈150°K may also be reproduced by coupled oscillator - RRK model calculations, as will be shown in Section V.

REFERENCES

1. D.P. Beggs and F.H. Field, J. Amer. Chem. Soc., 93, 1567 (1971).
2. J.J. Solomon, M. Meot-Ner and F.H. Field, J. Amer. Chem. Soc., 96, 3727 (1974).
3. S.-L. Chang and J.L. Franklin, J. Chem. Phys., 54, 1487 (1971).
4. M. Saporoschenko, J. Chem. Phys., 49, 768 (1968).
5. M.S.B. Munson, F.H. Field and J.L. Franklin, J. Chem. Phys., 37, 1790 (1962).
6. J.D. Payzant and P. Kebarle, J. Chem. Phys., 53, 4723 (1970).

7a. J.-H. Yang and D.C. Conway, J. Chem. Phys., 40, 1729 (1964).

b. D.A. Durden, P. Kebarle and A. Good, J. Chem. Phys., 50, 805 (1969).

8. D.C. Conway, J. Chem. Phys., 50, 3864 (1970).
9. A. Good, D.A. Durden and P. Kebarle, J. Chem. Phys., 52, 212 (1970).
10. D.K. Bohme, D.B. Dunkin, F.C. Fehsenfeld and E.E. Ferguson, J. Chem. Phys., 49, 5201 (1968).
11. D.K. Bohme, D.B. Dunkin, F.C. Fehsenfeld and E.E. Ferguson, J. Chem. Phys., 51, 863 (1969).
12. A.J. Cunningham, J.D. Payzant and P. Kebarle, J. Amer. Chem. Soc., 94, 7627 (1972).
13. A. Good, Trans. Faraday Soc., 67, 3495 (1971).

14a. R. Wolfgang, Accounts of Chemical Research, 3, 48 (1970).

b. S. Glasstone, K.J. Laidler and H. Eyring, in "The Theory of Rate Processes," McGraw Hill, New York, pp.127ff (1941).

15. H. Gershinowitz and H. Eyring, J. Am. Chem. Soc., 57, 985 (1935).
16. M. Meot-Ner, J.J. Solomon, F.H. Field and H. Gershinowitz, J. Phys. Chem., 78, 1773 (1974).
17. E. Herbst and W. Klemperer, The Astrophysical Journal, 185, 505 (1973).

IV.2 DECOMPOSITION RATES OF EXCITED REACTION COMPLEXES. TEMPERATURE AND PRESSURE EFFECTS IN ASSOCIATION REACTIONS INVOLVING NH_4^+, $CH_3NH_3^+$ AND $(CH_3)_2NH_2^+$

Introduction

The kinetics of the decomposition processes of excited reaction intermediates is a problem of central significance in determining the rates and results of chemical reactions. The study of reactions with well-established rates and lifetimes of excited reaction complexes and the effects of the structure, complexity, and energy content on the decomposition rates of such species. This Section reports the results of studies on the mechanism of clustering reactions of the ions NH_4^+, $CH_3NH_3^+$ and $(CH_3)_2NH_2^+$ and the effects of temperature and molecular complexity on the decomposition rates of the excited ion-molecule association complexes $(NH_4^+ \cdot NH_3)^*$, $(CH_3NH_3^+ \cdot CH_3NH_2)^*$ and $((CH_3)_2NH_2^+ \cdot (CH_3)_2NH)^*$. Some experiments were also done on clustering reactions of the larger alkylamine ions $C_2H_5(CH_3)_2NH^+$ and $(C_3H_7)_2NH_2^+$.

Experimental

The reactions were studied in mixtures of $\approx$1% NH_3 in CH_4 and $\approx$1% CH_3NH_2 or $(CH_3)_2NH$ in i-C_4H_{10}. Total pressures of 0.5 - 2.0 torr were used. Under these conditions most of the major ions of the reactant gas (CH_5^+ and $C_2H_5^+$; t-$C_4H_9^+$) react by fast H^+ transfer reactions to produce the protonated ions NH_4^+, $CH_3NH_3^+$ and $(CH_3)_2NH_2^+$. The protonated ions then react more slowly with additional molecules of the additive amine to form the association products $(NH_3)_2H^+$, $(CH_3NH_2)_2H^+$, and $((CH_3)_2NH)_2H^+$. In most cases the reaction systems were sufficiently removed from equilibrium that opposing dissociation reactions of the reaction products could be neglected; however, in some measurements at higher temperatures the opposing reactions were also considered. The kinetic analysis applied to the results was also described in previous publications.[1,2] Sample kinetic plots are shown in Fig. IV.2.1.

The overall forward reaction may be written as

$$BH^+ + B \xrightarrow{M} B_2H^+ \qquad \text{(IV.2.1)}$$

FIGURE IV.2.1

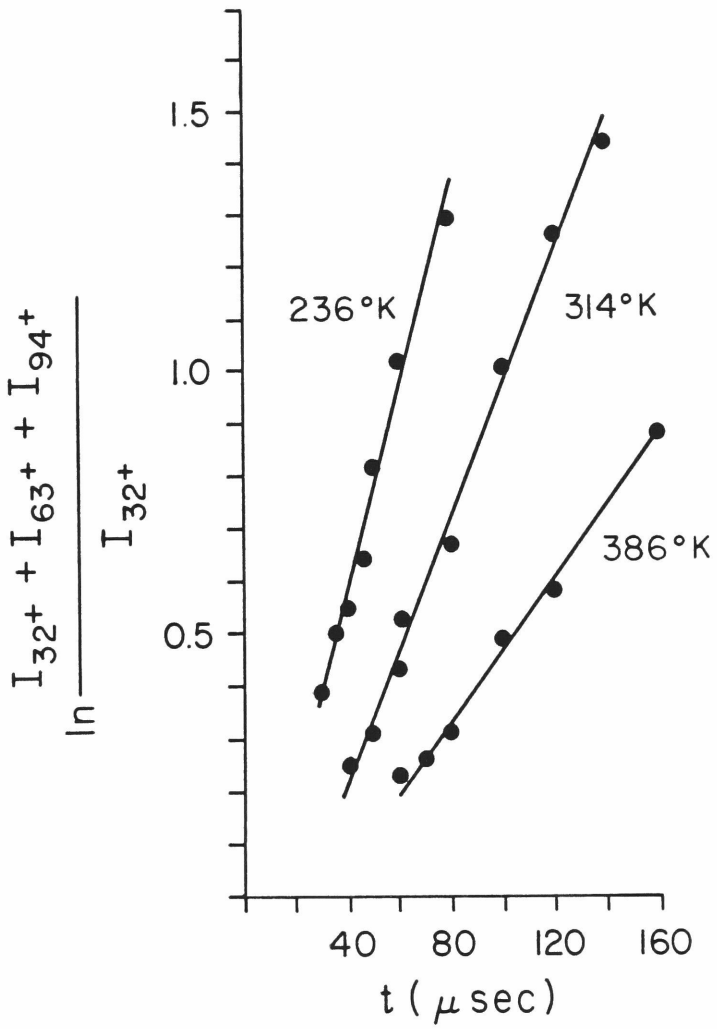

Sample pseudo-first-order kinetic plots for the association reaction $CH_3NH_3^+$ (m/e = 32) + CH_3NH_2 + i-C_4H_{10} $\longrightarrow$ $(CH_3NH_2)_2H^+$ (m/e = 63 + i-C_4H_{10}. Experimental conditions: $(M)_{i\text{-}C_4H_{10}} = 1.9 \times 10^{16}$ mol./cm.^{3}; $P_{CH_3NH_2}/P_{i\text{-}C_4H_{10}} = 0.00229$. The higher mass ion $(CH_3NH_2)_3H^+$, m/e = 94, when present, is assumed to be formed by a consecutive reaction of $(CH_3NH_2)_2H^+$. Note that since the association reactions are preceded by the protonation of CH_3NH_2 by t-$C_4H_9^+$ to form $CH_3NH_2^+$, the kinetic plots intercept the ordinate at t $\approx$30 usec. rather than at t = 0.

Since the concentration of the ions in the reaction mixtures is much smaller than the concentration of the neutrals, the kinetic measurements yield pseudo-first-order rate constants, k_1, for the disappearance of BH^+. From these the second-order rate constants are obtained as

$$k_f = k_1/(B). \qquad \text{(IV.2.2)}$$

The reproducibility of the rate constant measurements in each of the systems studied was found to be better than $\pm$ 10%.

We performed several measurements to check the agreement of the results of our measurements using the pulsed high-pressure mass spectrometric technique with published or theoretically expected equilibrium and rate constants. Using the pulsed technique to establish the attainment of equilibrium,[1,2] we measured the equilibrium constant for the reaction $(CH_3)_2NH_2^+ + (CH_3)_2NH_4^+$ $i\text{-}C_4H_{10} \rightleftharpoons ((CH_3)_2NH)_2H^+ + i\text{-}C_4H_{10}$ at 431, 437 and 468°K and obtained from the resultant van't Hoff plot for this reaction the values: ΔH° = -22.0 kcal/mole, ΔS° = -25.3 e.u. These are in acceptable agreement with the values published by Yamdagni and Kebarle:[3] ΔH° = -20.8 kcal/mole, ΔS° = -25.7 e.u. Similarly, we obtained for the reaction $C_2H_5(CH_3)_2NH^+ + C_2H_5(CH_3)_2N + i\text{-}C_4H_{10} \rightleftharpoons (C_2H_5(CH_3)_2N)_2H^+ + i\text{-}C_4H_{10}$, ΔH° = -20.2 kcal/mole, ΔS° = -29.6 e.u., in good agreement with published values for the analogous reaction involving the similar compound $(CH_3)_3N$, ΔH° = -22.5 kcal/mole, ΔS° = -32.e.u.[3] As a check on rate constant measurements, we obtained for the reaction $t\text{-}C_4H_9^+ + (CH_3)_2NH \xrightarrow{k} (CH_3)_2NH_2^+ + C_4H_8$ the value $k_{400^\circ K} = 1.45 \times 10^{-9}$ cm.^{3}/mol.sec., and for the H^+ transfer reaction from $t\text{-}C_4H_9^+$ to $(C_3H_7)_2NH$, $k_{380^\circ K} = 1.53 \times 10^{-9}$ cm.^{3}/mol. sec. These results are in very good agreement with the rate constants predicted for these reactions by the parameterized average dipole orientation theory,[4] 1.34×10^{-9} and 1.48×10^{-9} cm.^{3}/mol. sec., respectively; the former is also in good agreement with a measured experimental value,[5] 1.2×10^{-9} cm.^{3}/mol. sec.

As a further check on our technique we tested for the possibility of significant collisional dissociation of the B_2H^+ ions in the region

outside the source between the ion exit slit and ion focus plates. For this purpose we varied the potential difference between the ion exit slit and the ion focus plates, thereby varying the field strength in this region between 40 and 360 V/cm. We observed no effect of the field strength on the ion intensity ratio $I_{B_2H^+}/I_{BH^+}$. This indicates that collisional dissociation of the cluster ions is unlikely to be significant.

In summary, we observe that the results of our measurements using the pulsed ionization technique are in very good agreement with published results obtained with an instrument with a somewhat different source geometry,[3] and with theoretically expected results. Based on these reactions, we believe that our measured rate constants are accurate within 10% in absolute magnitude.

Results

1. Reaction Mechanism - Pressure Studies

The mechanism of three body ion-molecule association reactions is generally assumed to be the energy transfer mechanism:[6]

$$BH^+ + B \underset{k_b}{\overset{k_c}{\rightleftharpoons}} B_2H^+* \qquad \text{(IV.2.3)}$$

$$B_2H^+* + M \xrightarrow{k_s} B_2H^+ + M \qquad \text{(IV.2.4)}$$

The overall forward rate constant k_f may be defined be

$$\frac{d(B_2H^+)}{dt} = -\frac{d(BH)^+}{dt} = k_f\,(BH^+)(B) \qquad \text{(IV.2.5)}$$

If steady state considerations are applied to the concentration of the excited reaction complex B_2H^+*, it is readily shown that the overall forward reaction rate constant for the formation of the product ion B_2H^+ is given by

$$k_f = \frac{k_c k_s (M)}{k_b + k_s (M)} \qquad \text{(IV.2.6)}$$

If the rate of back-dissociation of the excited complex B_2H^+* is significantly larger than the rate of its deactivation, i.e., $k_b \gg k_s(M)$, then $k_f \approx \frac{k_c k_s(M)}{k_b}$, and the reaction exhibits third-order behavior. Most ion-molecule association reactions reported so far exhibit third-order behavior. On the other hand, if $k_s(M) \gg k_b$, $k_f = k_c$ and the association reaction proceeds with unit collision efficiency and exhibits second-order kinetics. In intermediate cases equation (IV.2.6) may be used to predict the dependence of k_f on (M). Comparison with experiment may then be used to test the applicability of the energy-transfer mechanism to the reactions of interest.

It is of interest to demonstrate the applicability of the energy-transfer mechanism to ion-molecule association reactions, since, although generally assumed, this does not appear to have been done before. A transition from third to second order kinetics in the clustering reactions of O_2^+ and N_2^+ with increasing third-order (He) pressure at 80^oK was reported, but the reported transition is much sharper than that predicted by equation (IV.2.6.)[7]

The model for unimolecular decomposition based on the redistribution of energy in a system of coupled oscillators (RRK model) indicates that the lifetime of excited complexes should increase with molecular complexity. Therefore, molecules with a larger number of internal degrees of freedom are good candidates even at moderately high temperatures to permit the magnitude of $k_s(M)$ to approach that of k_b, which is requisite for significant deviation from third-order behavior. Once the mechanism is established, equation (IV.2.6) may be used in conjunction with measured values of k_f and calculable values of k_c and k_s to obtain k_b, the rate constant for the decomposition of B_2H^+*, which is of much physical interest.

In Fig. IV.2.2 we show the experimental dependence of k_f on (M) at 210, 214 and 364^oK for reaction (II). (Throughout this section reactions will be referred to according to their number in Table IV.2.1). Calculated values of k_f as a function of (M) may be obtained by inverting equation

FIGURE IV. 2.2

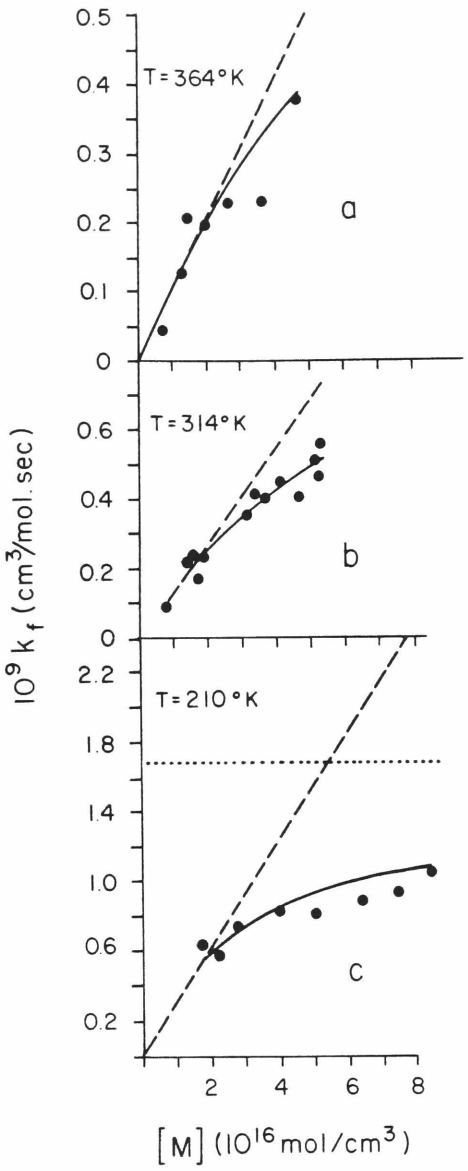

The dependence of the second-order rate constants k_f on third-body density (M) for the reaction $CH_3NH_3^+ + CH_3NH_2 \xrightarrow{M} (CH_3NH_3)_2H^+$ at 364, 314 and 210°K. The solid circles (•) are experimental values. The solid lines (——) show the dependence of k_f on (M) as predicted by equation (IV.2.6) in text, with the experimental point at (M) = 2×10^{16} mol./cm.^{3} as reference. The broken lines (---) show the calculated third-order behavior of k_f based on this reference point. The dotted line in (c) represents the collisional (ADO) second-order capture limit for k_f. M = i-C_4H_{10} in (a) and (b); M = CH_4 in (c). $(CH_3NH_2) \approx 0.01$ (M) in these experiments.

TABLE IV.2.1

Experimental Rate Constants for Clustering Reactions of NH_4^+, $CH_3NH_3^+$ and $(CH_3)_2NH_2^+$

Designation	Reaction	M	$(M)\times10^{-16}$ mol./cm.^{3}	$k_c \times 10^9$[a] cm.^{3}/mol.sec.		$k_s \times 10^9$[b] cm.^{3}/mol	$k_f \times 10^9$[c] cm.^{3}/mol.sec.		Calculated Third-Order Rate[d] Constants $k_3=k_c k_s/k_b$ (10^{-27} cm.^{6}/mol.^{2} sec.)	
				250°K	350°K		250°K	350°K	250°K	350°K
I	$NH_4^+ + NH_3 \xrightarrow{k_f} (NH_3)_2H^+$	CH_4	2.5	2.4	2.1	1.3	0.093	0.030	3.9	1.3[e]
II	$CH_3NH_3^+ + CH_3NH_2 \xrightarrow{k_f} (CH_3NH_2)_2H^+$	$i\text{-}C_4H_{10}$	1.8	1.7	1.6	1.2	0.40	0.23	30	16
III	$(CH_3)_2NH_2^+ + (CH_3)_2NH \xrightarrow{k_f} ((CH_3)_2NH)_2H^+$	$i\text{-}C_4H_{10}$	1.6	-	1.4	1.1	-	0.32	-	26

a. Capture collision rate constant for the process $BH^+ + B \longrightarrow B_2H^+*$. Since the neutral species are polar molecules, the parametrized ADO theory was used to calculate the rate constants.

b. Capture collision rate constants for the process $B_2H^+* + M \longrightarrow B_2H^+ + M$. Since CH_4 is non-polar and the dipole moment of $i\text{-}C_4H_{10}$ is small, the ADO and Langevin equations give similar rate constants for these processes. These rate constants are not temperature dependent.

c. k_f is calculated from the pseudo-first order rate constants k_1 which are directly measured in these experiments, i.e., $k_f = k_1/(B)$ where (B) is the number density of the neutral reactant B (mol./cm.^{3}).

d. k_3 is third-order rate constant for the association reaction. Since our reactions deviate from third order, k_3 is not generally directly available from our experimental observations. It is available as an approximation only under low pressure conditions. It is presented here to facilitate comparison with rate constants for other ion-molecule association reactions, which are usually published as third-order rate constants.

e. D.K. Bohme and F.C. Fehsenfeld, Can. J. Chem., 47, 2715 (1969), reported for the reaction: $NH_4^+ + NH_3 + O_2 \longrightarrow (NH_3)_2H^+ + O_2$, $k_3^{298} = 1.8 \times 10^{-27}$ cm.^{6}/mol.^{2}sec. Considering the higher third-body efficiency of CH_4, this compares well with the rate calculated from our data at 298°K: $k_3^{298} = 2.4 \times 10^{-27}$ cm.^{6}/mol.^{2}sec.

(IV.2.6) assuming k_c to be equal to the ion-molecule capture collision rate, and evaluating the ratio k_b/k_s from one experimental value of k_f and (M). These calculated values of k_f are represented in Fig. IV.2.2 by solid lines, and the agreement with the experimentally observed values is very good. The capture collision rates assumed for k_c is that predicted by the average dipole orientation (ADO) theory, and justification for its use is presented in the next section. At the lowest temperature studies ($210^{o}K$) the trend of k_f with pressure given in Fig. IV.2.2 shows that the reaction is predominantly second order in this pressure range. This undoubtedly is the result of a relatively low rate of back-dissociation of the intermediate complex. At higher temperatures the energy of the complex is higher; its dissociation rate is faster; and the pressure dependence of k_f shows that the reaction takes on more third-order character in the pressure range studied. As we show in Fig. IV.2.3 in the more complex compound $(CH_3)_2NH$ the reaction is closer to second than to third-order even at $314^{o}K$, and the experimental results agree reasonably well with the predictions of equation (IV.2.6).

For practical reasons no measurements were made of the effect of pressure on the association reaction in NH_3. Studies were made of the effect of temperature on the NH_3 reaction (see below), and in the course of these we found that NH_3 contaminated the mass spectrometer producing an unacceptable background for a long period of time. Consequently, the applicability of the energy transfer reaction to the ammonia system was assumed throughout the remainder of this Section.

2. Decomposition Rates of Excited Reaction Complexes: The Effects of Molecular Complexity.

Since the pressure studies on the kinetics of the clustering reactions of $CH_3NH_3^+$ and $(CH_3)_2NH_2^+$ confirm the applicability of the mechanism of equations (IV.2.3) (IV.2.4) we can use equation (IV.2.6) to calculate the decomposition rates of the excited reaction complexes involved in these reactions.

FIGURE IV.2.3

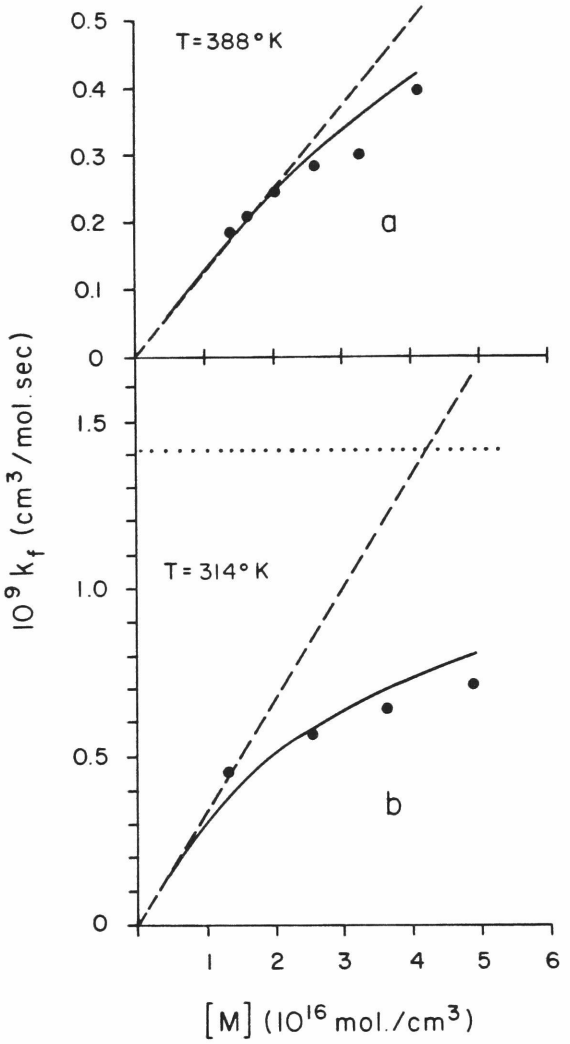

The dependence of the second-order rate constant k_f on third-body (i-C_4H_{10}) density for the reaction $(CH_3)_2NH_2^+ + (CH_3)_2NH \xrightarrow{M^f} ((CH_3)_2NH)_2H^+$. The meaning of the symbols is as in Fig. IV.2.2. The experimental point at (M) = 1.2×10^{16} mol./cm.^{3} was used as reference for the broken line in Fig. b.

It is well known that ion-molecule collisions within the critical parameter result in an orbiting ion-molecule complex which brings the reactants into close proximity. Therefore, each collision between BH^+ and B may be considered to result in an excited complex B_2H^+*, and we can take $k_c = k_{ADO}$. The ADO theory has been shown to account with good accuracy for the rate constants of ion-polar molecule reactions.[4,8,9] For the deactivation processes we selected CH_4 as the third body for the deactivation of $(NH_4^+ \cdot NH_3)*$ and $i\text{-}C_4H_{10}$ for the deactivation of $(CH_3NH_3^+ \cdot CH_3NH_2)*$ and of $((CH_3)_2NH_2^+ \cdot (CH_3)_2NH)*$. The numbers of internal degrees of freedom in the third bodies in each case is at least one half of those in the activated complexes. If equilibration of the internal energy takes place in each collision between B_2H^+* and M, one predicts that at least one third of the internal excitation energy of B_2H* is removed in each collision. Since the internal excitation energy may be taken equal to the dissociation energy of B_2H^+ ($\approx$20 kcal/mole), the removal of 6 - 7 kcal/mole from B_2H^+* will make the back dissociation of this complex negligibly slow. Therefore, the use of these efficient third bodies makes the assumption $k_s \approx k_{LANGEVIN}$ or k_{ADO} reasonable, and we used these values (Table IV.2.1), the measured values of k_f, and equation (IV.2.6) to calculate k_b, the dissociation rate constants for the activated complexes over a range of temperatures. The values of the quantities used in the calculations are given in Table IV.1.1.

The values of k_b for the reactions of this study obtained in the above manner at 250°K and 350°k are shown in Table IV.2.2. The absolute values of the dissociation rates of the excited complexes show the dependence on molecular complexity as may be expected; namely, the rate decreases as the molecular complexity increases.

3. Decomposition Rates of Excited Reaction Compelxes: Temperature Effects.

We have measured the effect of temperature upon the rate constants, k_b, for the back dissociations of the excited complexes involved in the

TABLE IV.2.2

Dissociation Half-Lives, Decomposition Rate Constants, and Temperature Dependence for Excited Reaction Complexes B_2H^+*

Complex	k_b^{EXP}[a] (10^7 sec.$^{-1}$)		Dissociative Half-Life of B_2H^+*, τ_b (10^{-9} sec.)		Temperature Dependence of k_b[b]
	250°K	350°K	250°K	350°K	
$(NH_4^+ \cdot NH_3)$*	81	220	0.86	0.32	$T^{3.2}$
$(CH_3NH_3^+ \cdot CH_3NH_2)$*	6.8	12	10	5.8	$T^{3.6}$
$((CH_3)_2NH_2^+ \cdot (CH_3)_2NH)$*	-	6.0	-	12	$T^{7.2}$

a. Obtained from k_f of the corresponding association reaction, the values of k_c and k_s as given in Table IV.2.1, and equation (IV.2.6) in text.

b. From the slopes of the plots of ln k_b vs. ln T at 375°K in Figure IV.2.4

reactions investigated. We find that the temperature coefficients of the rate constants vary with temperature; that is, the reaction rates do not have a simple functional dependence upon temperature. Representing this behavior in a convenient but meaningful way constitutes something of a problem. In the past we have represented[1,2] temperature coefficients by plotting ln k vs. ln T and for lack of a better procedure we continue this practice here in Fig. IV.2.4. As a measure of the temperature dependences for the rate constants, we have measured the slopes at 375°K of the experimental plots in Fig. IV.2.4, and the results expressed as $k_b = AT^n$ are given in Table IV.2.2. A more detailed consideration of these temperature dependences will be given later in this Section.

Third-order rate constants for our reactions are meaningful only at the low pressure limit, and may be calculated from our data as

$$k_3 = \frac{k_c k_s}{k_b} \qquad \text{(IV.2.7)}$$

To facilitate comparisons of our results with rate constants for other ion-molecule association reactions, which are generally published as k_3, we calculated k_3 for our reactions at 250 and 350°K using equation (IV.2.7). The values, which are rather large for this type of reaction, are shown in Table IV.2.1. The temperature dependences of k_3 are, of course, just as $1/k_b$, since the temperature dependences of k_c and k_s are negligible in the temperature range applied. (See Table IV.2.1). The third-order association rate constants therefore exhibit large negative temperature dependences. At 375°K these are: $T^{-3.2}$ for reaction I, $T^{-3.6}$ for II and $T^{-7.2}$ for III; the last is the largest negative temperature dependence observed for any ion-molecule reaction to date. The energy-transfer - RRKM theory predicts increasing negative temperature dependence with increasing molecular complexity. This is borne out in comparing reactions I, II and III.

FIGURE IV.2.4

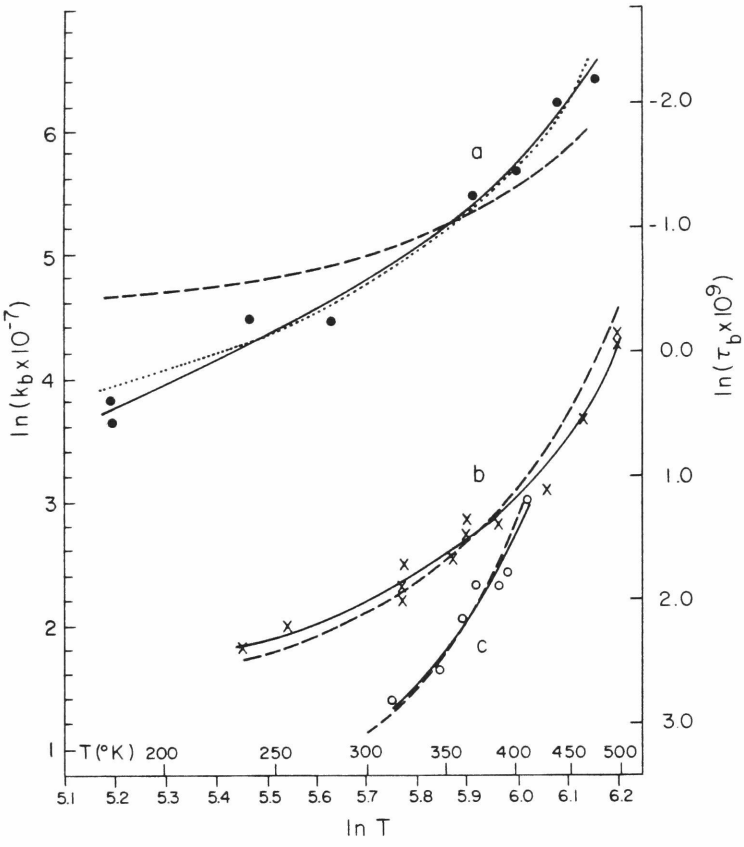

The temperature dependences of the dissociation rate constants k_b (in units of 10^7 sec.$^{-1}$) and of the dissociation half lives τ_b (in units of 10^{-9} sec.) of the excited complexes. a: $(NH_4^+ \cdot NH_3)^*$; b: $(CH_3NH_3^+ \cdot CH_3NH_2)^*$; c: $((CH_3)_2NH_2^+ \cdot (CH_3)_2NH)^*$. For ease of reference, the absolute temperature (^oK) is also indicated. The broken lines give the theoretical temperature dependences predicted by the RRKM theory, equation (V.9) (wide infra), with s=3N-6 and $\tilde{\nu}$ = 850 cm.$^{-1}$; for the dotted line in plot of $\tilde{\nu}$ = 650 cm.$^{-1}$ was used. For the sake of clarity the theoretical lines were translated such that they coincide with the experimental plots at 350^{o}K, i.e., these are plots of $\left[k_{b_{CALC}}^{T} \times (k_{b_{EXP}}^{350} / k_{b_{CALC}}^{350})\right]$ vs. ln T, where the values of $k_{b_{CALC}}^{350}$ are 4.4 x 10^6, 5.3 x 10^5 and 3.7 x 10^4 for the broken lines in plots a, b and c, correspondingly, and 3.2 x 10^6 for the dotted line in plot a.

4. Observations of the Kinetics of the Clustering Reactions of $C_2H_5(CH_3)_2NH^+$ and $(C_3H_7)_2NH^+$

In order to examine the dependence of reaction kinetics on further increase in molecular complexity, we attempted to conduct kinetics studies on the clustering reactions of $C_2H_5(CH_3)NH^+$ and $(C_3H_7)_2NH^+$. These reactions, however appear to proceed with a mechanism different from the association reactions involving the smaller reactants. A typical pressure study is shown in Fig. IV.2.5. The dependence of k_f on (M) does not follow the predictions of equation (IV.2.6), and, furthermore, k_f levels off to a second order limit which is different from the Langevin or ADO collision rate: e.g., for the case shown in Fig. IV.2.5, it is about 0.25×10^{-9}, which is 5 times less than the ADO value of 1.26×10^{-9} cm.^{3}/mol. sec. Unlike the capture collision rate, this second-order limiting rate exhibits large negative temperature dependence. We cannot readily explain this behavior; we wish to note, though, that the size of the reactant molecules in these reactions approaches the critical Langevin collision parameter. The kinematics of ion-molecule reactions in which the size of the reactants is too large to permit the formation of orbiting complexes in the traditional sense presents an interesting problem.

Discussion

In a previous publication[10] we proposed a simple application of transition state theory (TST) to the temperature dependence of termolecular ion-molecule association reactions. The temperature dependence was interpreted on the basis of the temperature dependences of the transitional and rotational partition functions of the reaction complex and of the reactants:

$$k_3 = AT \frac{(T_{trans})^{3/2} \quad (T_{rot})^{3/2}}{\prod_i (T_{trans}{}^{3/2})_i \quad (T_{rot}{}^{3/2})_i} \quad T_{int\ rot}^{r/2} \qquad \text{(IV.2.8)}$$

Here A is a constant; the product in the denominator is over the i reactants; and the term $T_{int\ rot}^{r/2}$ arises from the partition functions of the

FIGURE IV.2.5

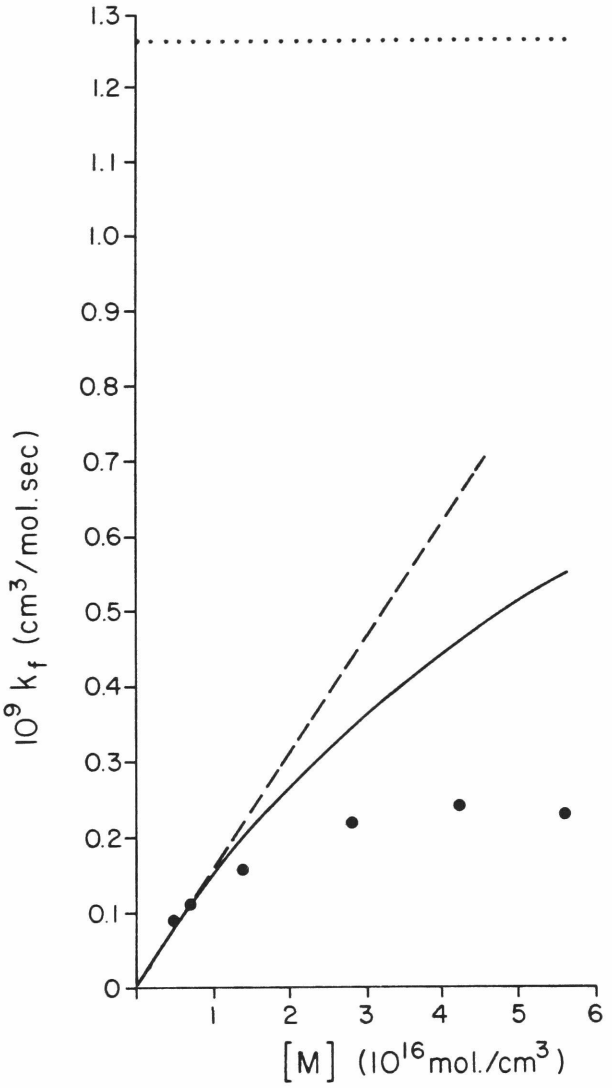

The dependence of the second-order rate constant k_f on third-body (i-C_4H_{10}) density for reaction $C_2H_5(CH_3)_2NH^+ + C_2H_5(CH_3)_2N \xrightarrow{M} (C_2H_5(CH_3)_2N)_2H^+$ at 354°K. The meaning of the symbols is as in Fig. IV.2.2. Note that the experimental points level off at $\approx 0.25 \times 10^{-9}$ cm.^{3}/mol.sec., rather than following the prediction of equation (IV.2.6). The levelling off is far below the ADO bimolecular collision rate, 1.26×10^{-9} cm.^{3}/mol.sec.

total number (r) of internal rotations created ($r > 0$) or destroyed ($r < 0$) upon the formation of the complex. In deriving equation (IV.2.8) it was assumed that no vibrational degrees of freedom of the activated complex or of the reactants were activated; that is, the vibrational partition functions were all taken to be unity. We found that equation (IV.2.8) represented well the experimental temperature dependencies of the rate constants of the association reactions of small ions and molecules.

The predictions of this model may be compared to our results if we recall that the temperature dependence of k_3 is equal to that $1/k_b$. Equation (IV.2.8) predicts a linear relation between ln k_3 (and ln $1/k_b$) and ln T. The curvature that is observed in the experimental plots of Fig. IV.2.4 cannot be easily explained on the basis of equation (IV.2.8). Inclusion of temperature terms from the partition functions of excited low-frequency vibrational modes in the complex will cause a curvature in the plots of ln k_3 vs. ln T based on IV.2.8, but the curvature will be of opposite sign to that observed experimentally. Thus transition state theory in the degree of sophistication entailed in the derivation of equation (IV.2.8) does not appear to be satisfactory for the reactions presently investigated. Transition state theory may be applied to the present reaction systems only if it is used in conjunction with the energy transfer mechanism. Collision rates for k_c and k_s can be obtained from TST, and these may be combined with values of k_b obtained from RRKM considerations to obtain values of k_3.

In conclusion, the results demonstrate the applicability of the energy transfer mechanism to ion-molecule association reactions. The rate constants of the dissociation of the excited association complexes are in the range $\approx 10^9 - 10^7$ sec.$^{-1}$. The dissociation rate constants decrease with increasing molecular complexity and increase with increasing temperature. These trends can be quantitatively reproduced by the coupled quantum oscillator RRK model, as will be shown in Section V.

REFERENCES

1. J.J. Solomon, M. Meot-Ner and F.H. Field, J. Amer. Chem. Soc., 96 3727 (1974).
2. M. Meot-Ner and F.H. Field, J. Chem. Phys., 61, 3742 (1974).
3. R. Yamdagni and P. Kebarle, J. Amer. Chem. Soc., 95, 3504 (1973).
4. T. Su and M.T. Bowers, Int. J. Mass Spectrom. and Ion Phys., 12, 347 (1973).
5. L. Hellner and L.W. Sieck, J. of Research of N.B.S., 75A, 487 (1971).
6. E. Rabinowich, Trans. Faraday Soc., 33, 283 (1937).
7. D.K. Bohme, D.B. Dunkin, F.C. Fehsenfeld and E.E. Ferguson, J. Chem. Phys., 49, 5201 (1968); E.E. Ferguson, in "Ion-Molecule Reactions," J.L. Franklin, ed., Plenum Press, New York, 1972, Vol. 2, p.371.
8. R.S. Hemsworth, J.D. Payzant, H.J. Schiff and D.K. Bohme, Chem. Phys. Letters, 26, 417 (1974).
9. M. Meot-Ner and F.H. Field, J. Amer. Chem. Soc., 97, 2014 (1975).
10. M. Meot-Ner, J.J. Solomon, F.H. Field and H. Gershinowitz, J. Phys. Chem., 78, 1773 (1974).

IV.3 ASSOCIATION AND SOLVATION REACTIONS OF PROTONATED GASEOUS AMINO ACIDS*

Introduction

Reversible association reactions of protonated ions with neutral molecules of the type

$$MH^+ + M \rightleftharpoons M_2H^+ \qquad \text{(IV.3.1)}$$

and the association of ions with gaseous solvent molecules of the type

$$X^+ + \text{SOLVENT} \rightleftharpoons X^+ \cdot \text{SOLVENT} \qquad \text{(IV.3.2)}$$

have been investigated extensively recently using high pressure mass spectrometric techniques.[1-4] The results are providing a better understanding of the intrinsic properties of ionic reactions, as in the gas phase such reactions are observed in the absence of liquid solvent effects.[5] To date, investigations of gaseous ion-solvent interactions have been limited to the reactions of small ions, mainly of inorganic interest.

In the present study we have investigated the association of protonated ions of the amino acids valine ($(CH_3)_2CHCH(NH_2)COOH$) and proline

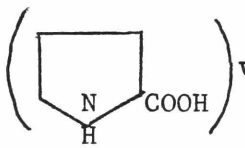

with neutral molecules of valine and proline, with the proton-bonding solvents H_2O and NH_3, and with the non-proton bonding solvent CH_3NO_2. In addition to their intrinsic interest as ion-molecule interactions, the energetics of the solvation reactions of protonated amino acid molecules are of potential interest in the physical chemistry of protein conformation, while the association reactions may be of potential interest in exobiological processes.

Experimental

The scope of quantitative mass spectrometric gaseous ionic studies is limited at the present time to compounds of relatively high volatility. Problems of volatility restricted our studies in amino acids to those

---

* M. Meot-Ner and F.H. Field, J. Amer. Chem. Soc., 96, 3168 (1974).

reported. The low volatility of these compounds also renders the pressure of the vapor of such samples in the ion source indeterminable, thereby imposing some restrictions and uncertainties on the experimentally available data for the association reactions, but not for the solvation reactions, as will be discussed below. Quantitative studies on the thermodynamics of ion-molecule reactions of compounds of comparably low volatility have not been reported previously.

In the present studies the major reactant gas was i-C_4H_{10}, and it constituted 90-100% of the reactant mixture. The solvent gases (NH_3, H_2O, and CH_3NO_2) were added to the i-C_4H_{10} in amounts between 2 and 10%. The mixtures of the solvent gases with i-C_4H_{10} were made up with quantitative accuracy so that the partial pressures of the solvents in the ionization chamber could be accurately calculated from the experimentally measured total pressures. The total source pressure was kept at 1.4 torr, except where otherwise specified. The amino acids were introduced into the flow of the reactant mixture 40 cm. upstream from the ion source, using a glass probe heated to 140°C. The temperature of the probe was kept constant during the course of each experiment in order to maintain a constant pressure of the amino acid vapor. Constancy of the presure of the amino acid vapor in the ion source was confirmed by the observations that the ratios $I_{MH}^+/I_{i\text{-}C_4H_9}^+$ and $I_{M_2H}^+/I_{MH}^+$ remained constant at constant source conditions for time periods which were considerably longer than the time required for a typical experiment. The ratios $I_{M_2H}^+/I_{MH}^+$ are dependent on the pressure of the amino acids, as $I_{M_2H}^+/I_{MH}^+ = K \cdot P_M$, where K is the equilibrium constant of the association reactions of the type given in equation (IV.3.1).

For some of the studies the mass spectrometer was operated in the pulsed mode, which permitted an examination of the variation of the apparent equilibrium constant with the residence time in the ionization chamber for the ions involved in the equilibria as described earlier. However, since chronologically this study was the first of those reported

in this thesis, most of the work was done in the continuous mode, in which the ions are generated by a continuous electron beam, diffuse continuously out of the source and are collected continuously at the detector. In this mode the average residence time of the ions under our conditions can be calculated at 50 - 100 μsec.

In the pulsed mode of the operation the mass spectrometer sensitivity is much reduced; consequently our pulsed studies were restricted to reactions of the more volatile of the two amino acids, valine.

Results and Discussion

Equilibrium constants for the solvation reaction (equation IV.3.2) were calculated as

$$K_a = \frac{I_{MH^+ \cdot SOLVENT}}{I_{MH^+} P_{SOLVENT}} \qquad \text{(IV.3.2)}$$

where $I_{MH^+ \cdot SOLVENT}$ = peak intensity of the solvated ion, I_{MH^+} = peak intensity of the unsolvated protonated ion, and $P_{SOLVENT}$ = pressure of solvent in atmospheres.

The presence of equilibrium in the solvation reactions under our experimental conditions was in part established by the dependence of the equilibrium constants on the total source pressure. The results for the solvation reaction of $ValH^+$ are shown in Fig. IV.1.1. $ProH^+$ behaved similarly. In these studies K_a shows an increase with increasing total source pressure up to P = 1.2 torr. The increase in K_a results from the increase of the number of ion-molecule collisions as well as from the increase of the residence time of the ions with increasing pressure. In the present experiments K_a obtains a constant value of $P \cong 1.2$ torr, indicating that equilibrium has been obtained in the solvation reactions. The presence of equilibrium in the solvation reactions was also tested by varying the pressure of the solvent by about an order of magnitude about the solvent pressure at which the temperature studies (vide infra) were conducted. The results showed no significant dependence of K on the pressure of the solvent; for example, the values of $\log K_{385}$ for the reaction

FIGURE IV.3.1

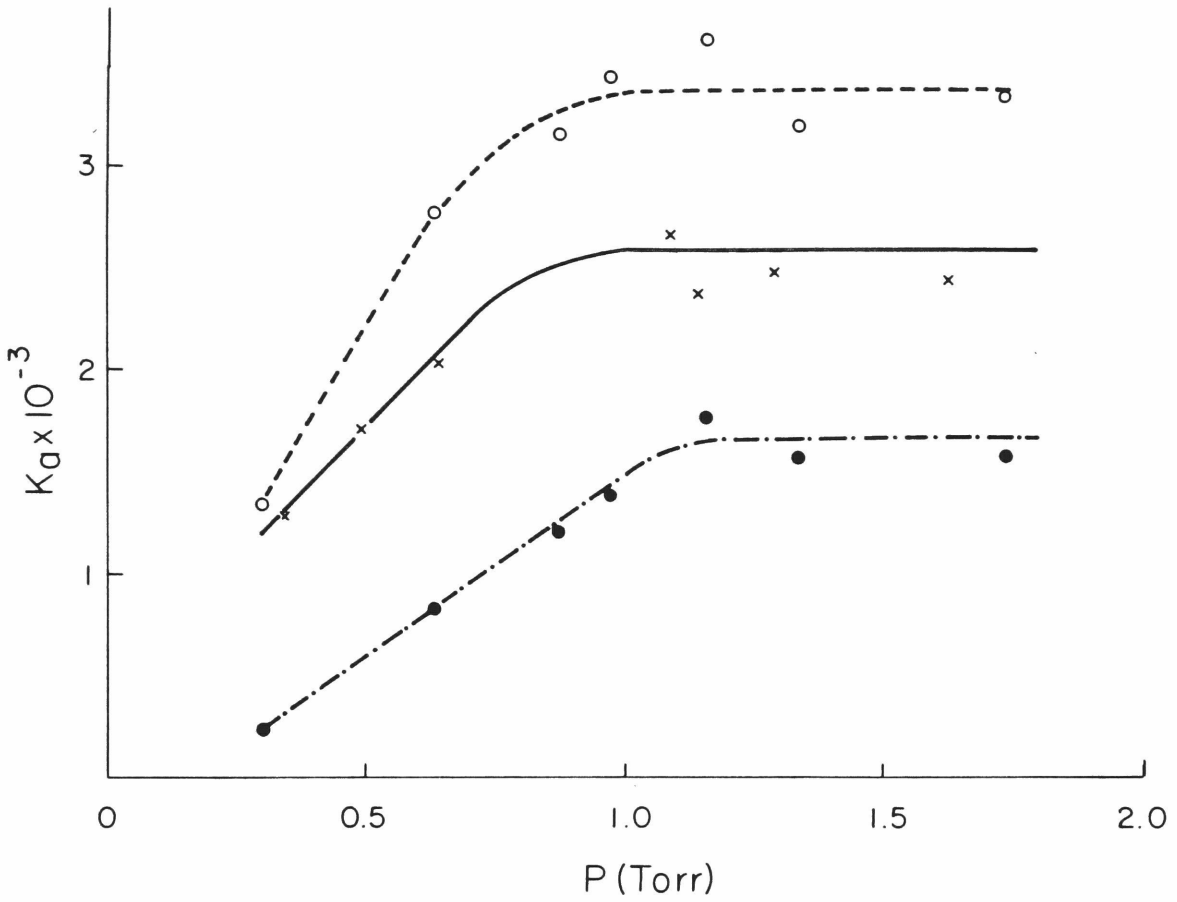

The dependence of the observed equilibrium constant of the solvation reactions, $K_a = 760 \frac{I_{VALH^+ \cdot SOLVENT}}{I_{VALH^+} P_{SOLVENT\ (torr)}}$ on the total source pressure.

(a) ✕——✕ : SOLVENT = H_2O, T = 385°K;

(b) o---o- Solvent = NH_3; T = 463°K;

(c) ●—●—● Solvent = CH_3NO_2; T = 463°K. Ordinate scale to be multiplied by 10 for graph (c).

$ValH^+ + H_2O \rightleftharpoons ValH^+ \cdot H_2O$ were measured as 3.29 at P_{H_2O} = 0.016 torr, 3.32 at P_{H_2O} = 0.230 torr, and 3.27 at P_{H_2O} = 0.620 torr. The latter pressure of H_2O vapor in the ion source was used in the temperature studies. The total source pressure was kept constant at 1.4 torr in the composition studies. The results constitute evidence that the ratios $\frac{I_{MH^+ \cdot SOLVENT}}{I_{MH^+} P_{SOLVENT}}$ are determined by equilibrium rather than kinetic effects in our experiments. Values of ΔG^o_{300}, enthalpies, and entropies for the solvation reactions, obtained from the van't Hoff plots of log vs. $\frac{10^3}{T}$ (Fig. IV.3.2), are reported in Table IV.3.1.

The validity of the thermodynamic values and of the assumption of equilibrium in the solvation reactions was further tested in the study of the behavior of the apparent equilibrium constant, $K_a = \frac{I_{MH^+ \cdot SOLVENT}}{I_{MH^+} P_{SOLVENT}}$ as a function of reaction time. The behavior of K_a for the reaction

$$ValH^+ + H_2O \rightleftharpoons ValH^+ \cdot H_2O \qquad \text{(IV.3.4)}$$

is shown in Fig. IV.3.3. We take the invariance with time of K_a, i.e., the ratio $\frac{I_{ValH^+ \cdot H_2O}}{I_{ValH^+}}$, as evidence that equilibrium has been obtained. The equilibrium constant corresponding to the time invariant portion of Fig. IV.3.3 is $K = 4.0 \times 10^4$ ($T = 328^oK$) (standard state = 1 atm.). From the thermodynamic values for this reaction listed in Table IV.3.1 we calculated the value $K = 8.80 \times 10^4$ (328^oK), and the agreement between these two values lies within the error limits of the thermodynamic values.

Equilibrium constants for the solvation of $ValH^+$ by NH_3 and CH_3NO_2 at 460^oK were determined by similar methods from the time invariant portions of the plots of K_a vs. reaction time. The values obtained were $K = 3.2 \times 10^3$ and 1.6×10^3 for NH_3 and CH_3NO_2, respectively. The values

FIGURE IV.3.2

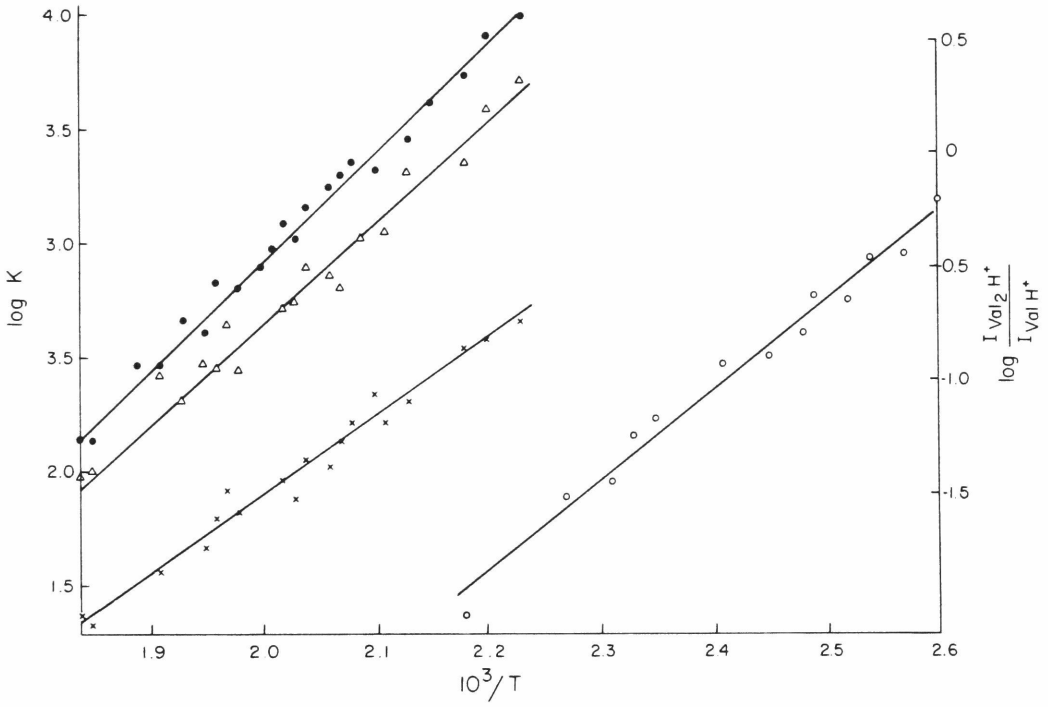

Sample van't Hoff plots for association and solvation reactions:

(a) ✕—✕ $ValH^+ + Val \rightleftharpoons Val_2H^+$;

(b) o—o $ValH^+ + H_2O \rightleftharpoons ValH^+ \cdot H_2O$;

(c) ●—● $ValH^+ + NH_3 \rightleftharpoons ValH^+ \cdot NH_3$;

(d) Δ—Δ $ValH^+ + CH_3NO_2 \rightleftharpoons ValH^+ \cdot CH_3NO_2$

In graph (a) $I_{Val_2H^+}/I_{ValH^+}$, rather than K_a vs. $\frac{10^3}{T}$ is plotted as P_{Val} is unknown. The ordinate scale on the right hand side relates to graph (a).

TABLE IV.3.1

Thermodynamic values for association and solvation reactions in protonated gaseous valine and proline. Error estimates are based on maximum deviation from the mean of values obtained in replicate experiments.

Reaction	ΔG°_{300} Kcal mole^{-1}	ΔH° Kcal mole^{-1}	ΔS° cal mole^{-1} degree^{-1}
$ValH^+ + Val \rightleftharpoons Val \cdot H^+ \cdot Val$	-	-20.7 $\pm$2.0	-
$ProH^+ + Pro \rightleftharpoons Pro \cdot H^+ \cdot Pro$	-	-20.0 $\pm$2.0	-
$ValH^+ + Pro \rightleftharpoons Val \cdot H^+ \cdot Pro$	-	-23.4 $\pm$2.0	-
$ProH^+ + Val \rightleftharpoons Pro \cdot H^+ \cdot Val$	-	-21.0 $\pm$2.0	-
$ValH^+ + H_2O \rightleftharpoons ValH^+ \cdot H_2O$	-8.4 $\pm$2.0	-19.3 $\pm$1.0	-36.3 $\pm$3.0
$ProH^+ + H_2O \rightleftharpoons ProH^+ \cdot H_2O$	-7.7 $\pm$2.0	-18.9 $\pm$1.0	-36.8 $\pm$3.0
$ValH^+ + NH_3 \rightleftharpoons Val \cdot H^+ \cdot NH_3$	-12.6 $\pm$2.0	-20.9 $\pm$1.0	-26.8 $\pm$3.0
$ProH^+ + NH_3 \rightleftharpoons Pro \cdot H^+ \cdot NH_3$	-11.9 $\pm$2.0	-20.6 $\pm$1.0	-28.9 $\pm$3.0
$ValH^+ + CH_3NO_2 \rightleftharpoons ValH^+ \cdot CH_3NO_2$	-12.4 $\pm$2.5	-19.8 $\pm$1.5	-27.8 $\pm$4.0
$ProH^+ + CH_3NO_2 \rightleftharpoons Pro \cdot H^+ \cdot CH_3NO_2$	-11.0 $\pm$2.5	-17.5 $\pm$1.5	-21.6 $\pm$4.0

FIGURE IV.3.3

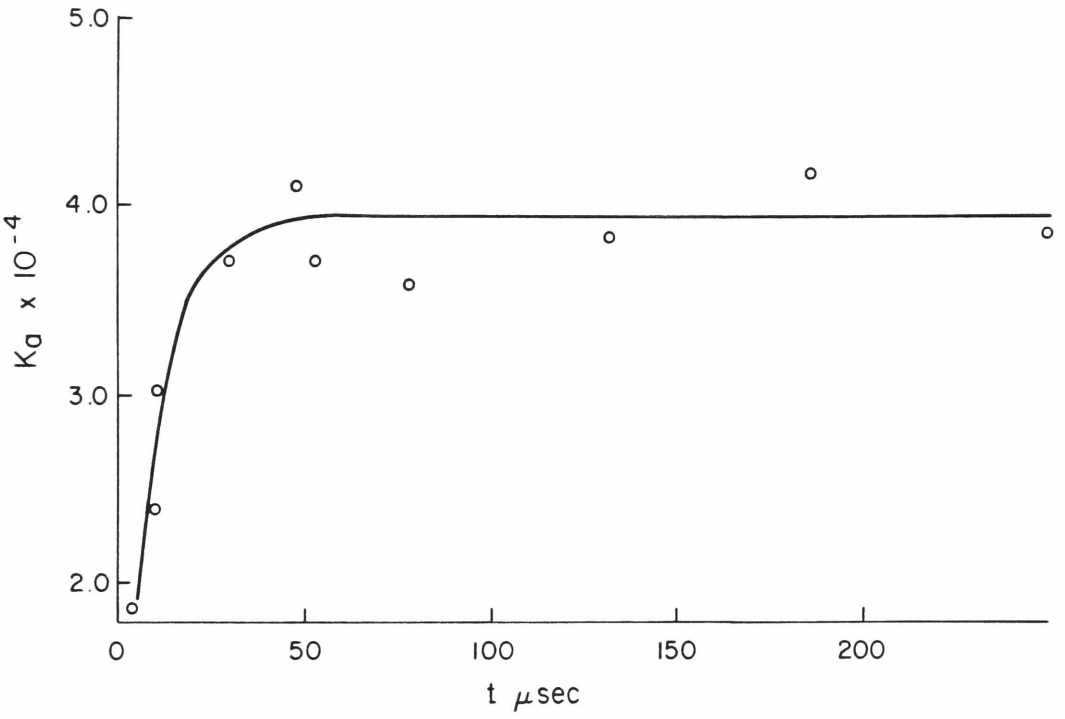

The dependence of $K_a = \frac{I_{ValH^+.H_2O}}{I_{ValH^+} P_{H_2O}}$ on reaction time at 328°K P_{TOTAL} = 1.2 torr, P_{H_2O} = 0.028 torr.

calculated from the thermodynamic data of Table IV.3.1 are 4.5×10^3 and 2.2×10^3, again in good agreement within the experimental error limits.

The satisfactory agreement between the equilibrium constant values obtained with continuous ionization (K_a invariant with pressure) and with pulsed ionization (K_a invariant with time) provides strong evidence that the systems had achieved equilibrium.

As discussed above, the pressure of the amino acids in the ion source may be assumed constant through each experiment, but its value is not known. Consequently $\frac{I_{M_2H^+}}{I_{MH^+}}$ vs. $\frac{10^3}{T}$ was plotter for these reactions. The value of the enthalpy, but not the entropy, for these reactions may be obtained from these plots since

$$\Delta H^o = -\frac{1}{R}\frac{d\ln K}{d\frac{1}{T}} = -\frac{1}{R}\frac{d\ln (I_{M_2H^+}/I_{MH^+})\cdot\frac{1}{P_M}}{d\frac{1}{T}} = -\frac{1}{R}\left(\frac{d\ln I_{M_2H^+}/I_{MH^+}}{d\frac{1}{T}}\right)_{P_M} \quad \text{(IV.3.5)}$$

Values of ΔH^o for the association reactions are also shown in Table IV.3.1.

Tests using the variation of pressure are not applicable to the establishment of equilibrium in the association reactions $MH^+ + M \rightleftharpoons M_2H^+$, since we do not know the actual pressure of the amino acid nor can we be sure that it would remain constant if the pressure of reactant gas mixture were varied. The existence of equilibrium in the reaction is implied, however, by the linearity of the van't Hoff plots and by the fact that the values of the enthalpy of the association reactions proved to be independent of the complexity of the reaction systems from which these values were obtained. For example, the value of ΔH^o for the reaction $ValH^+ + Val \rightleftharpoons Val_2H^+$ was measured as -21.1 kcal/mole in a reaction system of Val + i-C_4H_{10}, involving only one significant equilibrium reaction, and as -20.1 kcal/mole in a reaction system of Val + Pro + NH_3 + CH_3NO_2 + i-C_4H_{10}, which can be shown to involve 15 significant simultaneous association, solvation, and proton transfer equilibria. The lack of dependence of the equilibrium constants and of the thermodynamic values

obtained from this on the complexity of the reaction system is a consequence of the principle of microscopic reversibility as applied to gaseous ion chemistry.

The enthalpies of the association reactions (Table IV.3.1) are comparable to, although slightly lower than, the enthalpies of the association reactions between protonated and neutral gaseous amine molecules.[3] Comparison of the enthalpies of solvation of the $ValH^+$ and $ProH^+$ show no significant differences. It is interesting that the enthalpies of solvation of both ions by the solvents H_2O and NH_3 which are considered as hydrogen bonding in solution are quite comparable in magnitude to the enthalpies of solvation by the non-hydrogen bonding CH_3NO_2. It should be noted, however, that in the gas phase all of these solvents may serve as proton acceptors.

The thermodynamic parameters of the interactions of charged amino acid residues with solvent clusters of various sizes, from single molecules to full solvent, are an essential factor in the determination of biophysically important phenomena, such as the changes in the extent of solvation and in the pK values of amino acid residues upon conformational changes in proteins in protonating environments.[6,7] We think that the quantitative determination by mass spectrometric studies of solute-solvent interactions for ions of biologically important compounds will provide information relevant to the energetics of such ions in their biological environments. Similarly the information available from mass spectrometric studies on the energies of interaction between protonated and non-protonated amino acids may be helpful in the understanding of the role of such interactions on the determination of protein conformation.

Association complexes of the type $ValH^+ \cdot Val$ etc., were shown by Leclerq and Desiderio[4] to form preferentially in a "head-to-tail" configuration and to decompose in several condensation processes including the loss of H_2O, presumably leading to the production of protonated dipeptides. Association reactions of the types investigated in this study may therefore constitute the first step in reactions leading to the

abiotic synthesis of large molecules of potential biogenetic significance, under ionizing conditions that are frequently assumed in environments of interest in biogenetic and exobiological studies.

REFERENCES

1. F.H. Field, J. Am. Chem. Soc., 91, 2827 (1969).
2. S.L. Bennett and F.H. Field, J. Am. Chem. Soc., 94, 5186 (1972).
3. R. Yamdagni and P. Kebarle, J. Am. Chem. Soc., 95, 3504 (1973).
4. P.A. Lerlercq and D.M. Desiderio, Org. Mass Spectrom., 7, 515 (1973).
5. P. Kebarle in "Ion-Molecule Reactions," (J.L. Franklin, ed.) Vol. 2 Chapter 7 (Plenum Press, New York, 1972).
6. T. Schleich and P.H. von Hippel, Biochemistry, 9, 1059 (1970).
7. G.C.K. Roberts, D.H. Meadows and O. Jardetzky, Biochemistry, 8, 3053 (1969).

V. UNIMOLECULAR DISSOCIATION RATES OF EXCITED ION-MOLECULE ASSOCIATION COMPLEXES: AN RRKM DEGENERATE QUANTUM OSCILLATOR TREATMENT

Ion-molecule association reactions are generally assumed[1,2,3] to proceed through the energy transfer mechanism:

$$A^+ + B \underset{k_b}{\overset{k_c}{\rightleftharpoons}} AB^{+*} \qquad \text{(V.1.a)}$$

$$AB^{+*} + M \xrightarrow[k_s]{} AB^+ + M \qquad \text{(V.1.b)}$$

Assuming steady state for (AB^{+*}), the overall forward rate coefficient obtained for mechanism (1) is

$$k_f = \frac{k_c k_s (M)}{k_b + k_s (M)} \qquad \text{(V.2)}$$

The energy transfer mechanism was recently confirmed by the effect of (M) on k_f in the clustering reactions of $CH_3NH_3^+$ and $(CH_3)_2NH_2^+$. (Section IV.2) Using the energy transfer mechanism, and with k_c and k_s estimated from ion-molecule collision rate calculations, k_b^{EXP}, a quantity of much physical interest, can be found from the experimental value of k_f. To date, only the classical oscillator RRK model has been used,[1,2,3] mostly in a qualitative way, to interpret the dependence of k_f and k_b on molecular and experimental parameters. However, the classical oscillator model is known to give inaccurate results.[4,5] The interpretation of our detailed kinetic data on ion-molecule association reactions requires the application of more accurate forms of the kinetic theories. Thus, from the investigations on ion-molecule clustering reactions of CO^+, HCO^+, N_2^+ and N_2H^+ (Section IV.1) over an extended temperature range (100^o to 600^oK) the functional form of $k_b(T)$ may be meaningfully established. The dependence of k_b^{EXP} on molecular complexity has also been investigated experimentally in Section IV.2. The objective of the present work is to compare the predictions of the coupled quantum oscillator model for the decomposition of the excited reaction complexes with the values of k_b^{EXP} which may be obtained from these measurements.

Derivation of the Decomposition Rate Constant k_b^{CALC}

A special difficulty in applying the coupled oscillator model to ion-molecule association complexes is the fact that there are no spectroscopic data available on the structures of these species. The enthalpies of association, ΔH^o, which are in most cases -10 to -25 kcal/mole, indicate the presence of a weak bond and, presumably, low frequency modes associated with it, in ion-molecule complexes.

The observed strong temperature dependence of k_b down to 100°K also indicates the presence of low-frequency easily excitable modes in the complexes. In the absence of more detailed structural information, the RRKM model applied to the decomposition of a system of degenerate, weakly coupled low frequency quantum oscillators is the most rigorous model that can be meaningfully applied to the calculation of k_b^{CALC}. The equation developed by Johnston for this model[5] will be used in this work.

Another major problem in the application of the RRKM method to the calculation of k_b^{CALC} for the excited complexes is the question of the distribution of AB^+* over the manifold of available energy states. At low pressures, where k_f exhibits third order behavior, the lifetime of the complexes is shorter than the time between collisions with M. There is, therefore, no significant collisional thermal activation, deactivation or transition between the states. The relative rates of formation of the complex in each energy state AB_E^+ and the distribution of E into internal and external modes is a complex problem of molecular dynamics. To make the problem more readily tractable, we use the treatment as follows.

To establish the ratio between k_{c_E}, the rate constant for the formation of AB^+ in the energy state E, i.e., of AB_E^+, and between k_{b_E}, the rate constant for the back-dissociation from this state, we consider for the moment a situation of complete thermodynamic and chemical equilibrium in the reaction system. In this case each reaction and its opposite occur

at equal rates, and one can write:

$$k_{c_E}(A^+)(B) = k_{b_E}(AB_E^+) = k_{b_E}P_E(AB^+) \qquad (V.3)$$

Here (A^+), (B) and (AB^+) are the equilibrium concentrations of these species. Note that in equation (V.3) (AB^+) stands for the concentration of AB^+ in all possible states with E going from the ground-state energy to infinity. P_E in equation (V.3) denotes the thermodynamic probability of AB^+ being in the energy state E in the equilibrium system. Equation (V.3) may be rewritten as

$$\frac{k_{c_E}}{k_{b_E}} = P_E \frac{(AB^+)}{(A^+)\ (B)} = P_E K \qquad (V.4)$$

The relation of equation (V.4) between k_{b_E} and k_{c_E} are true also in the absence of equilibrium; this is evident on the basis of the principle that rate constants do not depend on the presence of opposing reactions.[6]

The energy transfer mechanism of equation (V.1) can be applied to the reaction proceeding via each available energy state AB_E^+ of AB^+*. This treatment yields for the concentration of AB_E^+, in a system similar to that of equation (V.1), i.e., in the absence of a reaction opposing V.1.b:

$$(AB_E^+) = \frac{k_{c_E}}{k_{b_E} + k_s(M)}(A^+)(B) \approx \frac{k_{c_E}}{k_{b_E}}(A^+)(B) \qquad (V.5)$$

The latter relation being accurate at low pressures, since $k_{b_E} \gg k_s(M)$. Comparing the concentrations of (AB^+) in two energy states $E_1 = (n_1+\frac{1}{2})h\nu$ and $E_2 = (n_2+\frac{1}{2})h\nu$, one obtains from equation (V.4) and (V.5).

$$\frac{(AB_{E_1}^+)}{(AB_{E_2})} = \frac{P_{E_1}}{P_{E_2}} = \frac{g_1 e^{-E_1/RT}}{g_2 e^{-E_2/RT}} \qquad (V.6)$$

Here g is the multiplicity of the state with energy E. For a system of s coupled equal oscillators with a total of n quanta of energy the multi-

plicity g is:

$$g = \frac{(n+s-1)!}{n!\ (s-1)!} \qquad (V.7)$$

Note that equation (V.6) was obtained by the use of the right most expression of V.5; therefore it is true at the low pressure limit where the distribution is not affected by collisions with (M) and where no direct transitions between the states of AB_E^+ are possible. The distribution V.6 is brought about by the rapid dynamic equation between the thermalized reactants and between the excited association complexes. Here, of course, stabilized AB^+ complexes are absent; i.e., each complex formed from the reactant has at least an energy equal to that required for the separation of AB^+ into A^+ and B. This critical energy will be called here $mh\nu$, where ν is the frequency of the oscillators of the decomposing system; in addition, i quanta of thermal origin may also be present. It is between the states with $E = (m+i)\ h\nu$, $i = 0$ to ∞, that the distribution of equation (V.6) applies.

In the RRKM model the decomposition rate $k_{b_E} = k_{(m+i)}$ of a system of s oscillators with total energy $E = (m+i)h\nu$ is a function of (m+i). Here m is the critical number of quanta which must be frozen in a given distribution - e.g., concentrated in the decomposing oscillator - such that decomposition will take place. In addition, j quanta ($j \leq i$) may be present in the reaction coordinate as translational energy; then k=i-j quanta remain to be distributed freely in s-1 oscillators (excluding the decomposing oscillator). The rate constant for the decomposition of the system with energy $E = (m+i)h\nu$, k_{b_E}, is in this theory given by ν multiplied by the probability that the system has a distribution of energies conducive to decomposition. The overall decomposition rate for an assembly of molecules is

$$k_b^{\ CALC} = \frac{\sum_E P_E k_{b_E}}{\sum_E P_E} \qquad (V.8)$$

Substituting for P_E from equations (V.6) and (V.7) and for k_E the expres-

sion given by Johnston,[5] (i.e., the bracketed term in the numerator of equation (V.9) one obtains:

$$k_b^{CALC} = \frac{\sum_{i=0}^{\infty} \frac{(m+i+s-1)!}{(m+i)!(s-1)!} e^{-(m+i)h\nu/kT} \left[\nu \frac{(s-1)!(m+i)!}{(m+i+s-1)!} \sum_{k=0}^{i} \frac{(k+s-2)!}{k!(s-2)!} \right]}{\sum_{i=0}^{\infty} \frac{(m+i+s-1)!}{(m+i)!(s-1)!} e^{-(m+i)h\nu/kT}} \qquad (V.9)$$

Results

For the reasons quoted earlier, we compare k_b^{EXP} for the decomposition of $CO^+ \cdot CO^*$ and $HCO^+ \cdot CO^*$ between 100 and 600°K with k_b^{CALC} computed from equation (V.9) for systems of s = 3,4,5,6 and 10 low-frequency oscillators of 100, 200 and 400°K. The values for k_b^{EXP} were obtained from the data of Section IV.1 for k_f, and the use of the low pressure limiting form of equation (V.2). The values $k_c = k_{LANGEVIN} = 8.14 \times 10^{-10}$ and $k_s = k_{LANGEVIN} = 7.05 \times 10^{-10}$ cm.^{3}/mol.sec. were used for the appropriate collision processes. The stabilizing efficiency of the third body, CO, introduces some uncertainty into the absolute values of k_b^{EXP} obtained this way; however, since k_c and k_s are not significantly temperature dependent, the temperature dependence of k_b^{EXP} is still well represented by these data. The values of k_b^{CALC} and k_b^{EXP} are shown in Fig. V.1 for the case representing k_b^{CALC} for $CO^+ \cdot CO^*$ ($|\Delta H^o| \approx 23$ kcal/mole) and in Figure V.2 for $HCO^+ \cdot CO^*$ ($|\Delta H^o| \approx 11$ kcal/mole). The best agreement between k_b^{CALC} and k_b^{EXP} in the case of $CO^+ \cdot CO^*$ is obtained for s = 3-4; $\tilde{\nu}$ = 200 cm.$^{-1}$ or s = 4-5; $\tilde{\nu}$ = 400 cm.$^{-1}$. Since a $CO^+ \cdot CO^*$ ion has 3N-6=6 internal degrees of freedom, of which 2 C≡O bonds are of high frequency, the presence of 3-5 low frequency modes in the complex is physically reasonable. For $HCO^+ \cdot CO^*$, the temperature dependence of k_b^{EXP} is best reproduced by k_b^{CALC} with s = 5-6, $\tilde{\nu}$ = 200 cm.$^{-1}$; the absolute value of k_b^{EXP} is best reproduced with s = 3to5, $\tilde{\nu}$ = 400 cm.$^{-1}$. (The uncertainty in k_b^{EXP} introduced by k_s must be kept in mind.) Since for $HCO^+ \cdot CO^*$ 3N-6=9 a number for s which is larger than that of $CO^+ \cdot CO^*$ is reasonable in this case.

The effect of the molecular complexity (represented here by s) on

FIGURE V.1

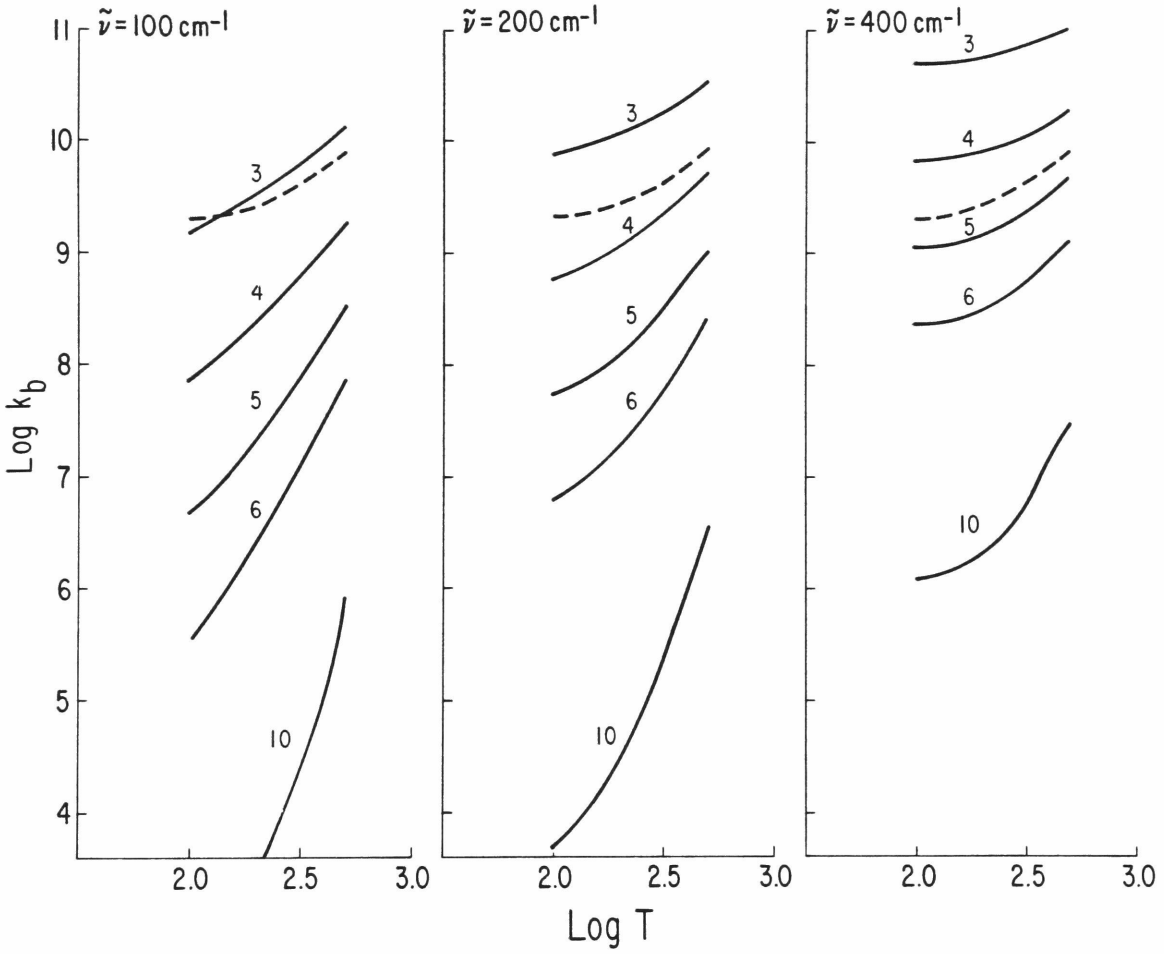

Plots of log k_b^{CALC} vs. log T between 100 and 500°K. k_b^{CALC} was calculated from equation (V.9), for the case when $\Delta H = 23$ kcal/mole. $\tilde{\nu}$ = 100 cm.$^{-1}$ (a); 200 cm.$^{-1}$ (b); 400 cm.$^{-1}$ (c). The numbers over each line indicate the number of oscillators, s, used in calculating k_b^{CALC} which is shown in the corresponding line. The broken line shows the experimental value, k_b^{EXP}, for the back-dissociation of $(CO^+ \cdot CO)^*$, obtained from the data of Section IV.1, as explained in the text.

FIGURE V.2

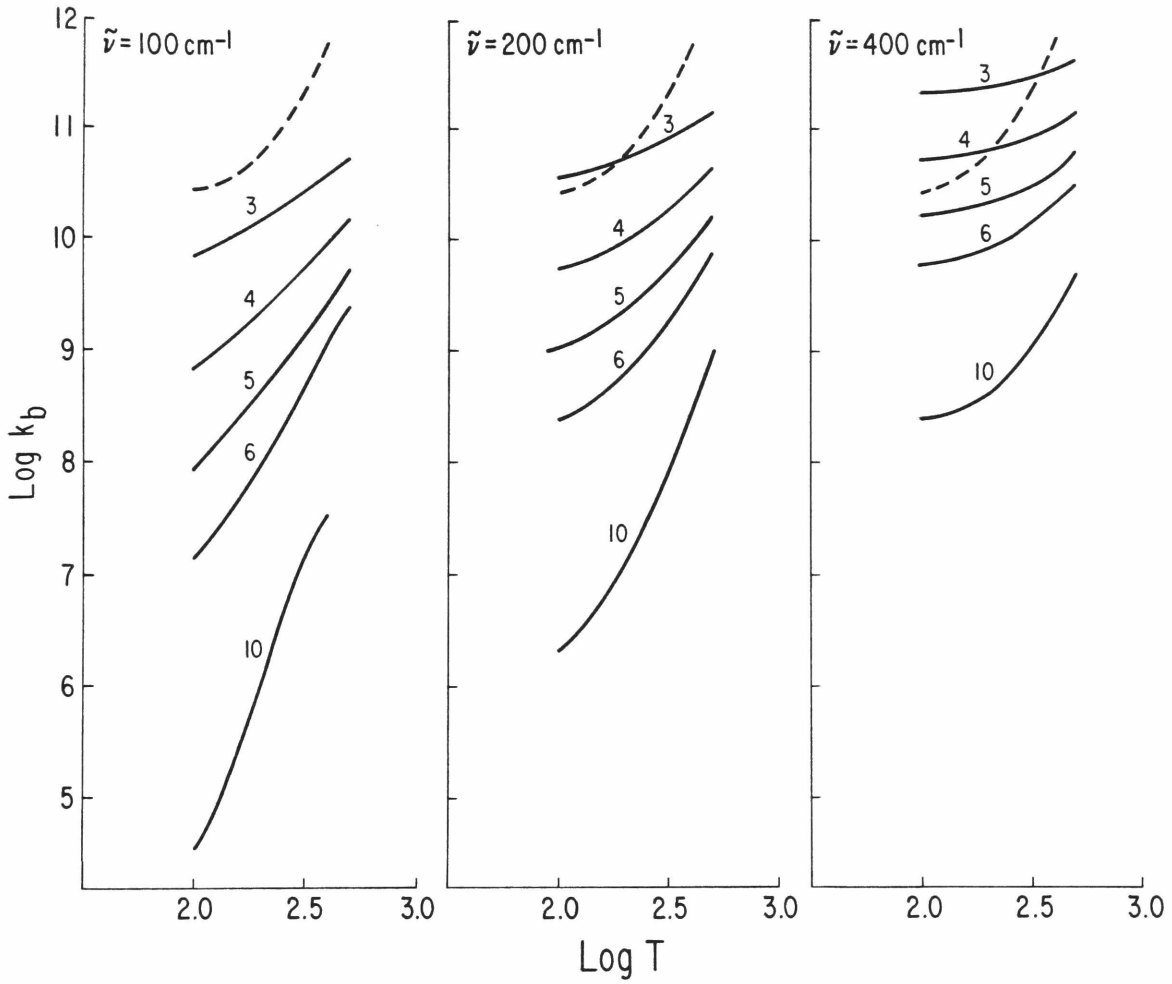

Plots of log k_b^{CALC} vs. log T as s in Fig. V.1.1, for the case ΔH = 11 kcal/mole. The broken line shows the experimental value, k_b^{EXP}, for the back-dissociation of $(HCO^+ \cdot CO)^*$

k_b^{EXP} was investigated in Section IV.2 in association reactions involving NH_4^+, $CH_3NH_3^+$ and $(CH_3)_2NH_2^+$. It is interesting to examine how the variation of s in equation (V.9) will reproduce the change of k_b^{EXP} with increasing molecular complexity. Our experimental results gave temperature dependences for these reactions between 350 and 400°K of the magnitude $k_b^{EXP} \propto T^3$ to T^7. The low energy bond ($\approx$20 kcal/mole)[7] presumably introduces low frequency modes in the complexes. However, computations based on equation (V.9) shows that, for example 8 oscillators of $\tilde{\nu}$ = 100 cm.$^{-1}$ or 18 oscillators of 500 cm.$^{-1}$ are required to reproduce the observed temperature dependences of k_b^{EXP}. The presence of such a large number of oscillators of such low frequencies in these complexes is physically unreasonable. These considerations indicate that the redistribution of the excitation energy in the higher frequency modes also significantly affects k_b in these complexes. For this reason computations were carried out using s=3N-6, the total number of internal degrees of freedom; $\tilde{\nu}$ was varied between 500 and 2000 cm.$^{-1}$.

The results with $\tilde{\nu}$ = 1750 cm.$^{-1}$ (Table V.1), show agreement within a factor of 6 between the absolute values of k_b^{CALC} and k_b^{EXP} at 350°K. The temperature dependence of k_b^{EXP} between 350 and 400°K are reproduced satisfactorily with $\tilde{\nu}$ = 650-850 cm.$^{-1}$. (See Fig. IV.2.4). This result illustrates the predominant effect of the low frequency modes on the temperature dependence of the decomposition rate.

Discussion

1. Examination of the results of the present calculations show that, in general, even the physically crude model of degenerate coupled quantum oscillators successfully reproduces the magnitude of k_b^{EXP} and its variation with the physical parameters. In particular:

(i) The model reproduces well the main features of the temperature dependence of k_b^{EXP} for the decomposition of the simpler ions $CO^+ \cdot CO^*$ and $HCO^+ \cdot CO^*$. These features are an approximately linear portion of the plot of log k_b vs. log T between 500 and 200°K, and a decrease in the extent of the temperature dependence of k_b^{EXP} at lower temperatures.

TABLE V.1

Calculated (RRKM) and Experimental Effects of Molecular Complexity and Temperature on the Decomposition Rates and Excited Reaction Complexes

No.	Complex	Internal Degrees of Freedom S=3N-6	k_b^{350} Calc[a]	k_b^{I}/k_b^{II}[b]		k_b^{II}/k_c^{III}[b]		Temperature Dependence of k_b[c] between 350 and 400°K		Exp.
			(10^7 sec^{-1})	Calc.	Exp.	Calc.	Exp.	(Calc. ($\tilde{\nu}$=1750cm^{-1})	Calc. ($\tilde{\nu}$=850cm^{-1})	
I	$(NH_4^+ \cdot NH_3)^*$	21	100	17.8	18.3	-	-	$T^{0.13}$	$T^{2.3}$	$T^{3.2}$
II	$(CH_3NH_3^+ \cdot CH_3NH_2)^*$	39	5.6	-	-	6.1	2.0	$T^{0.35}$	$T^{4.3}$	$T^{3.6}$
III	$((CH_3)_2NH_2^+ \cdot CH_3NH_2)^*$	57	0.91	-	-	-	-	$T^{0.36}$	$T^{6.3}$	$T^{7.2}$

. All the calculated values presented here except where indicated otherwise were calculated from equation (V.8), with $\tilde{\nu}$ = 1750 cm.$^{-1}$, S=3N-6 as shown in column 3. Values of j for these calculations were selected such that $jh\nu$ =22 kcal/mole, the average experimental value for these reactions. The summation over n was carried out not to ∞, but to values which contribute less than 2% to the overall decomposition rates.

. at 350°K.

. The calculated temperature dependence is smaller at lower temperatures. Such behavior was observed experimentally in Fig. IV.2.4 and in other ion-molecule association reactions.[3] The calculated temperature dependence given in this table is obtained from the ratio $\ln\left(k_{b_{CALC}}^{400}/k_{b_{CALC}}^{350}\right)/\ln\frac{400}{350}$.

(ii) Comparison of the plots of k_b^{CALC} in Fig. V.1 and Fig. V.2 show the increase in temperature dependence with increasing s. This is observed experimentally comparing the behavior of k_b^{EXP} of $CO^+ \cdot CO^*$ and $HCO^+ \cdot CO^*$. Similarly, the computational model with $\tilde{\nu} = 850$ cm.$^{-1}$ reproduces well the change between the temperature dependence of k_b^{EXP} in going from complex I to II to III in Table V.1. The RRKM model of equation (V.9) reproduces very well the temperature dependences of k_b^{EXP} when the values of s = 3N-6, and $\tilde{\nu} = 650$ cm.$^{-1}$ for complex I and $\tilde{\nu} = 850$ cm.$^{-1}$ for complexes II and III are used (Fig. IV.2.4).

(iii) The change in k_b^{CALC} with increasing s follows reasonably well the decrease of k_b^{EXP} (Table V.1) with increasing molecular complexity.

(iv) For constant values of s and , both k_b^{EXP} and k_b^{CALC} decrease when m increases, i.e., when $|\Delta H^\circ$ association$|$ gets larger (compare Figs. V.1 and V.2). This causes an overall increase of k_f for more exothermic reactions, as observed experimentally in Section IV.1.

2. Comparison of the quantum and classical oscillator models.

The classical approximation of the RRK model was applied to ion-molecule association reactions in the form

$$k_b = \nu \left(\frac{sRT}{|\Delta H^\circ| + sRT} \right)^{s-1} \qquad (V.10)$$

by several authors.[1,2,3] In Table V.2 the results of this equation are compared with that of the more accurate quantum oscillator model of equation (V.9) for several cases of interest in the present study. For the absolute values of k_b^{CALC}, the classical equation constitutes reasonably good approximation when s and $\tilde{\nu}$ are small; in other cases, the approximation is moderately to severly inaccurate. The temperature dependence of k_b^{CALC} is always poorly approximated by equation (V.10). The failure of the classical model is severe in particular for the cases of higher frequency oscillators ($\tilde{\nu} = 1750$ cm.$^{-1}$), i.e., when $h\nu \gg kT$, as might be expected. Consequently, equation (V.10) cannot give quantative insight

TABLE V.2

Values of k_b and its Temperature Dependence Calculated by the Exact Quantum Harmonic Oscillator Model Equation (V.9) and the Approximate Harmonic Oscillator Model Equation (V.10)

s^a	$\tilde{\nu}^a$ (cm^{-1})	ΔH^a (kcal/mole)	k_b^{350} (sec^{-1})		Temperature Dependence of k_b Between 350 and 400°K	
			Quantum	Classical	Quantum	Classical
4	400	22	1.2×10^{10}	1.7×10^{10}	$T^{1.1}$	$\approx T^3$
6	200	11	7.4×10^{9}	9.3×10^{9}	$T^{2.8}$	$\approx T^5$
21	1750	22	5.0×10^{9}	5.3×10^{5}	$T^{0.08}$	$T^{19.2}$
21	750	22	1.7×10^{6}	2.3×10^{5}	$T^{3.0}$	$T^{19.2}$
57	1750	22	1.1×10^{8}	9.0×10^{2}	$T^{0.26}$	$T^{11.7}$
57	750	22	3.0×10^{3}	3.9×10^{2}	$T^{8.5}$	$T^{11.7}$

a. The values of $s, \tilde{\nu}$ and ΔH selected here are those for which the quantum oscillator model approximates best the values of k_b^{EXP} and its temperature dependence.

into any aspect of the decomposition process, such as the number of active oscillators in the complex.[3] It may, however, be useful in some cases for qualitative arguments concerning the effect of ΔH^{o}, s and T on k_b.

3. A comment on the applicability of the RRKM model to ion-molecule transfer reactions.

It might be expected that transfer reactions proceed via a complex which may competitively decompose to products or back to reactants:

$$A^{+} + B \underset{k_b}{\overset{k_c}{\rightleftharpoons}} AB^{+}* \xrightarrow{k_p} \text{Products} \qquad \text{(V.11)}$$

In analogy with equation (V.2), the overall rate constant k_f is given by:

$$k_f = \frac{k_c k_p}{k_b + k_p} \qquad \text{(V.12)}$$

A mechanism essentially of this kind was proposed to account for the negative temperature dependence of some slow exothermic ion-molecule reactions.[1]

In exothermic transfer reactions in general the probability for decomposition to products is expected to be higher than the probability for back-dissociation to reactants. In such reactions, unless entropic factors strongly favor the back dissociation of $AB^{+}*$ to reactants, RRKM calculations will always give $k_p \gg k_b$, and, from equation (V.12) $k_f \approx k_c$. For example, the case of s = 84, $\tilde{\nu}$ = 1750 cm.$^{-1}$, with the chemical energy of $AB^{+}* \approx 10$ kcal/mole, and the overall exothermicity 3 kcal/mole was used as a crude model for the reaction t-$C_4H_9^{+}$(i-C_5H_{10}, i-C_5H_{12})t-$C_5H_{11}^{+}$. At 350^{o}K, equation (V.9) gives for this system $k_b^{CALC} = 1.53 \times 10^{10}$ sec.$^{-1}$; $k_p^{CALC} = 1.23 \times 10^{12}$ sec.$^{-1}$. With $k_{LANGEVIN} = 0.82$ cm.^{3}/mol.sec, equation (V.12) gives $k_f^{CALC} = 0.81 \times 10^{9}$ sec.$^{-1}$; however, $k_f^{EXP} = 0.013$ for this reaction at 350^{o}K. Thus, in general, RRKM considerations applied in the present sense will predict that all exothermic transfer reactions which involve negligible activation energies will proceed at the collision rate. Steric factors may render $k_c \ll k_{COLLISION}$, but this will not explain the negative temperature dependences often observed in such reactions. These considerations indicate

that slow transfer reactions with negligibly small activation energies do not proceed via complexes to which RRKM considerations are applicable.

In conclusion, the present calculations show that the dependence of ion-molecule association rate constants on the molecular complexity, on the enthalpy of the reaction, and the detailed form of the temperature dependence may be quantitatively accounted for by the RRKM model in conjunction with the energy transfer mechanism. Accurate information on the structures of ion-molecule association complexes should make the application of more advanced versions of the RRKM method to this type of reactions possible.

REFERENCES

1. E.E. Ferguson, in "Ion-Molecule Reactions," J.L. Franklin, ed., Plenum Press, New York, 1972, Vol. 2, pp.368 ff.
2. R. Wolfgang, Acct. Chem. Research, 3, 48 (1970).
3. A. Good, Trans. Faraday. Soc., 67, 3495 (1971).
4. P.J. Robinson and K.A. Holbrook, "Unimolecular Reactions," Wiley-Interscience, London, 1972, p.62.
5. H.S. Johnston, "Gas Phase Reaction Rate Theory," The Ronald Press Co., New York, 1966, p.281.
6. For example, see V.N. Kondrat'ev, "Chemical Kinetics of Gas Reactions," Pergamon Press, Oxford, 1964, p.175.
7. R. Yamdagni and P. Kebarle, J. Amer. Chem. Soc., 95, 3504 (1973).

PRO · BONO · HUMANI · GENERIS
The Rockefeller University
1901

THE LIBRARY

19010000002907

DeRAY
22 W 26
N Y

End